

Diss. ETH NO. 27637

The Role of Individuals
in the City-Scale Energy Transition:
An Agent-Based Assessment

A thesis submitted to attain the degree of

DOCTOR OF SCIENCES of ETH ZÜRICH
(Dr. Sc. ETH Zürich)

Presented by

Marco Ambrogio Pagani

M. Sc. ETH, ETH Zurich

Born on 03.01.1989

Citizen of Switzerland

Accepted on the recommendation of

Prof. Dr. Reza. S. Abhari, examiner

Prof. Dr. João Tomé Saraiva, co-examiner

Dr. Ndaona Chokani, co-examiner

Abstract

An energy transition in cities is underway, bringing new technical and financial challenges for multi-utility companies. The implementation of decarbonization policies has a long-term impact on the design, operation, and profitability of electrical, heat, and mobility infrastructure, resulting in significant investments and various types of risks. These risks are amplified by the individual choices of thousands of customers whose present and future behavior is uncertain. Therefore, it is necessary to analyze the interdependencies among the various actors in the energy transition and quantitatively assess its implications.

Multi-utility companies generally address these unknowns by relying on top-down models based on historical data, statistical models, and architectural standards. These models often do not provide the granularity needed for city-scale assessments and are not well suited to model discontinuities, such as the introduction of new technologies. Thus, this study's main contribution is the development of three predictive, integrated, bottom-up models to simulate electricity, heat, and electric mobility demand at the urban level. The most significant methodological advances of this study include the integration of the demand models into a single, high-resolution "digital twin" of an actual city, as well as the inclusion of behavioral models of individuals, obtained through the extensive and large-scale use of agent-based models.

Three case studies are used to evaluate the accuracy and performance of the developed models and their suitability in supporting a sustainable energy transition. In the mobility case study, it was found that providers face considerable financial exposure at today's low electric vehicle penetration, and the initial investment in public charging stations would only break even from a 4% electric vehicle penetration. Moreover, the study revealed that revenues based on parking duration break even faster than tariffs based on power supplied. However, the revenues from parking fees are also found to be more sensitive to user charging behavior. Furthermore, at 20% penetration, charging at public and charging at work can cause a local increase in grid load of up to 78%. In the heat case study, a model considering building occupants' behavior was found to quantify the time-resolved heat demand better, achieving an average annual error of -4.8%. To support the city's plans to expand the district heating network, the model was used in conjunction with a predictive model capable of quantifying the probability of a building connecting to the future network. By considering both the spatial distribution of heat demand and the probability that a building would connect to the future network, the internal rate of return of the district heat infrastructure could be increased by 25%, compared to a network extension in which the probability of connection was not modeled. Finally, the electricity study demonstrated how the implementation of behavioral models linked to location-specific habits improves electricity demand forecasts. The impact on the grid of future population dynamics and increased electricity demand due to the electrification of mobility and decarbonization of the building stock through heat pumps was quantified by identifying the areas of the city where the increase in load on the grid would be the greatest.

In conclusion, this study demonstrates the superiority of bottom-up agent-based energy demand forecasting models compared to other approaches, as well as the importance of incorporating individual behavioral patterns into the models. The results of this work have already been used in the test-case city to concretely support decision-making processes, improve business models, and ensure that future investments are socially accepted.

Sommario

Nelle città è in corso una transizione energetica e ciò, per le società multiservizi, comporta nuove sfide tecniche e finanziarie. L'implementazione di politiche di decarbonizzazione ha un impatto di lungo termine sulla progettazione, sul funzionamento e sulla redditività delle infrastrutture elettriche, di riscaldamento e di mobilità, da cui risultano importanti investimenti e vari tipi di rischi. Questi rischi sono amplificati dalle scelte individuali di migliaia di clienti il cui comportamento - nel presente e nel futuro - è incerto. Occorre quindi analizzare le interdipendenze tra i vari attori della transizione energetica e valutare quantitativamente le implicazioni di essa.

Generalmente le società multiservizi affrontano queste incognite affidandosi a modelli "top-down" basati su dati storici, modelli statistici e norme architettoniche. Questi modelli spesso non forniscono la granularità necessaria per valutazioni a livello urbano e non sono adatti a modellare discontinuità, come l'introduzione di nuove tecnologie. Il contributo principale di questo studio è quindi lo sviluppo di tre modelli previsionali, integrati e di tipo "bottom-up", in grado di simulare il fabbisogno elettrico, termico e di mobilità elettrica a livello urbano. Gli avanzamenti metodologici più significativi di questo studio sono rappresentati dall'integrazione dei modelli predittivi in un unico "gemello digitale" di una città reale ("*digital twin*"), ad alta risoluzione, così come dall'inclusione di modelli comportamentali dei singoli individui, ottenuti attraverso l'uso estensivo e su larga scala di modelli basati sugli agenti.

L'accuratezza e la performance dei modelli, nonché la loro adeguatezza nel supportare una transizione energetica sostenibile, sono stati valutati in tre studi. Nello studio sulla mobilità, si è evidenziato come l'attuale bassa penetrazione di veicoli elettrici sottoponga i provider ad una considerevole esposizione finanziaria; l'investimento iniziale in colonnine pubbliche verrebbe coperto (break-even) solo a partire da una penetrazione del 4%. Inoltre, lo studio rivela che introiti basati sulla durata di parcheggio permettono di raggiungere il pareggio dell'investimento più rapidamente che tariffe basate sull'energia fornita. Tuttavia, le prime, si dimostrano anche essere più sensibili al comportamento di ricarica degli utenti. Inoltre, ad una penetrazione del 20%, la ricarica presso colonnine pubbliche e sul posto di lavoro può localmente causare un aumento del carico sulla rete fino al 78%. Nello studio sul calore si è dimostrato come un modello, che consideri il comportamento degli abitanti negli edifici, sia migliore nel quantificare il fabbisogno termico nel tempo, ottenendo un errore medio annuale del -4,8%. Per sostenere i piani di ampliamento della rete di teleriscaldamento cittadina, il modello è stato utilizzato in abbinamento ad un modello predittivo in grado di quantificare la probabilità che un edificio si colleghi alla futura rete. Tenendo conto sia della distribuzione spaziale del fabbisogno energetico, sia della probabilità che un edificio si colleghi alla futura rete, il tasso interno di rendimento dell'infrastruttura può essere aumentato del 25%, rispetto a un'estensione della rete in cui il secondo aspetto non sia considerato. Lo studio sull'elettricità ha mostrato come l'implementazione di modelli comportamentali legati alle abitudini del luogo, migliori le previsioni della domanda elettrica. L'impatto sulla rete di distribuzione di future dinamiche demografiche e l'aumento della domanda elettrica in seguito all'elettrificazione della mobilità e alla decarbonizzazione del parco immobiliare mediante pompe di calore, è quantificato identificando le zone della città dove l'aumento del carico sulla rete sarà maggiore.

In conclusione, questo studio ha dimostrato la superiorità, rispetto ad altri approcci, di modelli di previsione della domanda energetica di tipo "bottom-up" e basati su agenti così come l'importanza di includere modelli comportamentali individuali alla base degli algoritmi. I risultati di questo lavoro sono già stati utilizzati nella città di studio per supportare concretamente processi decisionali, migliorare i modelli di business e assicurarsi che futuri investimenti siano accettati dalla popolazione.



Declaration of originality

The signed declaration of originality is a component of every semester paper, Bachelor's thesis, Master's thesis and any other degree paper undertaken during the course of studies, including the respective electronic versions.

Lecturers may also require a declaration of originality for other written papers compiled for their courses.

I hereby confirm that I am the sole author of the written work here enclosed and that I have compiled it in my own words. Parts excepted are corrections of form and content by the supervisor.

Title of work (in block letters);

THE ROLE OF INDIVIDUALS IN THE CITY-SCALE ENERGY
TRANSITION: AN AGENT-BASED ASSESSMENT

Authored by (in block letters):

For papers written by groups the names of all authors are required.

Name(s):

MARCO AMBROGIO

First name(s):

PAGANI

With my signature I confirm that

- I have committed none of the forms of plagiarism described in the '[Citation etiquette](#)' information sheet.
- I have documented all methods, data and processes truthfully.
- I have not manipulated any data.
- I have mentioned all persons who were significant facilitators of the work.

I am aware that the work may be screened electronically for plagiarism.

Place, date

Zürich, 10/03/2021

Signature(s)

Pagani

For papers written by groups the names of all authors are required. Their signatures collectively guarantee the entire content of the written paper.

Contents

Nomenclature	vi
1 Introduction	1
1.1 The Energy Transition	1
1.1.1 Ongoing decarbonization trends	3
1.1.2 The role of city multi-utilities in energy transition	7
1.2 Risks and Uncertainties	9
1.2.1 Techno-economic uncertainties	9
1.2.2 The human factor	11
1.3 Requirements for the Simulation Model	13
1.3.1 Agent-based	13
1.3.2 Bottom-up	15
1.3.3 Integrated	16
1.3.4 Large-scaled	17
1.4 Literature Survey	17
1.4.1 Electric mobility and EV charging infrastructure	17
1.4.2 Heat demand and district heat	19
1.5 Novelty of the Present Study and Thesis Goals	21
2 Methodology	24
2.1 Extension and Improvement of the <i>EnerPol</i> Framework	24
2.2 Methodology Outline	26
2.3 Digital Twin Development	28
2.3.1 Geo-referenced built infrastructure	28
2.3.2 Transformers data analysis	32
2.3.3 Smart meter data analysis	33
2.3.4 Power flow simulations of the low-voltage grid	43
2.4 Agent-Based Models	44
2.4.1 Agent-based population model	45

2.4.2	Agent-based daily activity model	45
2.4.3	Agent-based mobility model	46
3	Case Study: Electric Mobility	47
3.1	Methodology	48
3.1.1	Stochastic EV use model	48
3.1.2	Stochastic behavior model of EV users	49
3.1.3	Deterministic EV charging infrastructure model	51
3.1.4	Financial optimization of electric vehicle charging infrastructure	51
3.1.5	Evaluation of profitability of EV charging infrastructure	52
3.2	Scenarios	54
3.3	Results	56
3.3.1	Model validation	56
3.3.2	Business model, competition, and profitability of the existing charging infrastructure	58
3.3.3	Techno-economic consequences of increasing electric vehicle penetration	61
4	Case Study: Heat	72
4.1	Methodology	74
4.1.1	Characterization of agents	74
4.1.2	Agent-based model of building occupants' behavior	76
4.1.3	Agent-based heat demand model	77
4.1.4	District heat predictive model	84
4.1.5	District heat routing model	85
4.2	Scenarios	86
4.3	Results	87
4.3.1	Impact of individual behaviors on heat demand prediction	87
4.3.2	Findings on likelihood of connection of buildings to district heat network	90
4.3.3	Financial consequences of routing of new district heat pipelines	92
5	Case Study: Electricity	96
5.1	Methodology	97
5.1.1	Agent-based model of electricity demand of residential buildings	99
5.1.2	Agent-based model of electricity demand of office buildings	103
5.1.3	Smart meter- and norms-based model of electricity demand of other building types	105
5.2	Energy Transition Scenario	105
5.3	Results	106

5.3.1	Impact of individual behaviors on electricity demand prediction . .	108
5.3.2	Impact of energy transition on distribution grid	119
6	Conclusions	123
6.1	Concluding Remarks	123
6.2	Summary of Accomplishments	124
6.3	Other Accomplishments	128
6.4	Future Work	128
6.4.1	Database improvement	128
6.4.2	Model improvement	130
6.4.3	Suggested scenarios	131
	Acknowledgements	131
	List of Publications	133
	Student Projects Supervised	134
	Curriculum Vitae	136
	List of Figures	142
	List of Tables	145

Nomenclature

Abbreviations

ABM	Agent-based models
AF	Activation factor
CAPEX	Capital expenditures
DH	District heat
DHW	Domestic hot water
DSO	Distribution system operator
EKZ	Elektrizitätswerke des Kanton Zürichs
EV	Electric vehicle
GIS	Geographic information system
IRR	Internal rate of return
LEC	Laboratory for Energy Conversion
MAE	Mean absolute error
NACE	Statistical classification of economic activities
NPV	Net present value
OPEX	Operating expenses
SIA	Swiss Society of Engineers and Architects
sgsw	St. Galler Stadtwerke
SH	Space heating
SOC	State of charge (battery)

Symbols

α_{DSO}	DSO cost share	$[-]$
C	Thermal capacity	$[Wh/K]$
C_{Inv}	Investment costs (CAPEX)	$[CHF]$
C_{Maint}	Maintenance costs (OPEX)	$[CHF/year]$
h	Convection and radiation coefficient	$[W/(m^2K)]$
n	Ventilation rate	$[m^3/(m^2s)]$
$nRMSD$	Normalized root mean square deviation	$[\%]$
P^{Base}	Parking base fee	$[CHF/h]$
P^{Fee}	Parking fee	$[CHF/h]$
$\Delta P^{Surcharge}$	Parking fee surcharge (for charging)	$[CHF/h]$
Q	Heat flux	$[W]$
R	Conduction resistance	$[m^2K/W]$
$RMSD$	Root mean square deviation	$[OutcomeUnit]$
r	Discount rate	$[\%]$
t	Time	$[-]$
T	Temperature	$[K]$
T^{ext}	External/ambient temperature	$[C]$
t_{BE}	Time to break even	$[Years]$
U	Overall heat transfer coefficient	$[W/(m^2K)]$

Greek

μ	Average value	$[-]$
η	Thermal efficiency	$[-]$
σ	Standard deviation	$[-]$

Chapter 1

Introduction

1.1 The Energy Transition

The world is undergoing an energy transition. In cities, this implies profound and long-term changes to the urban electricity, heat, and mobility infrastructure. To reduce their carbon footprint and improve their overall energy efficiency, cities are implementing decarbonization policies. These include replacing fossil-fueled heating systems with more sustainable technologies (such as heat pumps and district heat [DH]), the electrification of private and public mobility, and distribution grid upgrades to support the additional electric power demand and the increased penetration of renewable energy sources.

Five years after the ratification of the Paris Climate Agreement [1], the goal of which being to limit the increase in global average temperature to 1.5°C above pre-industrial levels, national and supranational actors have defined plans for the long term. The EU, China, and Japan have committed to becoming climate neutral between 2050 and 2060. In the mid term, the EU's goal is to reduce emissions by at least 55% by 2030 (compared to 1990), Japan's goal is a reduction of 15% by 2030 (compared to 1990), and China's goal is to reach its emissions peak in 2030. Furthermore, the new US administration recently pledged to make the country climate neutral by 2050.

Figure 1.1 illustrates that, in 2020, 45% (252 TWh) of the total amount of electricity production in Germany was generated from renewable energy sources. Over the last 20 years, the share of electricity generated from renewable energy sources in Germany has increased considerably, while emission-intense coal and nuclear energy recorded a significant decline. Germany has been described as a global role model: It has already reached the 2025 goal of 45% electricity from renewable energy sources. Moreover, according to the German Atomic Energy Act (*Atomgesetz*), all German nuclear reactors will be shut down by 2022.

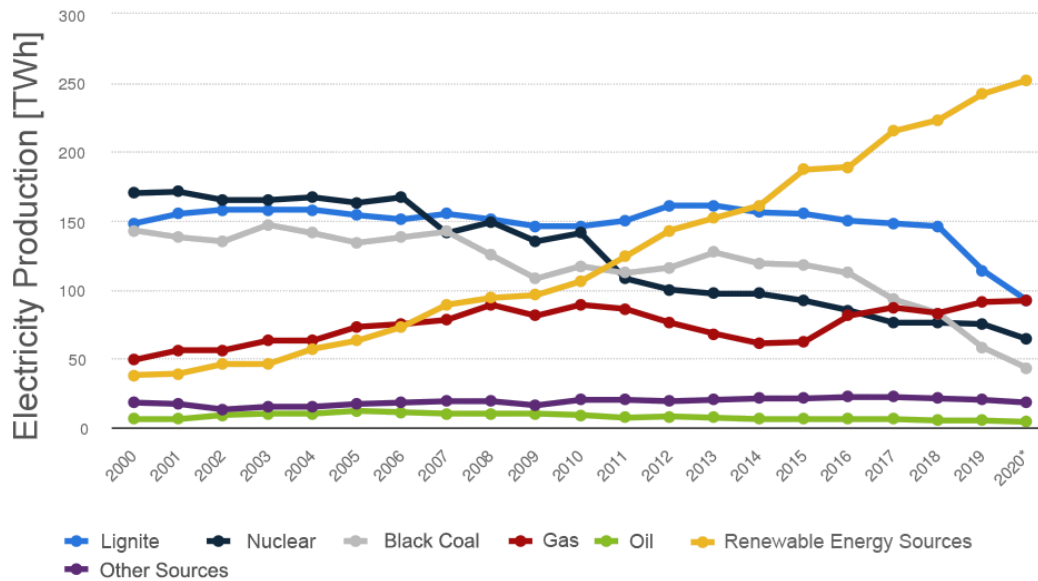


Figure 1.1: Gross electricity generation in Germany by energy source from 2000 to 2020 (in TWh/year). Elaborated from: [2] (*: values for 2020 are preliminary)

Figure 1.2 depicts the increase in the share of electricity generated from renewable energy sources in Germany and the increase of the EEG levy over the same time frame. The EEG is a surcharge for electricity end consumers used to finance the energy transition with a government-set feed-in tariff scheme. The EEG has been continuously increased over the last decade. Moreover, estimates predict that by 2050, around 110 billion euros will be required for the expansion and modernization of the German distribution grids. From these numbers, it is clear that the energy transition comes at a price and that this price should be sustainable for all actors involved, distribution system operators (DSOs) and cities included.

Cities have the critical role of driving the energy transition; therefore, they must to face opportunities, challenges, and risks arising from its implementation. For example, the design and operation of charging infrastructures for private and public mobility comes with large investment costs and raises the question of whether the power grid should be upgraded. Particularly high initial investment costs also mark the construction and extension of DH networks. Furthermore, cities must ensure cost neutrality compared to traditional heating systems to keep district heating economically attractive to end-users. Moreover, the individual choices of thousands of customers, whose present and future behaviors are associated with large uncertainties, amplify these and other risks.

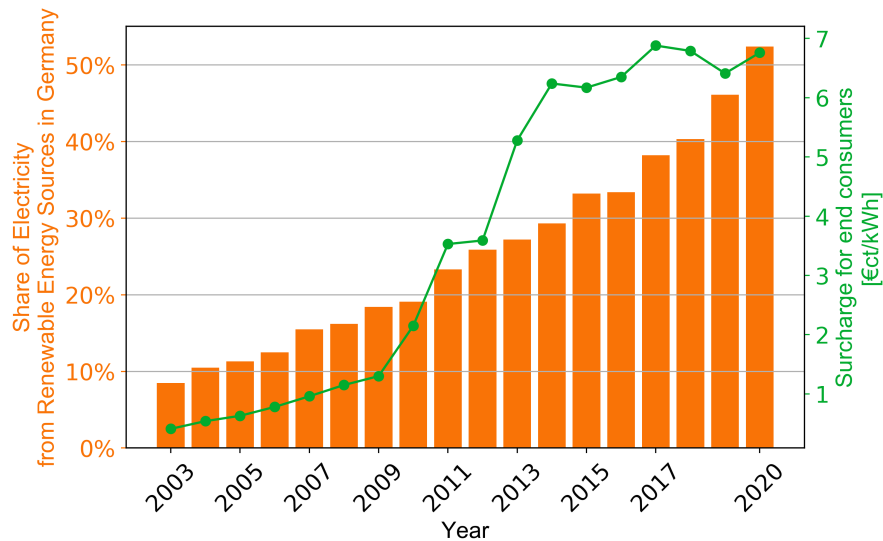


Figure 1.2: Share of renewable energy sources in German gross electricity generation and amount of EEG levy (surcharge for end consumers) for household electricity. Elaborated from: [3]

1.1.1 Ongoing decarbonization trends

The Paris Climate Agreement was signed in Paris on 12 December 2015 by 196 countries [1]. For the first time, almost all countries set common climate targets: In particular, they agreed that a further increase in global warming should be limited to 1.5°C. Although no binding reduction targets for greenhouse gases were specified, and some significant emitters (*e.g.*, the US, which is responsible for 14% of CO₂ emissions worldwide) are not part of the agreement, the Paris Agreement is an indicator of an increased awareness and sensitivity to the impact that economic activity has on the environment.

Environmental awareness, political accountability, and, above all, technical progress are the drivers of an energy transition that is broadly – yet heterogeneously – happening worldwide. Figure 1.3 presents the levelized cost of energy in Germany for various power sources in 2013 and 2018. In 2013, producing electricity from coal (lignite) was cheaper than using wind turbines and solar PV. In 2018, solar PV and onshore wind turbines were economically competitive with electricity generation from coal and cheaper than electricity generation from gas.

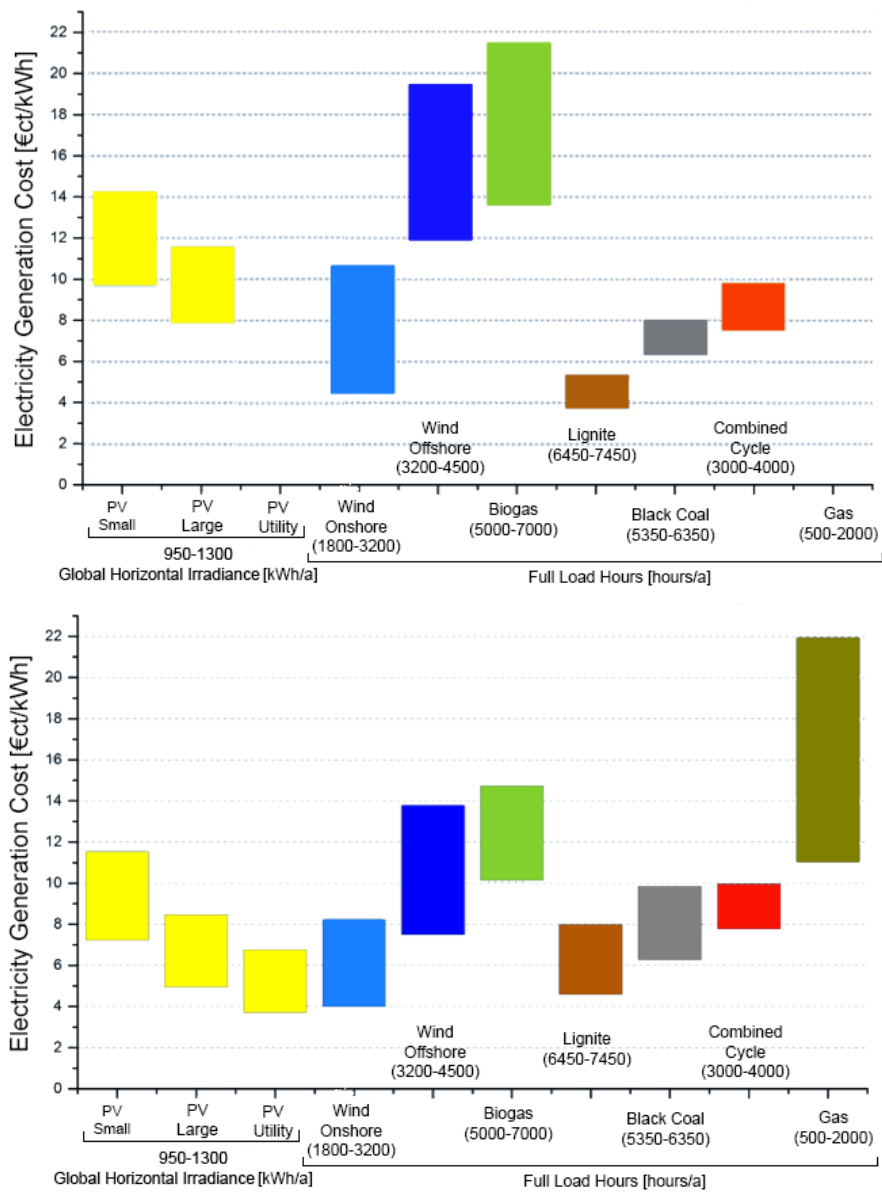


Figure 1.3: Levelized cost of energy for renewable energies and conventional power plants in Germany in the years 2013 (above) and 2018 (below). Elaborated from: [4]

As a result of technical progress and environmental awareness, national and supranational actors are and will be implementing new energy strategies to achieve the Paris Agreement's goals. Here follows an overview:

European Union

On 11 December 2020, the European Council approved the EU Commission's proposal to cut net greenhouse gas emissions by at least 55% compared with 1990 levels by the end of 2030 [5]. This new goal replaces the previous goal of a 40% emissions cut, which was considered insufficient to meet the Paris Agreement's environmental targets. The European Green Deal's main goal is for Europe to become the first climate-neutral continent by 2050 [5].

Switzerland

In 2017, the Swiss people approved an energy act called Energy Strategy 2050 [6] to restructure the overall energy system, including a progressive withdrawal from nuclear energy production. The implementation of Energy Strategy 2050 has and will have relevant consequences for cities and multi-utilities. In 2020, Switzerland approved the revision of the CO₂ law [7] that shall help attain a 50% emissions cut by 2030. However, only 37.5% needs to be reduced domestically. Moreover, the Swiss government has decided that Switzerland should become CO₂ neutral by 2050.

China

With a share of almost 30% of global emissions, China is the world's largest emitter of CO₂. The country aims to be carbon neutral by 2060, a target that was first announced in September 2020 by the Chinese president [8]. As China still depends on coal for more than half of its primary energy, the country's ambitions have a potentially significant impact.

United States

The United States withdrew from the Paris Agreement in 2020. The new administration elected in 2020 recently announced that the country would rejoin the agreement.

Are all these announcements, past and present, affecting greenhouse emissions? Figure 1.4 illustrates the forecasted greenhouse emissions for the coming decades as a function of the different policies that should be implemented until 2030. If countries were to continue with today's measures until 2030, the earth would warm up by about 2.9°C by the end of the century. With the implementation of the announced policies until 2030, the temperature will increase by just 2.5°C. More robust policies (such as CO₂ neutrality) are needed to reach the Paris goal.

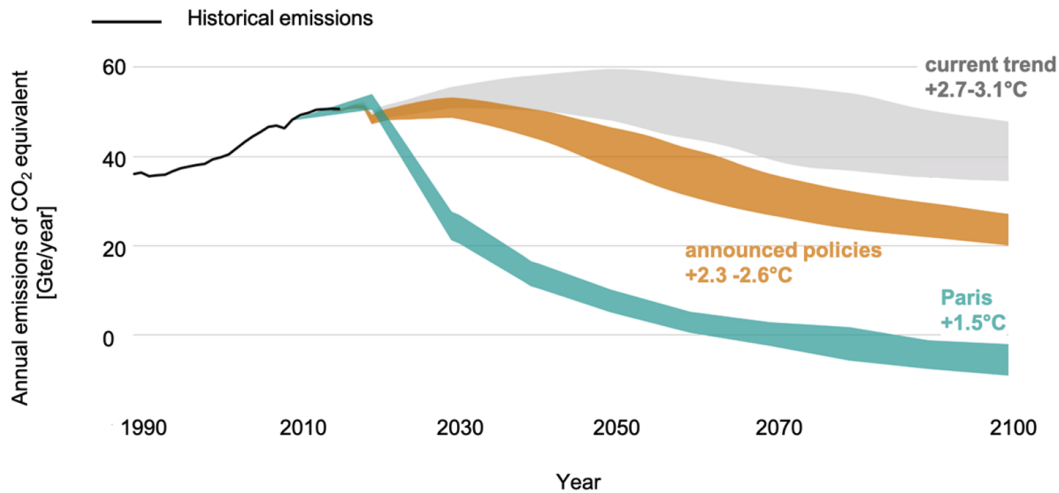


Figure 1.4: Forecast of global greenhouse gas emissions as a function of implemented policy and the resulting increase in world average temperature (width of the curve indicates inaccuracy). Source: [9]

Notably, the implementation of environmental policies does not occur at the same pace in different areas of the world:

- The European Union met its 2020 goal of a 20% reduction of greenhouse gas emissions by 2020 compared to 1990: The EU reduced its emissions by 24% between 1990 and 2019 [10]. Another 2020 goal was to reach a 20% share of electricity from renewable sources. In 2018, this goal was achieved by 13 member states, as shown in Figure 1.5 [11].
- Switzerland had the same goal as the EU, but, instead of the desired 20% reduction, Switzerland emitted only 14% fewer greenhouse gases in 2018 than in 1990 [12].
- In the United States, between 1990 and 2018, greenhouse gas emissions increased by 6% [13].
- In China, between 1990 and 2018, greenhouse gas emissions increased by 388% [14].

Therefore, it is clear that an energy transition is indeed occurring and that the latest announcements portend an acceleration. However, the transition is happening at a slower pace than what is needed or is sometimes portrayed by politics. Current concerns about the world economy's capacity to recover are certainly a restraining factor in its implementation.

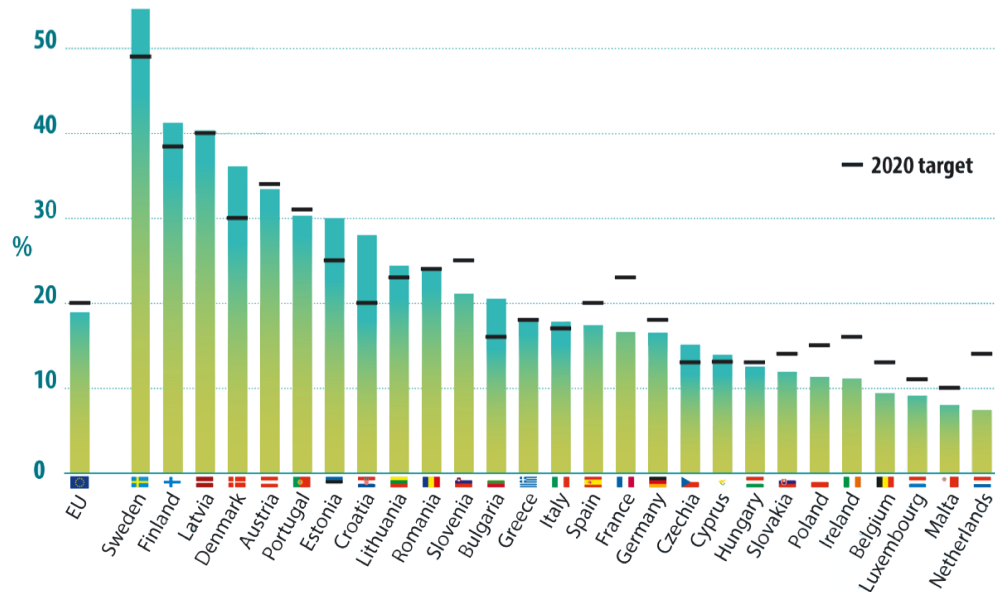


Figure 1.5: Share of electricity from renewable sources in the EU member states in 2018. Source: [11]

1.1.2 The role of city multi-utilities in energy transition

Cities play a central role in the energy transition: Worldwide, more than 50% of the population live in cities, and they are responsible for 70% of the greenhouse gas emissions [15]. On the one hand, the relevance of cities will continue to increase due to urbanization; on the other hand, cities have several opportunities to actively engage in the energy transition due to their dense and interconnected infrastructure. Furthermore, cities can set important impulses through their exemplary function in the areas of energy supply, mobility, area development, and the renovation of buildings [16].

The Swiss electricity market is highly fragmented; there are about 900 utilities in Switzerland that greatly vary in size and financial means. In general, midsized and large cities have their own publicly owned multi-utility companies. These companies are in charge of implementing the energy strategy at a city level, as they are particularly integrated into the economy of the city in which they operate and are subject to its political decisions and will. The public services they provide, *i.e.*, energy, water, telecommunications, transport, and waste disposal, are all energy transition actors.

Within the national context of Switzerland's Energy Strategy 2050 [6], Swiss multi-utility companies such as the St. Galler Stadtwerke (*sgsw*) [17] have elaborated their own energy concepts – in the case of *sgsw*, it is known as EnK³ [18]. The concept is

centered around three areas of focus – electricity, heat, and mobility – and is aligned with global climate targets and worldwide ongoing decarbonization trends. It is characterized by a holistic view in which energy transitions in the three mentioned areas are addressed either individually or by taking into account the overlaps between them, as graphically illustrated in Figure 1.6. The figure illustrates a selection of technologies and planning/financial tools that are considered drivers for the urban energy transition in EnK³.

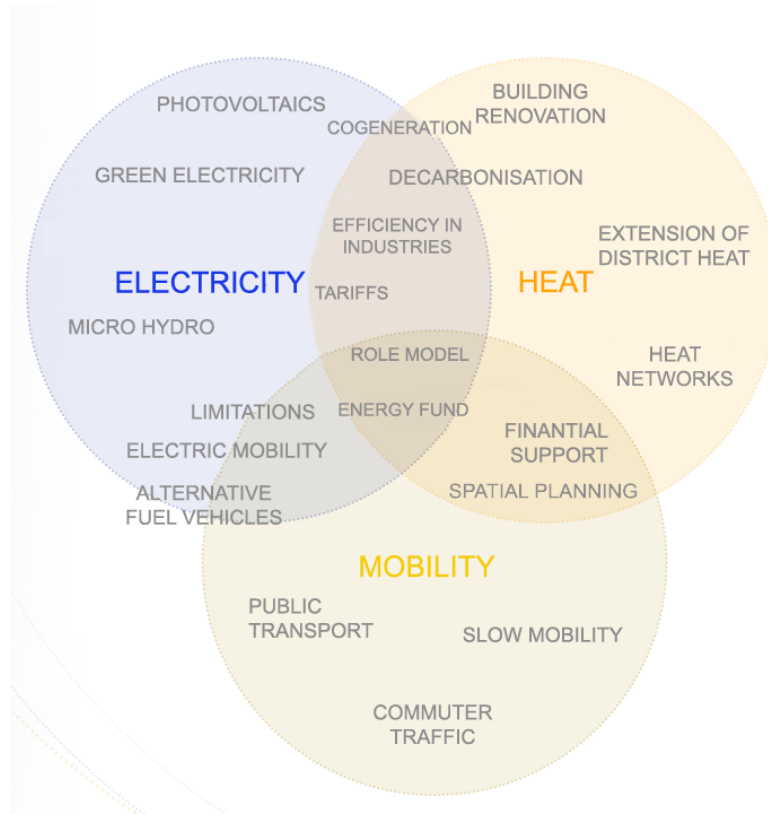


Figure 1.6: Ongoing technological, planning, and financial trends to support city-scale energy transition, classified according to the three pillars of the energy concept EnK³ – electricity, heat, and mobility. Elaborated from: [18]

Analyzing the energy transition implementation concepts worldwide reveals structures similar to EnK³ [19]. The technological and planning/financial tools that are generally put in place can be categorized as follows:

- *Energy system and electricity*
 - Electricity from renewable energy sources
 - Integrated supply concepts – for individual buildings or neighborhoods

- Smart grid technologies: demand-side management, virtual power plants, etc.
- Coupling of technologies (combined heat and power, batteries, power-to-gas, etc.)
- *Heat*
 - Heat from renewable energy sources
 - Heat from waste
- *Mobility*
 - Robust and optimized public transport
 - E-mobility private and public charging infrastructure
 - Innovative goods and freight transport

Therefore, a globally accepted paradigm suggests that a successful energy transition shall imply changes to the electricity, heat, and mobility infrastructure.

1.2 Risks and Uncertainties

The implementation of an energy transition in a city is associated with large investment expenditures and various types of risks. For a city, these risks encompass, for example, regulatory and governance (political) risks, financial and currency risks, counterparty risks, and operational and technological risks. Furthermore, the choices of individuals whose behaviors are associated with large uncertainties amplify these risks.

1.2.1 Techno-economic uncertainties

For the goals of EnK³ to be accomplished, several transformations in the generation mix of the multi-utility *sgsw* and in the energy and urban infrastructure must occur. Such transformations may, for example, include decarbonization of domestic heating, increased e-mobility, increased district heating, or active management of demand through load shifting and reduction. The main targets of EnK³ (schematically represented in Figure 1.7 through energy flow diagrams) foresee the following by 2050:

- A fourfold reduction/increase in non-renewable/renewable primary energy
- A 25% reduction in overall energy demand

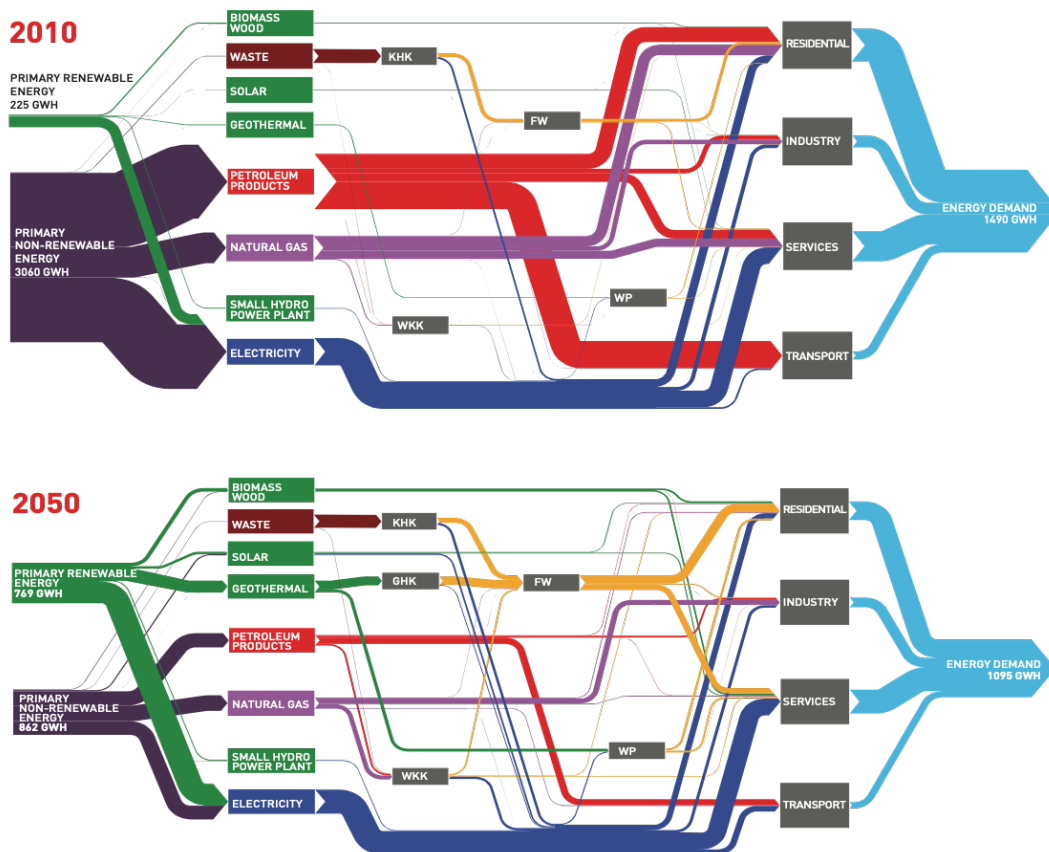


Figure 1.7: Energy flows for the city of St. Gallen in 2010 (above) and elaborated in energy concept EnK³ 2050 (below). Source: [18]

These main targets are to be achieved by implementing well-known technologies and policies (Section 1.1.2, Figure 1.6). Nevertheless, the possible transition pathways to accomplish the necessary transformations are numerous, which generates technical and financial uncertainties. For the decision makers, the ultimate goal of the energy transition is to ensure sustainability in the long term. The concept of sustainability requires, by definition, the balancing of several elements:

- From a *financial* point of view, the profitability of the multi-utility must be guaranteed. The implementation of the Energy Strategy 2050 is associated with considerable costs. However, the same goal could be achieved by generating very different costs. For example, the upgrade of the electricity distribution network in compliance with national guidelines entails investment costs ranging from 230,000 to 40 million Swiss Francs. As a reference, the net income of the multi-utility *sgsw*

in 2019 was 12.0 million Swiss Francs.

- From an *environmental* perspective, the transition must be aligned with the national energy strategy and global climate targets.
- From a *technical* perspective, the DSOs will need to handle long-term changes in energy demand characteristics for electricity, heat, and gas. In particular, the electrification of the mobility and the decarbonization of the building sector will have a profound impact on the distribution grid. Moreover, the daily operations of DSOs will change profoundly, with a shift from a one-way, demand-driven power flow to a two-flow power flow, where the variability in customer behavior will play a fundamental role. In particular, the management of demand peaks (caused by sudden loads from households and e-mobility) entails a significant technical effort for a small utility.
- From a *social* perspective, the economic benefit for the population and the city must be considered. If there is no consensus on the adopted measures, these are likely to fail, particularly in Switzerland, because of direct democracy.

Given the numerous interdependencies between the various elements and the overall complexity of a city-scale energy transition, only integrated assessments and quantitative analysis of the transition pathways' technical and economic consequences can help the stakeholders meet the targets of EnK³. In this way, risks and uncertainties are minimized. Therefore, for policymakers, a strategic decision-making process backed up with a data-driven and quantitative assessment of the costs and benefits of the different transition pathways is a way to overcome economic, political, and social barriers.

In the past, optimizations have taken place in nearly isolated compartments following a so-called silo-thinking approach. Establishing connections between different company departments makes the city a “system of systems” – also known as a *smart city*. Therefore, the prerequisite for creating an intelligent urban environment is to follow a holistic and data-driven approach – as the one applied in this work.

1.2.2 The human factor

When analyzing future scenarios of an energy system, population dynamics and human behavior cannot be neglected. The sustainable implementation of a broad energy transition requires a wide range of energy behavior changes among individuals. These changes include adopting sustainable energy sources and energy-efficient technology, investments in energy efficiency measures in buildings, and changes to direct and indirect energy use behavior [20]. These aspects can be analyzed at a macro and micro level.

At a macro level, these behaviors occur in a political and economic context; therefore,

it is crucial to integrate behavioral insights into the context of these larger systems [21]. On this matter, Switzerland is unique worldwide in that its citizens have the final say on political matters. By virtue of the direct democracy that is in place in Switzerland, citizens are always allowed to approve or reject public investments, regardless of their entity. The Energy Strategy 2050, which, for instance, envisages a maximum limit of 95 g of CO₂/km for gasoline cars by the end of 2020, as well as a ban on new nuclear power plants, was approved by 58.2% of voters in 2017 [22]. Although most layers of society supported the project, some heterogeneities could be observed: Acceptance was much greater among women than men, increasing as age decreased or with educational attainment. The Swiss implementation of the Paris Climate Agreement is closely linked to the revision of the CO₂ law [7], which will likely also be subject to a popular vote in 2021. It is, therefore, clear that energy transitions in participatory democracies cannot be efficiently implemented if citizens do not cooperate. Hence, some of the outcomes of this work aim to enhance social acceptance of long-term investments.

At a micro level, the behaviors, preferences, and choices of the individuals are even more relevant than in the macroscopic dimension; they can determine the success, or otherwise, of implementing an energy transition. These aspects are, by definition, heterogeneous throughout the population, as they generally depend on personal knowledge, motivations, and contextual factors.

To provide an example of the impact of customer preferences on adopting new technologies, many studies have analyzed the characteristics of households willing to connect to new DH pipelines, a problem which is also investigated in this work (Section 4.3). District heat network extensions are associated with large investment and political risks as, generally, there is no obligation for building owners to connect to an extended network. Ruokamo [23] found that Finnish households' views on heating alternatives are affected by socio-demographic characteristics and that homeowners valuing comfort, reliability, and environmental friendliness lean more towards DH. However, DH customers are sensitive to investment cost subsidization and are particularly sensitive to increases in operating costs. In a study on German households, Braun [24] found that multi-family buildings have a rather large probability of connecting to DH pipelines and that DH is predominantly applied by renters, particularly in Eastern Germany. The author also found that the probability of connection to DH is not a function of income and education level and that DH is less likely to be chosen for old buildings.

As another example, the willingness to pay for an electricity subscription for certified green electricity has been studied. Tabi *et al.* [25] conducted a study in which most respondents (80%) had a clear preference for electricity mixes derived from renewable energy sources, but only 7% of them had already translated their preferences into purchases of green electricity. They found that demographic variables played a marginal

role in explaining the difference. Instead, an analysis of psychographic and behavioral features revealed that adopters tended to perceive consumer effectiveness to be higher, placed more trust in science, tended to estimate lower prices for green electricity tariffs, were willing to pay significantly more for other eco-friendly products, and were more likely to have recently changed their electricity contracts than non-adopters [25]. The fact that many customers exhibit positive attitudes toward a new technology, but only a small percentage of them are willing to adopt it, translates into a high risk of investment for DSOs. This mismatch between how people respond to surveys and their actual choices is a well-known issue for multi-utilities.

The uncertainties related to human choices, particularly in the context of long-term investments, can be addressed by carrying out a series of “*what-if*” scenario assessments and quantifying the propagation of the uncertainties through sensitivity analysis. The need for an integrated approach in studying the human dimensions of a sustainable energy transition that increases our understanding is generally recognized in the scientific community[20]. Hence, the agent-based and bottom-up models developed in this work are best suited to provide these kinds of insight. However, it is worth noting that this work aims not to carry out a socio-economic study, but rather to develop a simulation framework in which behavioral aspects can be quantitatively converted into techno-economic considerations.

1.3 Requirements for the Simulation Model

For a multi-utility, the complexity and risks associated with implementing the energy transition represent economic, technical, and policy barriers that must be overcome. Simulation models facilitate a successful and sustainable energy transition as they provide answers and solutions to policy- and decision-makers by assessing future “*what-if*” scenarios and solving optimization problems. This section details the four requirements that the developed simulation models must satisfy.

1.3.1 Agent-based

The developed simulation framework must be agent-based. Agent-based models (ABMs) are a typology of models in which individual agents - which can include population individuals, dwellings, buildings, or vehicles - autonomously make decisions and interact among each other and with the environment, changing their status to pursue individual targets and goals [26], as schematically illustrated in Figure 1.8.

The most salient characteristics of ABM are that agents:

- Interact and mutually influence each other.

- Learn from experience.
- Adapt their behavior to the environment.

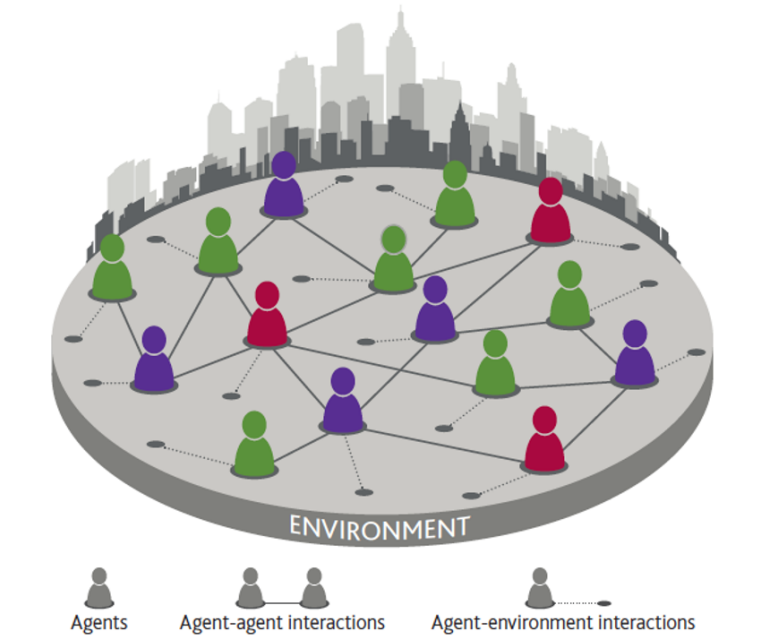


Figure 1.8: Schematic of an agent-based simulation environment. Source: [27]

Agent-based modeling is particularly suitable for developing models that simulate an environment in a life-like fashion. The modeling is achieved by linking agents to behavioral models; thereby, the simulated agents adapt to changes in the environment and the infrastructure through choices. Because of their inherent bottom-up nature, ABMs are best suited for integration into physical bottom-up demand models like those developed throughout this work.

Another advantage of ABMs is that agents can be characterized by a large number of parameters. For this reason, they are particularly indicated for usage with holistic frameworks that require flexibility and consistency in the simulation outputs and allow for the observation of propagation of behaviors at multiple scales [26].

The usage of ABMs in energy demand models has become increasingly established over the years (Section 1.4). The novelty of this work lies in the large scale of agent-based simulations, their combination with purely bottom-up models, and their integration into a high-resolution digital twin, in which the elements have been characterized by real-world data.

The disadvantages of ABMs are related to their complexity and can be summarized as

follows:

- They require a large number of variables to be modeled, calibrated, and validated. These steps are challenging since the availability of reference data is often limited or aggregated on a large scale.
- Due to the interdependence between agents, ABMs usually run on CPUs whose speed can be a limiting factor.
- They assume that agents are rational; therefore, ABMs are not capable of capturing irrational behaviors.

1.3.2 Bottom-up

One of the main requirements of the developed simulation framework for long-term strategic planning is the need to precisely estimate the agent's actual energy consumption. Various modeling techniques can be applied to calculate energy consumption at the city level; these are classified into top-down and bottom-up modeling approaches. The terminology refers to the hierarchical position of data inputs as compared to the sector as a whole. Top-down models *attribute* the total demand to agents based on their characteristics, while bottom-up models *calculate* each agent's energy consumption and aggregate it at an upper level [28].

The top-down approach is unsuitable for planning and modelling the energy transition: It models long-term forecasting in the absence of any discontinuity, whereas the energy transition involves a rupture of people's habits and mentalities and the introduction of new technologies [29]. In other words, top-down models are not able to cope with shock events [26]. Moreover, top-down approaches:

- Tend to have a lower resolution, which is of fundamental importance when modeling urban systems or distribution networks.
- Rely on historical demand profiles and scaling factors that might not be available for a given area.
- Cannot accurately account for changes in society due to changes in demographic structure or individual preferences.
- Do not easily integrate behavioral models.

In contrast, bottom-up models, which determine each end user's contribution to the aggregate value, are more appropriate for modeling an energy transition, as they provide a greater level of detail and the ability to model technological options. They can follow either a statistical or an engineering approach. Statistical methods utilize samples of customers' energy billing information as a data source and combine them with agents'

attributes (such as building age, type, or size). They can account for behavioral patterns; however, they rely on historical data [29].

In bottom-up engineering models, the characteristics of individual agents are used to determine the energy consumption of individuals, buildings, or vehicles through physical models as, for instance, heat transfer calculations [29]. Thus, each element's physical properties need to be modeled - for example the conduction resistances of different building components in the case of buildings. Therefore, bottom-up engineering models are generally computationally intense since they require a significant amount of geometrical and parametric input building data (such as 3D building models). In return:

- They are advantageous in that historical data are not required, whereby historical data are used for calibration and validation.
- They can explicitly account for the behavior of building occupants [28].

1.3.3 Integrated

The third requirement for the simulation models is that the developed models must be integrated into a single simulation framework. When implementing a city-scaled energy transition, a holistic approach is paramount. The investigated energy concept EnK³ itself and the Energy Strategy 2050 pursue a holistic approach by considering the mutual interactions and feedback loops occurring between the areas of heat, electricity, and mobility. These interactions may be more or less noticeable; for example:

- Increased EV penetration may cause an additional load on the distribution grid, which will need to be upgraded in some areas.
- The multi-utility sells both DH and gas; buildings connected to new DH pipelines will no longer buy natural gas, causing revenue loss.
- At a national level, the promotion of renewable energies must be supported by the expansion and optimization of electricity storage.

A silo thinking approach, often found in multi-utilities of a certain size, would result in a suboptimal implementation of the energy transition. Individual departments would try to get the most out of the energy transition for themselves, losing sight of the greater goal.

Most energy models (Section 1.4), regardless of their bottom-up or agent-based approach, fail to provide a holistic picture. By creating a modular architecture in which the developed models are integrated into a single digital twin, the holistic view is ensured while assessing scenarios.

1.3.4 Large-scaled

The simulation framework requirements previously formulated (agent-based, bottom-up, and holistic) generally collide with the need to carry out large-scale assessments. Large-scale population or network simulation (with hundreds of thousands of links and nodes) models that include ABMs, too, are generally constrained by computational power limitations.

However, only large-scaled simulations ensure that the outcomes are realistic and reliable. The reason is self-explanatory: A city cannot be simulated as an island because, for example, its daily traffic does not only start and end within it, but the commuter flows also strain its road infrastructure, the resident population is exposed to migration flows, and energy systems are connected to national grids.

Several studies (Section 1.4) have developed accurate, bottom-up, and behaviorally provided energy models; however, due to their limited scope of application, they are likely to remain academic studies with no practical purpose. This risk can be avoided by ensuring the planning ability of the models developed in this work. For this reason, no aggregations or down-scaling of the elements of the digital twin must occur. In other words, simulations must model each inhabitant of the country, each vehicle traveling along the network, and each building of the investigated city.

1.4 Literature Survey

1.4.1 Electric mobility and EV charging infrastructure

Increase in electric mobility

Worldwide sales of new electric vehicles (EVs) surpassed 1 million units in 2017, a 54% increase compared to sales in 2016 [30]. Indeed, the global stock of EVs is expanding rapidly, having crossed the threshold of 3 million vehicles in 2017. There are several drivers for this transition to EVs, including policies and incentives, cost reductions, and more stringent CO₂ targets for cars. From the perspective of policies and incentives, rebates to EV owners in the state of California, as well as cost-free license plates for EVs in Shanghai, are among the drivers for the transition. The cost of batteries used in EVs is now decreasing faster than historical data suggest [31, 32], and, together with the entry of traditional manufacturers of internal combustion engine vehicles into the EV market [32, 33], substantial cost reductions of EVs entering the market are anticipated. Cities such as Cologne, Hamburg, and Stuttgart, among many others, have undertaken clean city initiatives that limit or entirely ban diesel or petrol cars. Indeed, until now, the growth in the number of EVs has been driven primarily by their urban use [33].

Thus, for cities and, in particular, distribution system operators (DSOs), there are significant challenges in the EV transition. One of the main challenges for DSOs is to anticipate the development in electric mobility and then to adapt, in advance, the infrastructure for the anticipated development. Planning tools that can accurately assess the impact of EVs on the infrastructure and optimize the finances of DSOs to ensure the best benefit-to-cost ratios are required to support a successful transition to EVs. However, the development of such tools is challenging, as EVs' deployment is accompanied by new technologies and changes to current and future EV users' perceptions and habits. Fast chargers, new grid management solutions such as "controlled charging" and "smart charging", and individual preferences in regard to charging at home, work, or public chargers translate into significant economic and technical uncertainties, around which DSOs must make planning decisions for both the short- and long-term.

State of the art of simulation models

Various approaches have been used to assess the impacts of increased EV penetrations. [34] coupled a MARKAL model with a static transportation model to demonstrate that EVs have little effect on the energy system. The behavior of EV users and the characteristics of EVs were assessed on a 34-node IEEE test feeder model in [35], which suggests that peak loads may be of concern. Using two real distribution grids, with assumed charging and driving behaviors of EV users, [36] found that peak hour charging had the most significant impact on the distribution grid. In addition, the placement, size, and operation of public charging stations have been investigated in several different studies. A genetic algorithm technique was used in [37] to determine a layout that minimized the total cost of deploying charging stations. To investigate and optimize the utilization of charging stations, [38] used the formulation of a classic set covering problem. Recently, the optimal layout of multi-types of public chargers, derived using a two-step equivalence method, was investigated [39]. By using a 31-bus distribution system, the overall cost of the EV charging infrastructure could be reduced with the optimal layout. Furthermore, coupled models of the distribution and transportation networks have been used to identify locations of the least expensive charging stations [40]. A K-means clustering method was used to determine the optimal number, location, and capacity of public charging stations that maximize the profits of a distribution system operator [41]. Considering the characteristics and number of EVs and the technical specifications of charging stations, the locations and sizes of charging stations on the Italian highway system were assessed in [42]. Finally, in [43], a Markov chain model coupled with geospatial maps was used to estimate the charging load arising from EVs in a city; three distinct charging profiles (home, work, and other) were modeled and applied to a model of the city of Uppsala, Sweden.

Some previous studies have also focused on issues that arise from EV charging at home.

For example, the coordination of EV charging at homes to avoid grid congestion and voltage problems was examined [44]. As exact forecasting of household loads is not possible, stochastic models of load profiles have been studied to develop optimal charging profiles that minimize the power losses associated with charging EVs at homes [45]. Moreover, [46] developed a stochastic bottom-up model that accounts for socio-economic, technical, and spatial factors and found that uncoordinated EV charging at home profoundly impacts the distribution grid. The economic rationale of EV charging infrastructure has not been extensively studied. In [47], the authors examined the uncertainties of EV rollout and demonstrated that the investment in fast-charging infrastructure is hardly profitable at low EV penetrations. [48] suggests that the needs of specific EV users should be accounted for in the development of networks of standard chargers. Furthermore, [41] argues that a DSO's profits do not necessarily increase with increased EV penetration, as the costs of establishing parking lots are often higher.

1.4.2 Heat demand and district heat

Heat demand of the residential sector

The European Union consumes half of its total final energy for heating and cooling purposes, with space heating and hot water preparation being responsible for 27% and 4% of the total final energy demand, respectively [49]. With more than 2800 TWh consumed per year, the residential sector is the largest consumer of heat, consuming 43% of Europe's heat demand [49]. In 2017, in the EU-28 countries, more than half of this heat was still obtained from fossil fuels, with gas and oil accounting for more than 57% of space heat production and hot water preparation in households [11]. In Switzerland, where 38% of the country's final energy consumption is attributable to buildings for heating, air conditioning, and hot water purposes [50], the residential sector accounts for more than 60% of this, and almost 2/3 of buildings are heated with oil or gas [51]. Aside from Luxembourg, no other European country consumes as much oil per capita for heating purposes as Switzerland [51].

Decarbonization through district heat

One possible way to comply with CO₂ reduction policies is to incentivize the decarbonization of residential buildings with measures aiming to improve the energy efficiency of buildings or support the dismantling of fossil-fuel heating systems [50].

On a municipal level, the extension of DH networks is a way for cities and local multi-utility companies to decarbonize the building stock. District heat has long been considered a resource- and cost-efficient means of supplying heat to buildings and a promising method to mitigate climate change [52]. Connolly *et al.* [52] demonstrated that, by exploiting the potential district heating in the EU, the EU could reach its target of an

80% reduction in annual greenhouse gas emissions by 2050 at a 15% lower cost than in a baseline scenario. However, the potential of district heating is not yet fully exploited, as revealed by Persson and Werner [53]; in fact, the excess heat recovery potential could cover 90% of the total heat demand of residential and commercial buildings in the EU.

Thus, in Switzerland, many cities are currently implementing network extension projects as well [54]. However, for local multi-utilities, this task is accompanied by significant multi-annual investments and uncertainties related to the local building stock's characteristics, the distribution of heat demand over the territory, and the occupants' habits and personal choices. From a city perspective, a significant uncertainty is that there is generally no obligation for buildings to connect to new DH pipelines, because, in general, neither the building owners nor the city has such a legal obligation [54]. To guarantee economic sustainability, DH pipelines should be built in city areas where buildings have both large heat demand and a sufficient likelihood of connecting to the future network and generating revenues.

Bottom-up models for heat demand calculations

In bottom-up models, the characteristics of individual buildings are used to determine their energy consumption. Thus, buildings' physical properties, such as the conduction resistances of different building components, need to be modeled. Perez *et al.* [55] compiled a comprehensive set of physical properties of building walls, roofs, and windows, from which conduction resistances were inferred in this work. Cesaratto and De Carli [56] evaluated the correlation between design and in situ-measured conduction resistances and found that the differences in heat demand ranged from 11–14%. Convective heat transfer coefficients for external building surfaces are a function of building geometry, surroundings, facade roughness, local airflow patterns, and temperature differences [57]. Liu *et al.* [58] found that the total heating energy consumption within similar-sized urban neighborhoods varies as much as 32% in a dense city compared to a less dense city because of the different magnitudes of convective heat transfer from exterior building surfaces due to the effects of shading and wind sheltering. Mirsadeghi *et al.* [57] provide an extensive review of convective heat transfer coefficient models for bottom-up modeling of heat demand and identify their applicability range; most models define the convective heat transfer coefficient as a function of a reference wind speed.

Behavior of building occupants: Agent-based and other modeling techniques

Bottom-up demand models can explicitly account for the behavior of building occupants [28]. In recent work, people's social and behavioral aspects have been integrated into energy models, generally with stochastic heat demand models [59]. One approach uses random patterns of occupancy, for instance, by applying Monte-Carlo algorithms that randomly assign parameters from probability distributions of empirically observed data

[60]. Another approach, proposed by McKenna [61], is to use a first-order Markov chain to stochastically model the occupancy and activity of the building occupants. Heterogeneous Markov chains were also used in [62] to model individuals' activity patterns to quantify the electricity consumption in an average American household. An alternative approach is to use activity-based models, whereby the modeling of occupancies and activities is based on time-use surveys [60]. Subbiah *et al.* [63] used logistic and Poisson regressions of survey data to model the total household energy demand based on the building occupants' energy-consuming activities. A limitation of stochastic models is that, as the models are based on historical data, such models cannot account for events – such as climate change or the introduction of new technologies – that have not previously occurred.

On the other hand, ABMs can account for the heterogeneity in the heat demand and capture the interactions between different system components. Azar and Menassa [64] used an agent-based approach to model building occupants' behavior to determine a single commercial building's energy demand. Similarly, Bustos-Turu *et al.* [65] used the behavior of building occupants derived from an ABM to assess the heat demand in different zones of an urban area. However, the heat demand was determined in a manner similar to that of the traditional heating degree day method. Finally, Chingcuanco and Miller [66] coupled an agent-based choice model with a building energy simulation software to stochastically simulate residential space heating demand.

1.5 Novelty of the Present Study and Thesis Goals

This work focuses on the three pillars that commonly sustain a city's energy transition: electricity, heat, and mobility infrastructure. It investigates their role in the energy transition with the intent to assess and minimize the uncertainty that accompanies the implementation of energy policy in the next 10 to 30 years.

More precisely, the following elements of energy transition are investigated in detail:

- *Mobility*: the technical and financial consequences of a larger penetration of EVs.
- *Heat*: the implementation of the extension of the DH network.
- *Electricity*: the impact of population dynamics on the electrical distribution grid.

It is evident from the aforementioned literature that a variety of behavioral, economic, technological, and sociological factors are driving the urban energy transition. This complexity applies, for example, to the EV transition and the decarbonization of the building stock. The literature survey indicates that a comprehensive simulation framework that integrates agent-based, bottom-up, holistic, and large-scale energy demand models into

a highly resolved digital twin is still missing.

In this Ph.D. project, to holistically plan and assess a successful energy transition, three novel bottom-up physical models of demand (electricity, heat, and electric mobility) have been fully coupled and applied to an integrated digital twin of a mid-sized town, which was developed during the Ph.D. project. The digital twin provides high temporal resolution and spatial granularity (individual buildings and low-voltage network elements) and builds an integrated and holistic framework that allows for addressing “*what-if*” scenarios and optimization problems, where large databases from different sources are bridged together.

Human behavior patterns have been included in all developed models through the extensive use of large-scale (country-wide) agent-based simulations to ensure realistic assessment of future scenarios and, in particular, to account for future population dynamics and mobility needs. Moreover, smart meter data analysis results and other measurements have been applied to calibrate and validate the developed models. Additionally, four tools are included in the developed framework:

- A power flow simulation tool that, for the first time, has been used to simulate the low-voltage distribution grid of the investigated city.
- A predictive algorithm to quantify via machine learning the willingness of building owners to connect to future DH pipelines.
- A routing algorithm for future DH pipelines to maximize revenues for the multi-utility.
- A model for the optimal placement of an EV charging infrastructure.

Thus, the **main objectives** of this research are as follows:

- To study the impact of individuals' characteristics and behaviors on the techno-economic consequences for a city going through an energy transition.
- To quantify the sensitivity associated with the developed bottom-up models' input variables on the techno-economic consequences of the energy transition.
- To assess how agent-based, holistic, and data-driven model predictions compare with norm-based top-down approaches.
- To understand how agent-based, holistic, and data-driven predictions can help overcome economic, technical, and policy barriers to the energy transition.

Chapter 2

Methodology

2.1 Extension and Improvement of the *EnerPol* Framework

EnerPol is a bottom-up integrated simulation framework that has been in development since 2009 at the Laboratory for Energy Conversion (LEC), which is used to support strategic decision making through data-driven and scenario-based assessments. Originally, *EnerPol* was used primarily for the performance evaluation of gas and electric infrastructure. The extensive and granular database and the physical models' resolutions provided by the gas and electricity models guarantee a high spatial and temporal resolution. Many studies have proven the suitability and the accuracy of *EnerPol* to model large-scale interconnected systems:

- Singh *et al.* presented an integrated approach of geographically indexed electricity production, demand, and grid modeling for large-area power systems and applied *EnerPol* to assess wind power development in Switzerland [67].
- Eser *et al.* extended *EnerPol* with a gas system model, which captures the market behavior of both gas traders and gas system operators, as well as investigated the impact of the new gas pipeline *Nord Stream 2* on gas trade and security of supply in the European gas network [68].

Moreover, *EnerPol*'s modular architecture and the integration of all developed models into a single digital twin ensure the capability of *EnerPol* to provide a holistic view in the scenario assessment. The following are some examples of holistic assessments carried out with *EnerPol* and their findings:

- Eser [69] demonstrated that the increased penetration of renewables in 2020 will

induce an increase in the number of starts of conventional plants and that the number of load ramps significantly increases by 63–181%, which underlines the need for action for equipment manufacturers and utilities.

- Eser [70] also showed that increased penetration of EVs in Europe with the current electricity generation mix would imply that 65% of the electricity used to charge the EVs is produced by conventional power plants. Consequently, the intrinsic CO₂ emissions of EVs are found to be up to 25% higher than those of gasoline cars. Therefore, the decarbonization of personal transport requires more effort than simply promoting the sales of EVs.
- In the development of an agent-based mobility model, Saprykin [71] illustrated how only a holistic and integrated approach that combines different elements (population synthesis, job assignment, car ownership, and mode choice models) is capable of generating a realistic synthetic population and agents' daily plans for a large-scale scenario.

More recently, *EnerPol* has been extended by three large-scale ABMs: a population model, a daily activity model, and a mobility model, illustrated in detail in Section 2.4. These models have allowed a paradigm shift in the modeling of individuals within *EnerPol*. For example, an agent-based daily activity model simulates the daily routine of all inhabitants of a given domain. The top-down approach previously used in *EnerPol*, in which, for example, electricity demand, obtained from historical time series, was distributed and then up-down-scaled to simulate future scenarios, does not lend itself to simulations of urban systems. The ABMs were used to carry out assessments of transportation infrastructure [72, 73], land use, and urban development [74, 75].

Therefore, *EnerPol* provides an initial framework suitable to support an urban energy transition as it satisfies the previously stated requirements for a simulation framework: agent-based, bottom-up, holistic, and large-scale. In this work, the *EnerPol* framework has been extended and improved to enhance its capabilities to model energy transitions at a city-scaled level. Furthermore, the new models are demonstrated using the digital twin of an entire city; GPUs' architecture is used to overcome the large computational requirements.

For the project to proceed systematically, the four overall phases of the project were dictated by the existing *EnerPol* structure, well established in the past ten years of development at LEC. The *EnerPol* structure is based on four pillars: Data, Models, Scenarios, and Results Aggregation, as schematically represented in Figure 2.1. Data digitally represent the infrastructure, the environment, the energy, mobility, and the economic systems, and the population of the investigated area. In *EnerPol*, data constitute the foundation of models, and their quality is essential to guarantee accurate simula-

tions. Models interlink the data to assess “scenarios” for decision makers. “Results” are then aggregated to be displayed to different audiences.

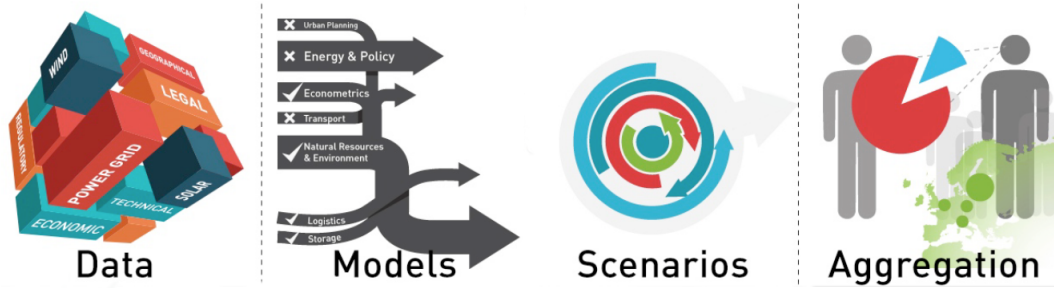


Figure 2.1: Schematic of *EnerPol*’s four pillars on which the *EnerPol* framework is based.

To manage a large number of variables, the high temporal resolution, the level of detail of the simulation domain, and the resulting large number of agents, the models were developed and run on the hybrid CPU-GPU architecture that has recently been incorporated into *EnerPol* [26]. Thanks to the hybrid CPU-GPU architecture, no aggregations or down-scaling of the digital twin elements occurred in this work. In other words, each inhabitant of the country, each vehicle traveling along the network, and individual buildings of the investigated city are modeled.

2.2 Methodology Outline

Following the previously explained *EnerPol* structure, this project’s methodology is hereby presented as it was developed and applied:

1. *Data*: The creation of a real digital twin of the built infrastructure, the analysis of real measurements data from low-voltage transformers and smart meters, and a tool to run power flow simulations of the low-voltage grid are presented in Section 2.3
2. *Models*: The integration into the digital twin of various large-scaled ABMs of population, daily activities, and mobility simulations is presented in Section 2.4
3. *Models*: The methodology applied in the development of the new agent-

based bottom-up demand model for electricity, heat, and electric mobility is presented in the case study Chapters 3, 4, and 5 (specifically in Sections 3.1, 4.1, and 5.1)

4. *Scenarios*: The scenarios investigated in the case studies are detailed in Sections 3.2, 4.2, and 5.2.
5. *Results and Aggregation*: The results of the case studies are presented in the respective chapter sections (3.3, 4.3, and 5.3).

2.3 Digital Twin Development

2.3.1 Geo-referenced built infrastructure

An actual and comprehensive digital twin of the investigated city's energy and urban infrastructure was developed in this project; Figure 2.2 shows an example detail of the digital twin. The model functions as a digital twin of the city and interfaces the geo-referenced highly resolved datasets with the agent-based and bottom-up physical models. The usage of geo-referenced data, particularly of the ESRI shapefile format – a geospatial vector data format for geographic information system (GIS) software – facilitates the identification of interdependences between databases.

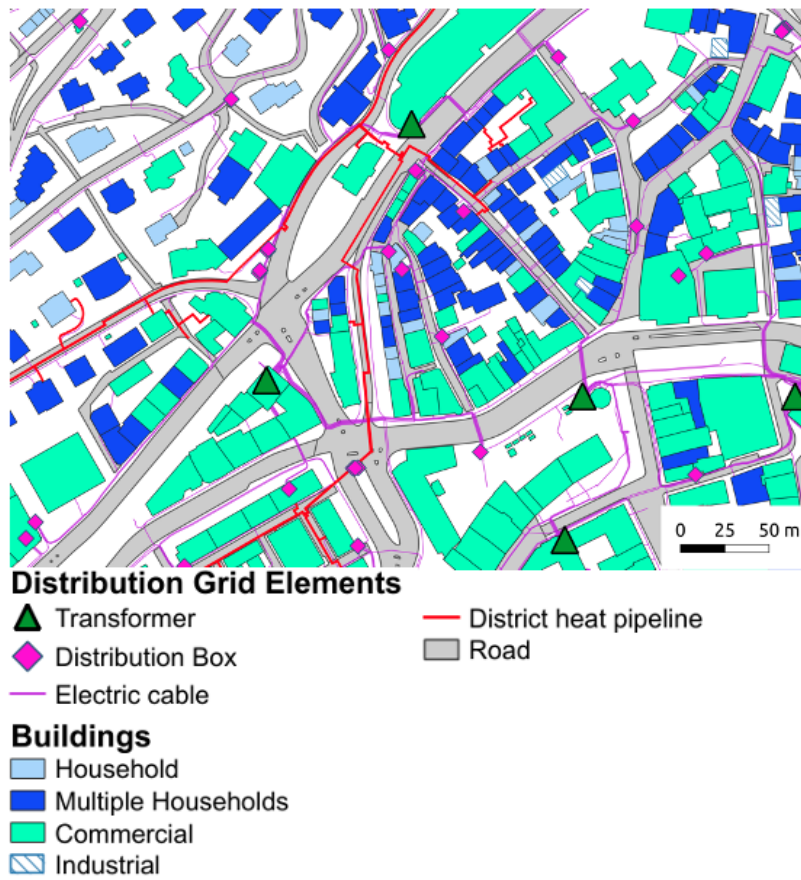


Figure 2.2: Detail of the digital twin with elements of the energy and the urban infrastructure

The following tables summarize the geo-referenced datasets that were included in the digital twin. Table 2.1 and Table 2.2 detail the geo-referenced datasets utilized to model the city's real estate and mobility infrastructure, respectively. Table 2.3 and Table 2.4 describe the geo-referenced datasets utilized to model the city's electricity and DH infrastructure, respectively. More details on the datasets' attributes are explained in the methodology sections of the respective case studies. The tables specify the datasets' source: Seven datasets contain proprietary data and were made available by the multi-utility *sgsw*. These data were verified and standardized to comply with *EnerPol* standards. The other datasets are part of the *EnerPol* database and were obtained from open-source data sources and federal registers.

The geo-referenced digital twin of the city's real estate contains 14,000 buildings' roof print areas and the respective building heights; the building geometry is approximated to prisms with the roof surface parallel to the basis. A set of architectural (height, perimeter, build year, renovation year) and functional attributes (typology, ownership, end-use, purchase value, garage availability) characterizes each building. The buildings' functional attributes were either obtained from the land surveying office of the city of St. Gallen or official federal registers (Federal Register of Buildings and Dwellings and Federal Register of Commercial Activities). Each building is also characterized by an energy-demanding area in m^2 , and annual electricity and heat consumption data were obtained from the multi-utility customer database.

The geo-referenced digital twin of the city's mobility infrastructure contains 230 km of primary, secondary, tertiary, and residential roads; the locations of 7,045 public and private parking lots; and the locations of the existing 11 parking lots with public chargers with a total of 23 chargers (year 2018).

The geo-referenced digital twin of the city's distribution grid includes, among others:

- 15,391 power lines: 9 high-voltage (110 kV) cables, 291 middle-voltage (10 kV) cables, and 15,091 low-voltage (400 V) cables
- 192 transformers
- 1,216 smart meters

The geo-referenced digital twin of the city's DH network includes 50 km of DH supply pipelines in operation and 3 DH plants.

Table 2.1: Description of the geo-referenced database included in the digital twin of the investigated city to model the city’s real estate

Category		Dataset	Attributes	Resolution		Data Source
				Spatial	Temporal	
Urban infrastructure	Real estate	Buildings	<ul style="list-style-type: none"> • Geometric attributes • Architectural attributes • Functional attributes • Energy demand measurements 	<ul style="list-style-type: none"> • Individual buildings • 0.2-1.5 meters 	<ul style="list-style-type: none"> • Year 2019 	<ul style="list-style-type: none"> • Land surveying office of city of St. Gallen [76] • Federal office of topography (<i>swisstopo</i>)
		Garages	<ul style="list-style-type: none"> • Location 	<ul style="list-style-type: none"> • Individual private and public garages 	<ul style="list-style-type: none"> • Year 2018 	<ul style="list-style-type: none"> • Land surveying office of the city of St. Gallen [76]
		Federal Register of Buildings and Dwellings	<ul style="list-style-type: none"> • Resident attributes • Household attributes • Dwelling attributes 	<ul style="list-style-type: none"> • Individual buildings 	<ul style="list-style-type: none"> • Year 2015 	<ul style="list-style-type: none"> • Federal registers [77, 78]
		Federal Register of Commercial Activities	<ul style="list-style-type: none"> • Building end-use • Job properties 	<ul style="list-style-type: none"> • Individual buildings 	<ul style="list-style-type: none"> • Year 2013 	<ul style="list-style-type: none"> • Federal register [79]

Table 2.2: Description of the geo-referenced database included in the digital twin of the investigated city to model the city’s mobility infrastructure

Category		Dataset	Attributes	Resolution		Data Source
				Spatial	Temporal	
Urban infrastructure	Mobility	Roads	<ul style="list-style-type: none"> • Geometric attributes • Functional attributes 	<ul style="list-style-type: none"> • <5 meters [80] 	<ul style="list-style-type: none"> • Year 2019 	<ul style="list-style-type: none"> • Open street maps [81]
		Parking lots	<ul style="list-style-type: none"> • Ownership • Location • Capacity 	<ul style="list-style-type: none"> • <5 meters 	<ul style="list-style-type: none"> • Year 2018 	<ul style="list-style-type: none"> • Land surveying office of the city of St. Gallen [76]
		Existing EV public chargers	<ul style="list-style-type: none"> • Location • Capacity 	<ul style="list-style-type: none"> • Aggregated at parking lots 	<ul style="list-style-type: none"> • Year 2018 	<ul style="list-style-type: none"> • Own research

Table 2.3: Description of the geo-referenced database included in the digital twin of the investigated city to model the city’s electricity infrastructure

Category		Dataset	Attributes	Resolution		Data Source
				Spatial	Temporal	
Energy infrastructure	Electricity	Electrical distribution grid	<ul style="list-style-type: none"> • Distribution lines • Network elements: substations, transformers, distribution boxes, house connections 	<ul style="list-style-type: none"> • Individual line segments • Individual network elements 	<ul style="list-style-type: none"> • Year 2017 	<ul style="list-style-type: none"> • <i>sgsw</i> [17]
		Smart meters	<ul style="list-style-type: none"> • Real power consumption with a time resolution of 15 minutes 	<ul style="list-style-type: none"> • Individual customers 	<ul style="list-style-type: none"> • April 2015-April 2017 	<ul style="list-style-type: none"> • <i>sgsw</i> [17]

Table 2.4: Description of the geo-referenced database included in the digital twin of the investigated city to model the city’s DH infrastructure

Category		Dataset	Attributes	Resolution		Data Source
				Spatial	Temporal	
Energy infrastructure	Heat	District heat pipelines	<ul style="list-style-type: none"> • Geometric attributes • Functional attributes 	<ul style="list-style-type: none"> • Individual line segments • Individual pipeline elements 	<ul style="list-style-type: none"> • Year 2018 	<ul style="list-style-type: none"> • <i>sgsw</i> [17]
		District heat plants	<ul style="list-style-type: none"> • Location • Power production with a time resolution of 15 minutes 	<ul style="list-style-type: none"> • 1 waste incinerator & 2 district heat plants 	<ul style="list-style-type: none"> • January 2013-May 2018 	<ul style="list-style-type: none"> • <i>sgsw</i> [17]

2.3.2 Transformers data analysis

The distribution grid of St. Gallen comprises 192 transformers on grid level 6 that connect the mid-voltage grid (10 kV, grid level 5) to the low-voltage grid (400 V, grid level 7). A power quality system for fault analysis and monitoring of power quality tracks the power flow through 17 transformers that supply to different city areas. Therefore, the power flow measurements were aggregated for clusters of, on average, 75 buildings of various types. The measurements had a time resolution of 15 minutes and covered the period from November 2018 to May 2020. The locations of the transformers with available measurements are displayed in Figure 2.3, and Figure 2.4 presents an example power demand profile of a period of one year for a transformer located in a residential area. The supplied demand had a time resolution of 15 minutes and followed a daily and a seasonal trend: The demand peak over a day was reached at 18:00, and the demand for summer months was lower than in other months because heat pumps and other electric heating systems were not used, and building occupants spent less time at home during dark hours. Moreover, demand drops due to school holidays are visible. The demand drop to 0 kW in March was due to a temporary change in network switch status.

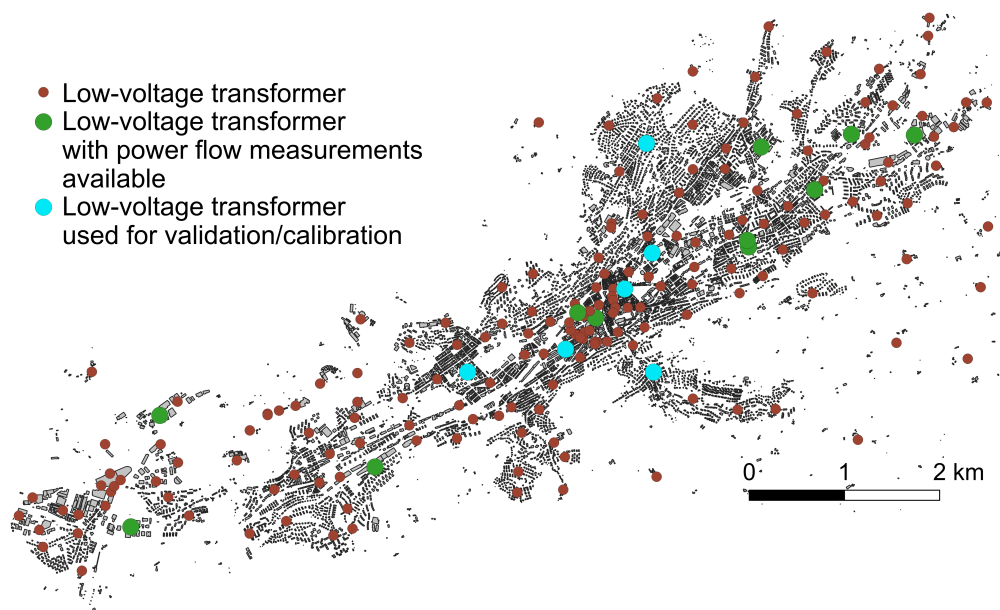


Figure 2.3: Map of low-voltage transformers with indication of power flow measurement availability.

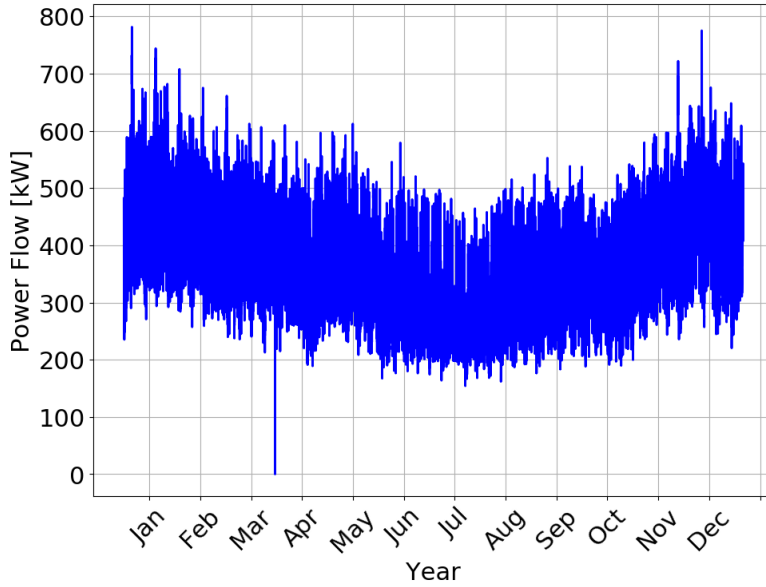


Figure 2.4: Annual aggregated power demand at a low-voltage transformer in a residential area in grid level 7 with a time resolution of 15 minutes (source: Power Quality System of *sgsw*).

The mid- and low-voltage distribution network's digital twin was applied to determine which buildings were connected to a specific transformer. Figure 2.5 illustrates an example topography of the network layout around a transformer. A correct allocation of buildings to the supplying transformer was crucial to correctly interpret the calibration and validation results of power flow simulations. The electricity demand of a building is not necessarily supplied by the closest transformer since the distribution network depends on the city's topography; in addition, it includes redundant pathways (mesh network). Therefore, the allocation of buildings was not based on nearest neighbor searches but on the actual network topography as modeled in the SQL network database of the multi-utility, which had been imported into the digital twin.

Power flow simulations were used to simulate the demand at transformers to verify both the functioning of the digital twin and the results of the electricity demand model. Six of the transformers for which power flow measurements are available were used in the calibration and validation of the electricity demand model.

2.3.3 Smart meter data analysis

The smart meters installed in the city track the real power consumption of 13 typologies of customers with a frequency of 15 minutes. The measurement pool consisted of 1,216 customers of various types, as reported in Table 2.5. The total measurement duration

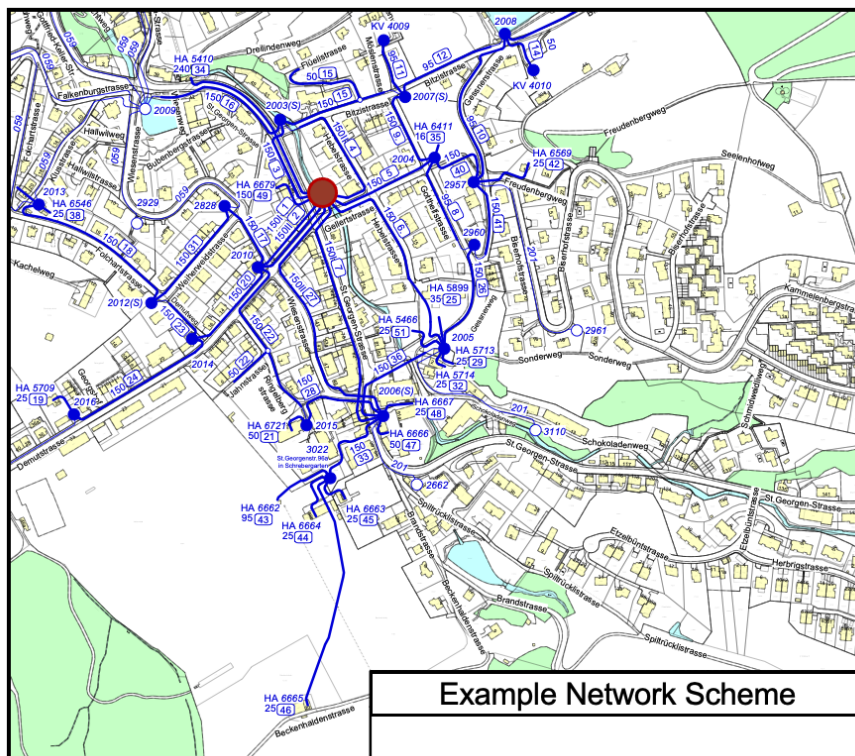


Figure 2.5: Example of low-voltage network topography around a low-voltage transformer (brown circle) as it is modeled in the digital twin; blue circles are network nodes placed at a lower hierarchical level in the network.

covered the period from April 1, 2015 to April 30, 2017. Nevertheless, the measured time for an individual customer may be shorter. Each smart meter is uniquely identified with an anonymized 33-digit code and, in the case of St. Gallen, by a city address. The address was used to geo-reference all measuring points. Subsequently, through a nearest neighbor search algorithm (*cKD-Tree*), a building was assigned to each smart meter; in this way, each smart meter could be characterized with the following characteristics:

- Building end-use: household or, for other kinds of buildings, NACE code of level 1 for economic activities, as reported in Table 2.5
- Energy-consuming area [m²]

In addition to the smart meters from the city of St. Gallen, a second pool of measurements was made available by the *Elektrizitätswerke des Kantons Zürich (EKZ)*. This second measurement pool consisted of 4,630 customers of various types, as also reported in Table 2.5. For all customers, the total measurement duration covered the year 2016. The time resolution of the power demand in kW was 15 minutes. Unlike the first measurement pool, the measurements were fully anonymized and could not be geo-referenced. An official *EKZ* classification was made available and used.

A single shared pool was created to increase the number of available customers and the results' representativity. To allow the merge, both *sgsw* and *EKZ* categories were converted into NACE codes of level 1. All customers who behaved as “prosumers” (meaning that they did not only draw electricity from the grid but also fed self-produced electricity back into the network) were filtered out from the shared pool.

An automatized pre-processing analyzed the quality of the available yearly time series day by day. Due to flawed or missing data, primarily as a result of technical problems with the smart meters, not all time series could be used. Flawed/missing data were substituted, when possible, with interpolated data. With a set data quality criterion (maximum 5% of missing/flawed data per day), about 15.7% of data needed to be discarded. In particular, 44.4% of data on households needed to be discarded. Measurements from building categories “Energy”, “Construction”, and “Real Estate” were also not used because the number of accepted time series was too little to guarantee representativity.

The results extracted from the analysis were typical normalized power demand profiles and baseload distributions for the 13 customer typologies reported in Table 2.5. Both outcomes were used to calibrate the electricity demand model presented in Chapter 5.

Typical normalized power demand profiles

The normalization for N customers of the same customer typology took place according

Table 2.5: Categorization and quality assessment of smart meter data delivered by St. Gallen and EKZ.

	Customers		Accepted Yearly Time Series	Acceptance Ratio [%]	Typical power demand profiles implemented
	sgsw	EKZ			
Household	361	300	1383	55.6	No
Agriculture	0	61	57	93.4	Yes
Manufacturing - Industrial	67	379	537	92.6	Yes
Energy	11	9	28	66.7	No
Water Supply, Sewerage, Waste Management	4	45	50	87.7	Yes
Construction	4	4	12	75	No
Wholesale, Retail	128	540	884	95.7	Yes
Transportation, Storage	0	34	33	97.1	Yes
Accommodation, Food Services	17	294	338	98	Yes
Financial and Insurance Activities	0	29	27	93.1	Yes
Real Estate	4	0	8	66.7	No
Scientific, Technical	0	35	34	97.1	Yes
Public Administration	9	5	89	96.7	Yes
Education	59	150	301	92.1	Yes
Health	11	84	111	94.9	Yes
Entertainment, Recreation, Arts	69	89	263	88.9	Yes
Offices and Other Services	382	230	1285	93.4	Yes
Total categorized customers	1126	2288	7727	84.3	-
Total uncategorized customers	90	2342	-	-	-

to Equation 2.1, where nDF stands for normalized power demand factor.

$$nDF = \frac{1}{N} \sum_{n=1}^N \frac{demand(t)}{\overline{demand}} \quad (2.1)$$

Normalized power demand factor curves were defined for a period of one year. Figure 2.6 illustrates the trend of normalized power demand factor over one average year for customers belonging to the “Education” category. The demand dropped over the summer; school holidays were clearly visible and were therefore accounted for in modeling power demand in the electricity demand model. Figure 2.7 provides some examples of normalized demand factors over an average week for customer typologies “Manufacturing/Industrial” and “Education”. The electricity demand dynamic was strictly related to the type of activity: For example, in industrial customers, the peak-to-base ratio over the workweek was always smaller than $1.4/1$, while it was $2.7/1$ for customers belonging to the “Education” category.

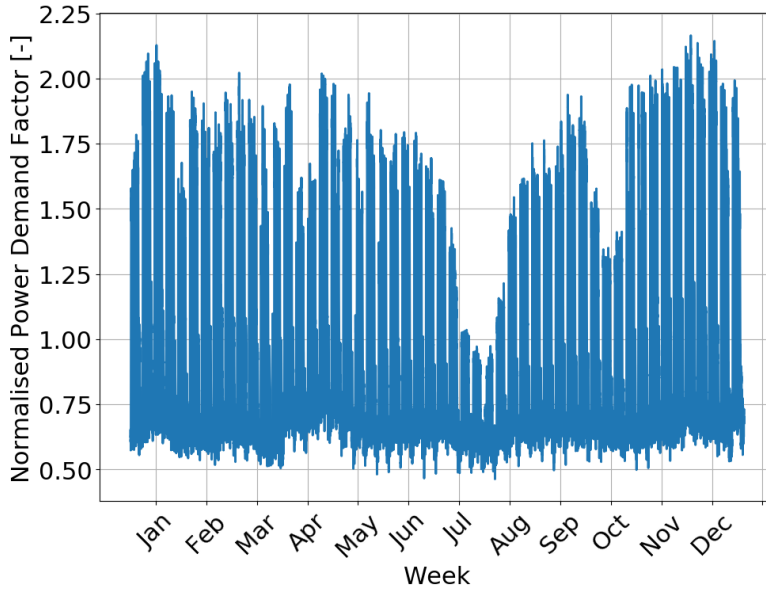


Figure 2.6: Normalized power demand factor over an average year for customers belonging to “Education” category calculated from smart meter measurements.

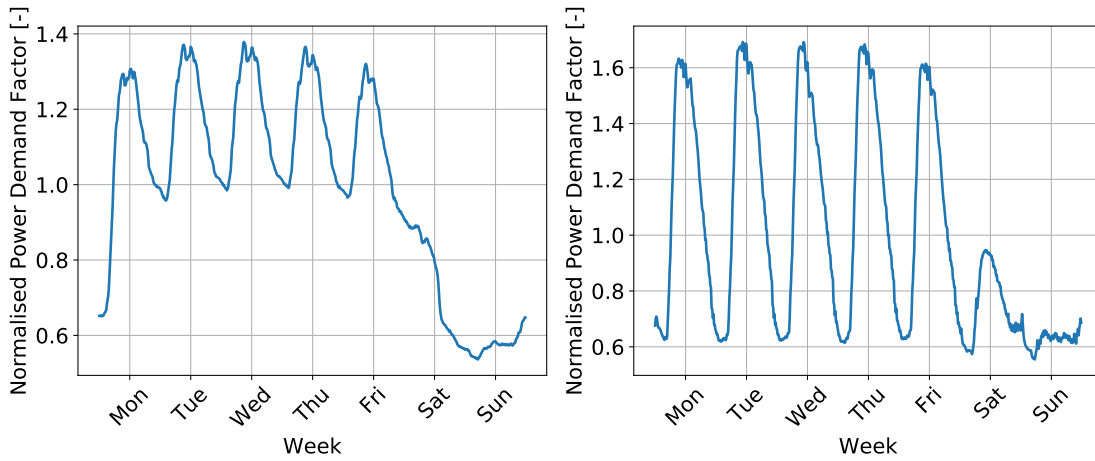


Figure 2.7: Normalized power demand factor over an average week for industrial customers (left) and customers belonging to “Education” category (right) calculated from smart meter measurements.

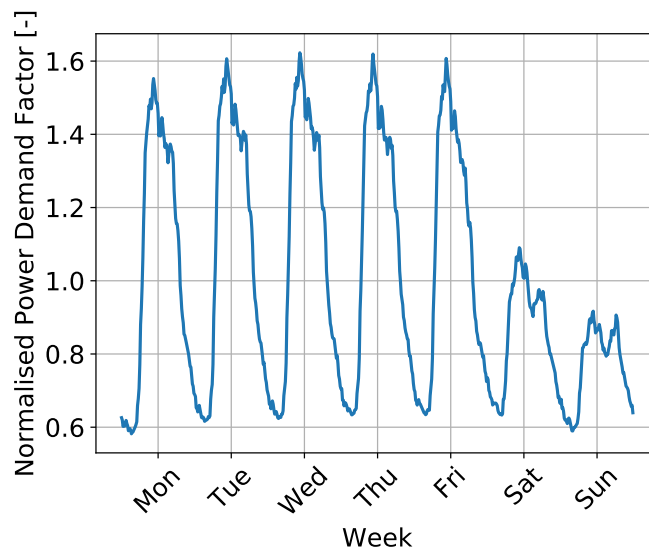


Figure 2.8: Normalized power demand factor over an average week for households calculated from smart meter measurements.

To evaluate a specific power demand factor's representativity, the standard Pearson correlation factor between the typical trend and the available trends used to define it was calculated. The mean absolute error (MAE) between the typical trend and the available trends was also calculated. The resulting values are reported in Table 2.6. This data indicates whether the defined typical power demand factor was representative for its customer category or whether the variance between customers' demand profiles was too large to obtain any representative trend. For customers belonging to the categories "Manufacturing/Industrial", "Wholesale/Retail", "Accommodation", "Scientific/Technical", "Education", "Health", and "Entertainment", the typical load profiles were found to be representative and would be used in the electricity demand model. For the "Households" category (Figure 2.8), that was not the case: A correlation factor of 0.12 and MAE 0.76 suggest that different households show very different demand patterns. This inhomogeneity is due to different family sizes, compositions, ages, preferences, daily routines, and other household characteristics. Hence, accurate modeling of electricity demand for households necessitates the inclusion of individuals' preferences and choices, which provides an argument for the development of an agent-based electricity demand model.

Table 2.6: Assessment of representativity of typical normalized power demand profiles obtained from smart meter data analysis – by customer category

	Variability of Demand		Typical power demand profile implemented in electricity demand model?
	Average Correlation Coefficient [-]	Average Normalized MAE [-]	
Household	0.12	0.76	No
Agriculture	0.11	0.77	No
Manufacturing/Industrial	0.53	0.56	Yes
Water Supply, Sewerage, Waste Management	0.05	0.44	No
Wholesale, Retail	0.65	0.41	Yes
Transportation, Storage	0.17	0.32	No
Accommodation, Food Services	0.48	0.46	Yes
Financial and Insurance Activities	0.38	0.37	No
Scientific, Technical	0.58	0.2	Yes
Public Administration	0.54	0.36	Yes
Education	0.61	0.43	Yes
Health	0.69	0.3	Yes
Entertainment, Recreation, Arts	0.43	0.54	Yes
Offices and Other Services	0.6	0.45	Partially

Distribution of baseload demand, normalized to the surface area in m^2

When defining the baseload distributions, it must be noted that only *sgsw* smart meter data can be geo-case studied and, therefore, linked to a building for which the energy-consuming area is known. Thus, *EKZ* smart meter data were not used to obtain baseload distributions. From the baseload distributions, baseloads outside the 90% percentile were discarded as they did not represent typical customers. Figure 2.9 provides examples of baseload demand distributions calculated on a yearly basis for customers belonging to categories “Education” and “Wholesale/Retail”. The standard deviation of the distribution for customers belonging to “Education” was smaller than that of “Wholesale/Retail”, indicating that the former category presents more homogeneous demand patterns; the electricity demand model considers these aspects.

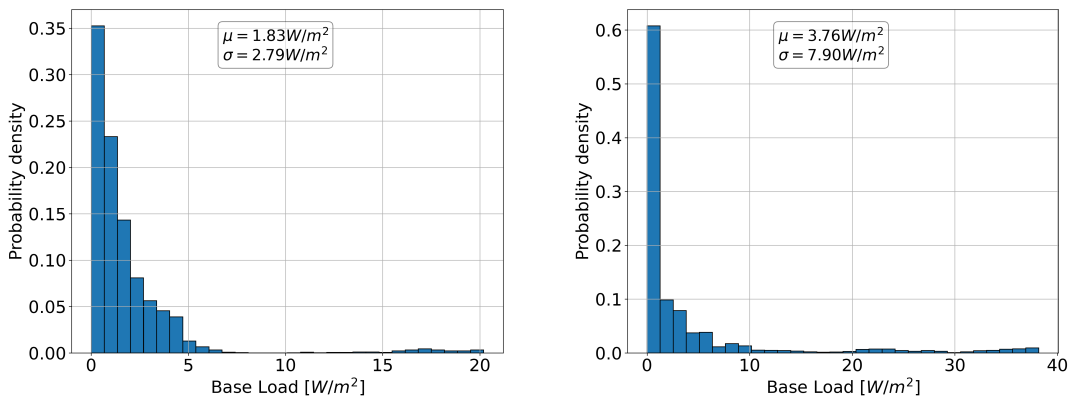


Figure 2.9: Distribution of base loads normalized with energy-consuming area for customers belonging to category “Education” (left) and category “Retail” (right) calculated from smart meter measurements with indication of average value and standard deviation.

The peak-to-base ratios for weekdays and weekends, as well as the baseload distribution’s mean and standard deviation values, calculated on the 0–90% percentile range, are reported in Table 2.7. The results are reported only for customer categories whose typical power demand load profiles have been implemented in the electricity demand model. For the sake of completeness, Table 2.7 also reports the baseload distribution’s mean and standard deviation values calculated over all available measurements.

Table 2.7: Results of the analysis of smart meter measurements: (i) Peak-to-base ratios for weekdays and weekends, and (ii) baseload distribution's mean and standard deviation values for customers categories whose typical power demand load profiles have been implemented in the electricity demand model

	Peak-to-base Ratio		Base Load [W/m ²]			
			90% Percentile		All	
	Weekdays	Weekends	μ	σ	μ	σ
Household	2.8	1.9	1.4	1.8	2.3	5.4
Manufacturing/Industrial	1.6	1.7	4.6	8.9	13.9	51.8
Wholesale, Retail	4.5	3.8	3.8	7.9	6.2	13.2
Accommodation, Food Services	2.3	2.1	4.1	2.9	4.5	3.4
Scientific, Technical	1.3	1.1			n/a	
Public Administration	2	1.5			n/a	
Education	3.1	1.8	1.8	2.8	4.4	13.4
Health	2.4	1.7	9.8	23.0	15.5	33.4
Entertainment, Recreation, Arts	2.8	2	1.9	1.8	2.4	2.7
Offices and Other Services	3.4	2.5	2.1	2.7	3.9	11.7

2.3.4 Power flow simulations of the low-voltage grid

Variations in electricity demand – both in magnitude and time dynamics – as predicted by the electricity demand model presented in this work were investigated using power flow simulations of the low-voltage network.

Power flow modeling is generally recognized as an essential tool for investors and policymakers to support the development of energy technologies, power security and trade, and policymaking [67]. When the high temporal and spatial resolutions provided by the bottom-up and the ABMs are combined with power flow modeling, the consequences of the energy transition on the grid can be precisely assessed by identifying lines that necessitate an upgrade due to increased load. The consequences of the electrification of mobility or the decarbonization of heating systems are particularly significant at the distribution level [82, 83].

The predicted normal steady-state operation of a power system can be analyzed by numerically determining, among others, the magnitude and phase angle of the voltage at each bus, as well as the real and reactive power flowing in each line. Figure 2.10 illustrates a typical result of power flow simulations (*i.e.*, the day-averaged line loading as a percentage of the individual lines' loading limit). Thereby, the cables' thermal limit was chosen as the constraint for the maximum available power flow. More details on the approach used in *EnerPol* to model power flow simulations can be found in [67]. It must, however, be noted that the approach applied in this work differentiates from previous *EnerPol* simulations:

- The simulated network was a mid- to low-voltage distribution grid instead of a high-voltage transmission grid.
- The electricity demand was modeled in a bottom-up way instead of being allocated according to a top-down approach.
- The generation of electricity was not accounted for in the digital twin; hence, power flow simulations, rather than optimal power flow simulations, were carried out.

All distribution grid elements needed to run power flow simulations were included in the digital twin and were used in combination with the Python-based open-source power flow solver *pandapower* [84], which combines the data analysis library *pandas* and the power flow solver PYPOWER. The solver was applied at a quarter-hourly time resolution. Since some distribution grid elements could not be univocally identified and characterized, the demand at some distribution boxes (15.4% of the city's total demand) could not be precisely allocated when defining the power flow simulation problem. This missing demand has been homogeneously distributed over the city domain. However, it is worth noting that these results represent the first full-scale simulations of the low-voltage

distribution grid ever carried out in the investigated city.

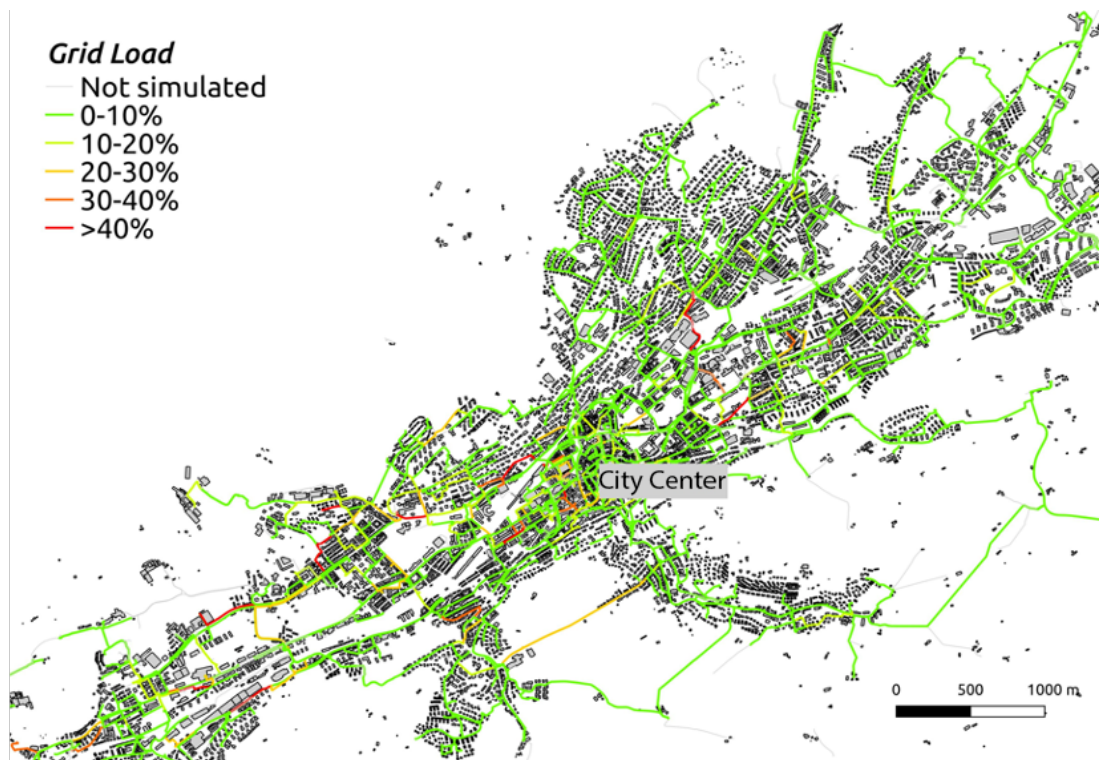


Figure 2.10: Day-averaged line loading as % of the line thermal limit in the city's low-voltage distribution grid.

2.4 Agent-Based Models

Three existing *EnerPol* agent-based models (ABMs) – population, daily activities, and mobility- were used and extended with the ABMs developed in this work. For completeness, salient features of these three models are presented in this section.

The existing *EnerPol* ABMs have been extended to make them suitable for simulating the urban energy transitions. Two main extensions have been made:

- In the electricity and heat case studies, the agent activities occurring inside the buildings needed to be accounted for to predict the electricity and heat demand at home or at the workplace. These activities, simulated with a 15-minute temporal resolution, include being at home, sleeping, cooking, and washing. The modeling approach, applied in both the electricity and the heat demand model, is based on reservoir-based variables and probability distributions calibrated on survey data.

- In the mobility case study, EV users' preferences and charging behaviors needed to be accounted for when designing an EV charging infrastructure.

The modeling details and the specific utilization of the extended ABMs are explained in the respective case studies.

2.4.1 Agent-based population model

In the agent-based population model [26, 74, 75, 85], a synthetic population of individual agents is generated from population statistics at the municipal level and housing stock and activities databases. Characteristics such as total population, age distribution, income distribution, household structure, and employment status are among the population statistics. Examples of individual agents' activity locations in the synthetic population include office workplaces, shops, or schools. Each agent is linked to a household and is assigned a dwelling and, if relevant, a workplace. The demographics and the activity locations of each agent provide the basis for generating the activity-based demand, which comprises a set – typically three – of daily activities for each agent; each daily plan consists of travel start times, destinations, and the preferred mode of transport. The characteristics of individual buildings and the locations of activities are extracted from highly detailed databases such as the Swiss Federal Registries of Residential Buildings and Dwellings [77, 78] and the Swiss Federal Registry of Economic Activities [79]. In the present work, the entire population of Switzerland, 8,534,667 individuals, is considered, with a focus on the city of St. Gallen in Eastern Switzerland, which has 80,000 inhabitants.

2.4.2 Agent-based daily activity model

The agent-based activity model [71] simulates the daily routines of the synthetic population generated by the agent-based population model. Microscopic daily-activity plans are generated for those agents that need to leave their home during the day to accomplish some daily tasks, related to either work, leisure, education, shopping, or business.

The 8.5 million agents select a mode of transport through a mode choice model that assigns a transportation mode (car, public transport, or walking). The assignment process uses characteristics of the household, such as household size and income, as well as location-specific information, such as the quality of public transport in one's surroundings. In this work, micro-census data on mobility and transport, which provided the personal attributes and the detailed travel behavior of 57,090 participants in Switzerland, were used to sample activity chains, and aggregated micro-census data were used to calibrate the models [71].

Moreover, a car ownership model is used to assign the number of cars owned by each of

the synthetic households that selected “car” as a transportation mode. A discrete choice model is applied to these synthetic households to estimate the number of cars owned; monthly income, household typology, public transit quality, and municipality typology are the household characteristics that impact the choice.

By considering the geographic locations of houses, jobs, and economic activities included in the agent-based population model, the daily activity model generates the agents’ daily activities with a time resolution of 1 second. These include start and end locations, departure and arrival times, transport mode, and travel purpose.

2.4.3 Agent-based mobility model

The outcome of the agent-based daily activity model is used in *EnerPol*’s agent-based mobility model developed by Saprykin *et al.* [73]. This mesoscopic, queue-based model is multi-modal; the choice of transportation mode depends on the agent’s characteristics, such as age, as well as the accessibility to the given means of transport at the agent’s location. The agent-based mobility model simulates, with a one-second temporal resolution, the entire country’s vehicular transportation using a digital twin of the road network [81] and the official public transit schedule. In a mobility simulation, with one daily plan per agent, the agents perform their daily activities as specified in the agent-based daily activity model and travel between locations of activities. Each mobility simulation is scored based on a cumulative utility function that accounts for all agents’ travel times. Based on a given probability, a sample of the agents modify, or leave as is, their individual daily activities; re-routing on account of traffic congestion or changing transportation mode are two examples of modifying the daily activities. The daily activities of the agents are iteratively varied until the population reaches a Nash equilibrium. For EVs, the simulated driven distance, travel time, and time of arrival at home or at the workplace are subsequently used to quantify the electric consumption of each EV. In this work, the entire Swiss driving population of 5,200,000 agents was simulated. For the city of St. Gallen, it was considered that there were 23,000 internal daily commuters and 39,000 external commuters circulating by car in the city each weekday.

Chapter 3

Case Study: Electric Mobility

The transition to electric mobility is accelerating worldwide. However, the transition is often happening at a pace that is slower than what is necessary for cities to meet their goals. Figure 3.1 depicts a comparison between the current trend of EV penetration in the city of St. Gallen and the mid- and long-term goals set in the city's Energy Concept (EnK³), which plans for 50% of mobility demand to be covered electrically by 2050. In 2018, the EV penetration of 0.3% was slowly moving towards the city of St. Gallen's goals; the transition is lagging.

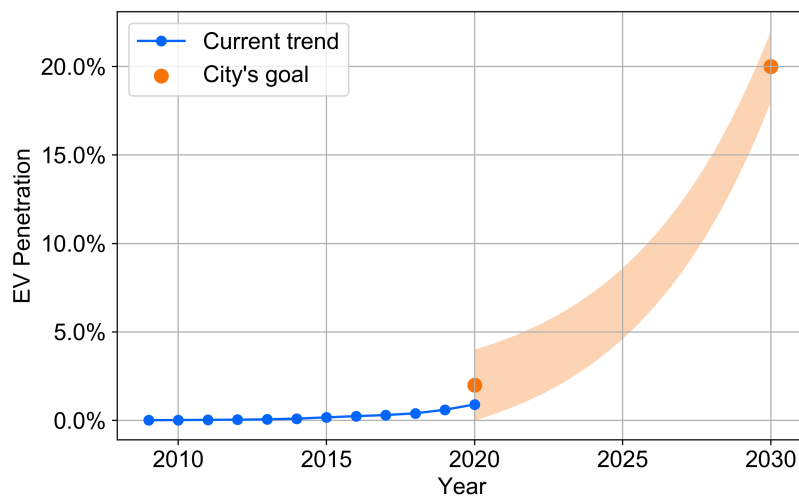


Figure 3.1: Current trend of EV penetration in the city of St. Gallen versus mid- and long-term goals of the EnK³.

As a consequence, the economic and operational implications for DSOs of the transi-

tion to electric mobility are not obvious; numerous factors are beyond the control of the DSO (for example, customers' charging behavior). Thus, to ensure a financially sustainable transition, it is increasingly important to be able to anticipate and adapt future development of the EV charging infrastructure. To assess the implications of the energy transition of the mobility sector for the investigated city, we integrated into *EnerPol* newly developed agent-based, bottom-up models – specifically (i) an agent-based electric mobility demand model that accounts for the characteristics, preferences, and behavior of the EV owners and (ii) a Monte-Carlo-based optimizer, which optimizes the placement of the EV public charging infrastructure across the city.

In the results section, business models that enhance the profitability of public charging infrastructure are identified. Moreover, it is quantified how the behavior of EV users affects the profitability and the operation of the EV charging infrastructure. These findings are highly relevant for DSOs, who seek to anticipate and adapt their infrastructure in a rapidly changing marketplace.

3.1 Methodology

The outcomes of the ABMs previously presented were used as the main inputs of the electric mobility demand model. Likewise, elements of the digital twin of the built infrastructure were used to further characterize the EV charging infrastructure. An overview of the ABMs' output and elements of the digital twin utilized by the electric mobility demand model is presented in Table 3.1.

3.1.1 Stochastic EV use model

For a given penetration of EVs, the total number of EVs was determined, and multiple different sets of distributions of these EVs were generated in the stochastic EV use model. In each set, the EVs were randomly assigned to eligible agents of the working population. An agent is eligible to have an EV assigned to him/her if the EV has a range that is equal to or greater than twice the distance between the agent's dwelling and workplace. As the users of EVs are generally not known a priori, this stochastic EV use model allows the extended *EnerPol* framework to be applied even in geographic areas where either no survey of EV use or ownership exists, or where there is not yet penetration of EVs in vehicle fleet.

Table 3.1: Outcomes of agent-based and elements of digital twin used by the electric mobility demand model

Source	Attributes
Agent-based population model	Total population, age distribution, income distribution, household structure, employment status
Agent-based daily activities model	Agent presence time at home and at the workplace, travel start times, destinations, preferred mode of transport
Agent-based mobility model	Simulated driven distance, travel time, and time of arrival at home/workplace are used to quantify the electric consumption of each EV
Digital twin of built infrastructure	3D building model, building end-uses Availability of a parking garage Distribution of private and public parking lots Locations of activities of individual agents of the synthetic population (office workplaces, shops, schools, ...) Electricity distribution grid

3.1.2 Stochastic behavior model of EV users

The human patterns of EV charging behavior were stochastically modeled. In this regard, when the battery state of charge was less than 50%, the probability of charging was determined. This work considered three different behaviors – a price-driven behavior, a comfort-driven behavior, and a mixed behavior – and the respective probabilities of charging at a given instant in time were modeled as follows:

- A Price-driven behavior: The probabilities were assumed to be inversely proportional to the price of charging at a home, work, or public charger at the time of the opportunity to charge; and
- B Comfort-driven behavior: The probabilities were derived from a recent analysis of surveys of EV charging behavior [86]. These probabilities are summarized in Table 3.2. For example, the probabilities of an agent who lives in a single-family house charging at a home, work, or public charger are 81%, 9%, and 10%, respectively. Scaling factors (k) were applied to ensure that the sum of probability is unity.
- C Mixed behavior: a mix between price-driven and comfort-driven behaviors was assumed to be the most realistic. Today, EVs are generally adopted by younger males with higher income [87] who are less sensitive to price variations. However, the technical development of EVs will enhance their affordability such that broader layers of society will have access to electromobility. As a result, it is expected that

price-driven consumers will gain importance. In fact, although the price of car fuel in relation to income in Switzerland and other wealthy countries is currently among the lowest worldwide [88], 59% of drivers in the United States choose a specific gas station because of its lower prices [89]. The income-to-price ratio in the United States is even more favorable for drivers than in Switzerland. For these reasons, in future simulations, EV drivers with income below the Swiss median according to agent-based population simulations were assigned a price-driven behavior; the other half, a comfort-driven behavior.

Table 3.2: Summary of probabilities of charging at home, work, or public chargers when an agent with comfort-driven behavior has an opportunity to charge his/her EV. k is scaling factor.

Place of Charging	Dwelling Type		
	Single-family	Multi-family	
		No garage	With garage
Home	0.81	0.00	$k \cdot 0.81$
Work	0.09	0.09	$k \cdot 0.09$
Public Charger	0.10	0.91	$k \cdot 0.10$

3.1.3 Deterministic EV charging infrastructure model

Consistent with other studies (for example, [30, 86]), the three charging options – home, work, or public chargers – were modeled as follows:



Home charging: charging duration of up to 16 hours using standard home AC plugs; and



Workplace charging: charging duration up to 8 hours using wall-boxes installed at the EV user's workplace; and



Charging at public chargers, with a minimum charging duration of 15 min, up to 4 hours, using either:

- AC chargers (having a nominal power of 15-20 kW) that are installed in public parking lots, or
- Fast DC chargers (having a nominal power of 100-150 kW) that are installed at hotspots

The public chargers were assumed to operate with a conversion efficiency of 90%. Tapering of the charging speed occurred from a battery state of charge (SOC) of 80%, and charging ended when the battery SOC reached 95%. The investment and annual maintenance costs of the EV charging infrastructure are summarized in Table 3.3. It should be noted that discount factors were applied when multiple chargers were installed at the same location [90].

3.1.4 Financial optimization of electric vehicle charging infrastructure

To assess future EV public charging infrastructure, the *EnerPol* simulation framework was further extended by embedding the agent-based electric mobility demand model within an optimizer, which optimized the placement of the EV public charging infrastructure across the city. The optimal placement maximized the load factor of public chargers and, therefore, the profitability of the infrastructure.

As shown in Figure 3.2, for a given penetration of EVs, a sequence of placement and mobility simulations was used to determine this optimal placement.

Table 3.3: Modeled charging elements and associated investment and maintenance costs.

Charging Option	Element	Power [kW]	Investment (Swiss Francs)	Annual Maintenance (Swiss Francs)	DSO Cost Share $\alpha_{DSO}(\%)$
Home	Plug	2.3	–	–	0
Workplace	Wall Box	10	6,000	1,200	20
Public	AC (2018)	15	20,000	1,200	100
	AC (future)	20	25,000	2,000	
	DC (2018)	70	100,000	2,500	
	DC (future)	150	110,000	2,500	

Initially, similar to the approach used in the modeling of power systems in *EnerPol* [69], a Voronoi tessellation centered on the locations of the low-voltage transformers was established. Then, in the first step of the sequence of simulations, one public charger was allocated to each Voronoi cell, and then in a second step of the sequence, a mobility simulation was conducted to assess the usage of the public chargers. In subsequent iterations of the sequence, public chargers were added or removed with the goal of maximizing the load factor of the public chargers. In particularly busy locations, which have more than 20 users per day, AC chargers were substituted with DC fast chargers to minimize the queuing time of EV users. Further, if the load factor was less than 1 hour per day, then chargers were removed. A Monte Carlo approach was employed, as in each iteration one of the sets of randomly distributions EVs for the given penetration of EVs, which were generated in the stochastic EV use model (3.1.1), was used. The iterative sequence of placement and mobility simulations was considered converged when there was less than 5% difference in the successively predicted: electricity supplied for charging at (i) all homes, (ii) all workplaces, and (iii) all public chargers; (iv) usage of each charging station; (v) number of required public chargers; and (vi) share of agents not able to find an available public charger. The agent-based mobility model and agent-based population model were run on GPUs and, therefore, provide high-resolution simulations in a reasonable amount of time. Since our methodology is based on agent-based mobility and population simulations, very detailed data and high-performance computing resources were required.

3.1.5 Evaluation of profitability of EV charging infrastructure

The profitability of the EV charging infrastructure is was evaluated in terms of time to break even (t_{BE} in Eq. [3.1]). This period between the first year of operation and break-even year is was determined when the net present value of the infrastructure is was equal to or greater than 0. A discount rate r of 5% is was used. The revenues and costs of all components of the infrastructure (chargers and wall-boxes) are were considered; thus, it

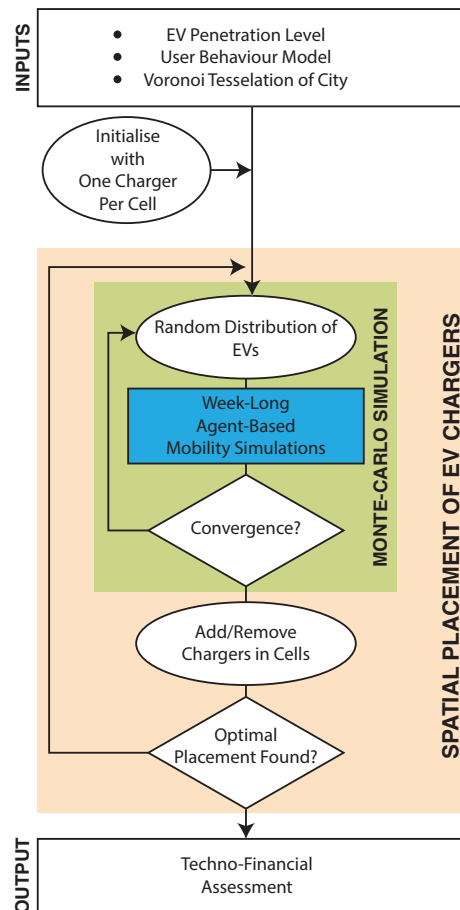


Figure 3.2: Schematic of iterative sequence of placement and mobility simulations that is integrated into the *EnerPol* framework.

is possible that EV users who charge at home may also pay back for the investment in public chargers. From the DSO's perspective, this approach provides the most complete evaluation of profitability.

$$0 = NPV(t_{BE}) = -C_{Inv} \cdot \alpha_{DSO} + \sum_{t=0}^{t_{BE}} \frac{Revenues - C_{Maint} \cdot \alpha_{DSO}}{1 + r} \quad (3.1)$$

Other financial assumptions are as follows:

- The cash flows were assumed to be unlevered (cash flow without financing).
- The discount rate r did not include an interest rate; it only represented the risk of investment.
- The lifetime of the chargers was 15 years.

3.2 Scenarios

For the case of the existing EV charging infrastructure in the city, 1260 scenarios were evaluated, in which the EV penetration, the source of revenues, the charging behavior of EV users, and the preferences of EV users were varied. For the case of new EV charging infrastructure in the city, 1308 scenarios were assessed.

The simulation parameters can be described as follows:

- *EV penetrations.* The ratio of EVs and the entire vehicle fleet circulating to or within the city that were simulated were 0.3%, 2%, 5%, 10%, 15%, and 20%. The EV penetration of 0.3% was the 2018 EV penetration in Switzerland [91]; the EV penetration of 2% was the 2020 goal for the city [18]; and the 20% EV penetration was the city's 2030 goal and the EV penetration that is anticipated for Europe in 2030 [30]. In the 20% EV penetration case, 12,078 EVs were simulated. For all EV penetrations greater than 0.3%, on account of the expected improvements in technology, the efficiencies of EVs were increased up to 25% over the baseline case used in the 0.3% EV penetration case [86], and the conversion efficiency of chargers were increased to 94%.
- *EV models.* The top 10 EVs in terms of 2019 sales in Switzerland ([92, 93]), Table 3.4, were included in the model.
- *Source of revenues.* Two alternative options were considered. In the first option, EV users were charged by the amount of power used to charge the EV. The power charge per kWh was a multiple ($\pi_{Power}^{Multiplier}$) of the average Swiss electricity price, which was 0.20 Swiss Francs/kWh in 2018 [94]. The marginal gain

Table 3.4: Characteristics of electric vehicles. Sources: [92, 93]

EV model	Share of sales [%]	Autonomy range [km]	Consumption [kWh/(100 km)]
Tesla Model 3 – Long Range	38.2	499	16.1
Renault Zoe	13.7	315	16.5
BMW i3	8.1	183	18.0
Hyundai Kona EV	6.5	415	17.4
Audi e-tron	5.2	328	28.6
VW e-Golf	4.7	201	17.4
Nissan Leaf	4.0	243	18.6
Tesla Model X – Long Range	4.0	523	21.7
Tesla Model S	3.8	417	20.5
Jaguar I-Pace	3.4	377	27.3

for the DSO was assumed to be a multiple of 0.16 Swiss Francs/kWh, which was the difference between the European Energy Exchange wholesale electricity price in Switzerland and the electricity price for households [94]. In the second option, EV users were charged by parking duration. The parking charge was $P_{Parking}^{Fee} = P^{Base} + \Delta P^{Surcharge}$, where the base fee, P^{Base} , was the same as the city’s current market price for parking of traditional vehicles, which is 2 Swiss Francs/hour. The base-case values of $\pi_{Power}^{Multiplier}$ and $\Delta P^{Surcharge}$ were set by analyzing the tariffs of some Swiss chargers’ operators and service providers, which in Switzerland vary greatly depending on the provider (Table 3.5). In the base-case scenario, the surcharge, $\Delta P^{Surcharge}$, was 2 Swiss Francs/hour: a value obtained by averaging the price per hour reported in Table 3.5.

- *Preferences of EV users.* Three charging preferences of EV users were considered: (i) leaving the parking space immediately after completion of charging, (ii) leaving the EV plugged in for a buffer time, and (iii) moving the EV after work.
- *Charging behavior of EV users.* Price-driven, comfort-driven, and mixed behaviors were simulated, each with respective probabilities of charging at home, work, or public chargers.
- *Pricing policy.* In addition to the base-case prices, the response of the price-driven EV users to pricing policies was assessed by including public charging locations where EV users are only charged for the parking but not for the charging. This is a widespread policy among many retailers [96, 97] and car manufacturers that offer free supercharging to their customers [98]. The possibility to charge at work for a

Table 3.5: Prices for EV charging at public chargers in Switzerland for three of the main national providers (rated power at AC chargers: 22 kW; at DC chargers: 150 kW). Roaming fees and subscriptions are not included. Source: [95]

Provider	Price per kWh		Price per hour	
	[Swiss Francs/kWh]		[Swiss Francs/hour]	
	AC	DC	AC	DC
PlugnRoll	0.43	0.62	3.60	10.8
Move	0.35	0.59	1.8 (+1.5/process)	6 (+1.5/process)
Swisscharge	0.25	0.44	0.5	3

discounted price is also a common practice, sustained by DSOs [99]; therefore, the possibility to charge at the workplace for a discounted power fee (25% discount on the power charge per kWh) was implemented as well.

3.3 Results

The results section is structured as follows: In the first section, the model predictions are compared with data on the actual usage of the existing public charger infrastructure. In the second section, the profitability of the existing charging infrastructure is assessed based on an evaluation of present and future scenarios characterized by different business models, as well as by the entry of new providers of charging stations into the market. The last section assesses the resulting financial and technical consequences of a future infrastructure designed to accommodate the increasing number of EVs.

3.3.1 Model validation

Figure 3.3 compares the predicted and actual monthly charging cycles in 2017 at the four most widely used public charging stations of the city. The geographic locations of the four charging stations are also shown in Figure 3.3. In 2017, the city had a total of 23 public chargers, and the EV penetration was 0.3%. In the simulations, a comfort-driven charging behavior of the EV users was assumed. It is clear that there was overall good agreement between the predicted and actual monthly charging cycles. For all public chargers, simulations predicted an average of 106 charging cycles per month, a 4.3% difference from the actual average of 110.8 charging cycles per month. For the city's 23 public chargers, the predicted and actual monthly supplied electricity were 1.18 MWh and 1.05 MWh, respectively: a difference of 12%. This overall good agreement between predictions and data validated our novel agent-based simulation methodology.

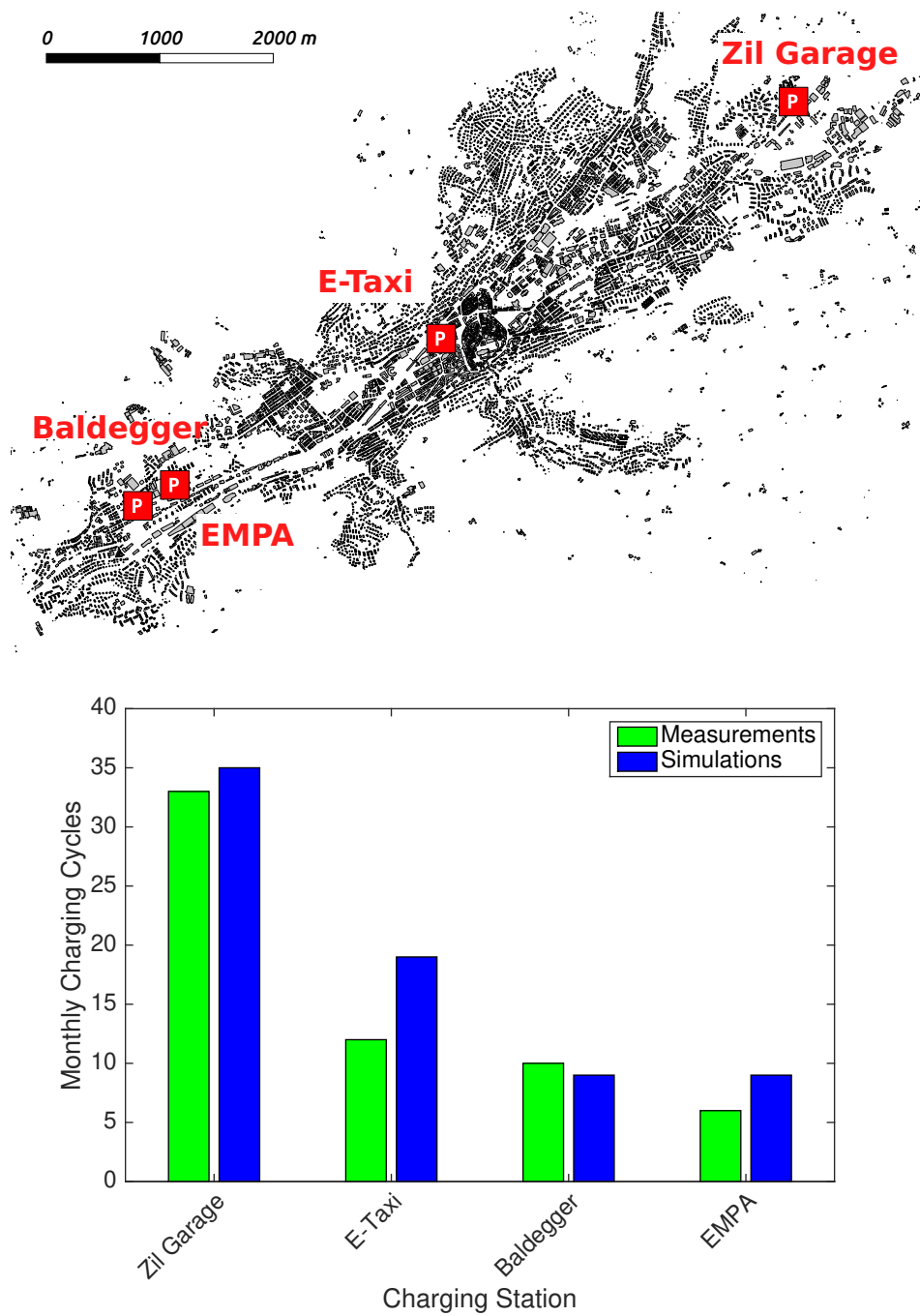


Figure 3.3: Locations (upper) and comparison of predicted and actual monthly charging cycles (lower) in 2017 at the four most widely used public charging stations of the city.

3.3.2 Business model, competition, and profitability of the existing charging infrastructure

This section assesses scenarios where, as the EV penetration increased, the city's existing EV infrastructure of 23 public charging stations was unchanged. Figure 3.4 compares the DSO's revenues from charging at home, work, and public chargers, for the two options of paying for the use of public chargers – sales of power and parking duration. In the first option, power sales, the price of charging was 0.20 Swiss Francs/kWh, which was the 2018 market price for EV charging in the city; in the second option, parking fees, the price of charging of 4 Swiss Francs/hour was the city's current market price for the parking with a surcharge, $\Delta P^{Surcharge}$, of 2 Swiss Francs/hour.

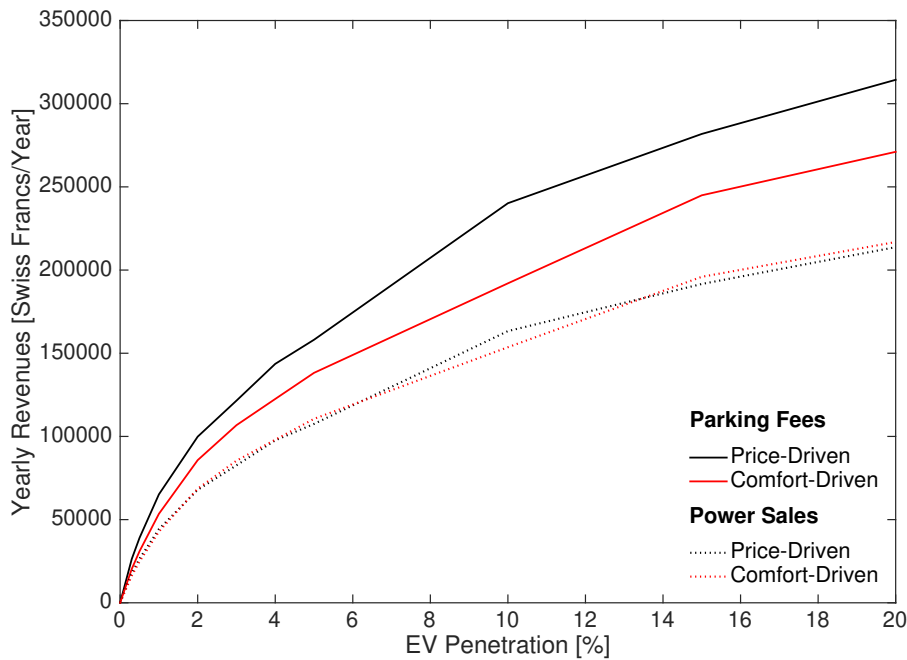


Figure 3.4: Comparison, for EV users with price-driven and comfort-driven charging behaviors, of the effect of EV penetration on the DSO's revenue for EV charging based on parking duration (solid lines) and power sales (dotted lines).

Further, in Figure 3.4, the two different charging behaviors of EV users – price-driven behavior and comfort-driven behavior – are assessed. It can be seen that for a given EV penetration, the DSO's revenue from parking fees was greater than the revenue from power sales, both for price-driven and comfort-driven charging behaviors. Even though a business model based on parking fees rather than power sales generated more revenue, this business model showed greater sensitivity to the charging behavior of EV

users, and the revenue was lower for comfort-driven charging behavior compared to price-driven charging behavior. This observation also highlighted an advantage of ABMs in comparison to models that forecast based on historical statistical data, as ABMs can account for the interactions between agents and their environment, whereas statistically based models do not account for such interactions. Because of the feedback included in our agent-based simulation framework, changes in pricing systems affected the choices of EV users and, in turn, the design, costs, and revenue of the EV charging infrastructure. For example, doubling the electricity price neither doubled revenue nor halved the time to break even.

The effect of EV penetration on the time to break even of the city's existing EV infrastructure is shown in Figure 3.5. Two business unit cases were compared: (i) the business unit managed all EV charging infrastructure, and (ii) the business unit managed only the public EV charging infrastructure. In both cases, the DSO's revenues came from parking fees, and the EV users had price-driven charging behavior. Whereas a business unit that manages all EV charging infrastructure will have a time to break even of 11 years at today's EV penetration of 0.3%, and subsequently shorter times to break even as the EV penetration increases, a business unit that manages only public EV charging infrastructure will only break even when the EV penetrations are 4% or higher.

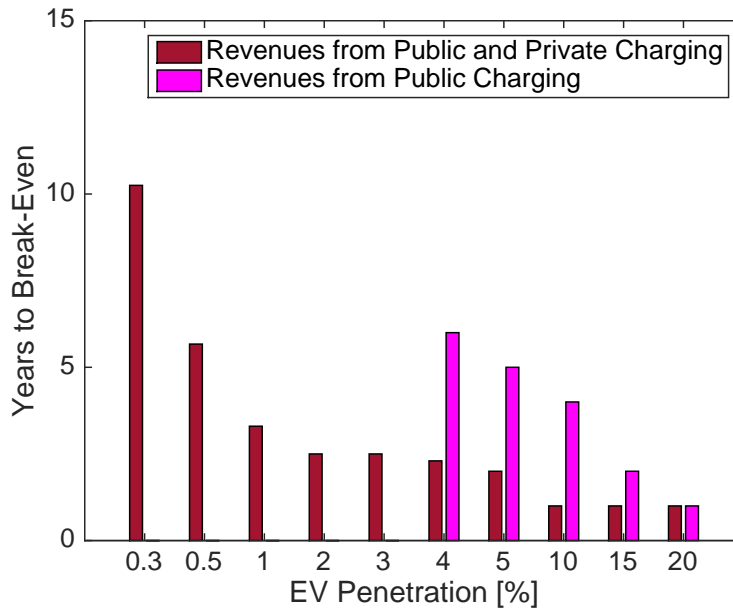


Figure 3.5: Comparison of time to break even for the cases when revenue comes from all EV charging infrastructure and for when revenue comes only from public EV chargers are considered. The revenue comes from parking fees, and the EV users have price-driven charging behavior.

In 2017, it was announced that private companies plan to enter the market of public EV chargers in St. Gallen [100]. As illustrated in Figure 3.6, the impact of 10 proposed privately owned public chargers on the DSO's existing infrastructure was assessed. In the assessment, the DSO's revenues were based on parking fees, and the EV users were assumed to have a price-driven charging behavior. It can be seen that the privately-owned public chargers had a substantial adverse impact, with a 35% decrease in load factor for a 2% EV penetration, on the DSO's revenue from its existing infrastructure, Figure 3.6 (a). At two representative public charging stations of the DSO, the impact of competition on the annual revenue is shown, Figure 3.6 (b). It can be seen that at both public charging stations, there was an adverse impact on the DSO's revenue, even at high penetrations of EVs.

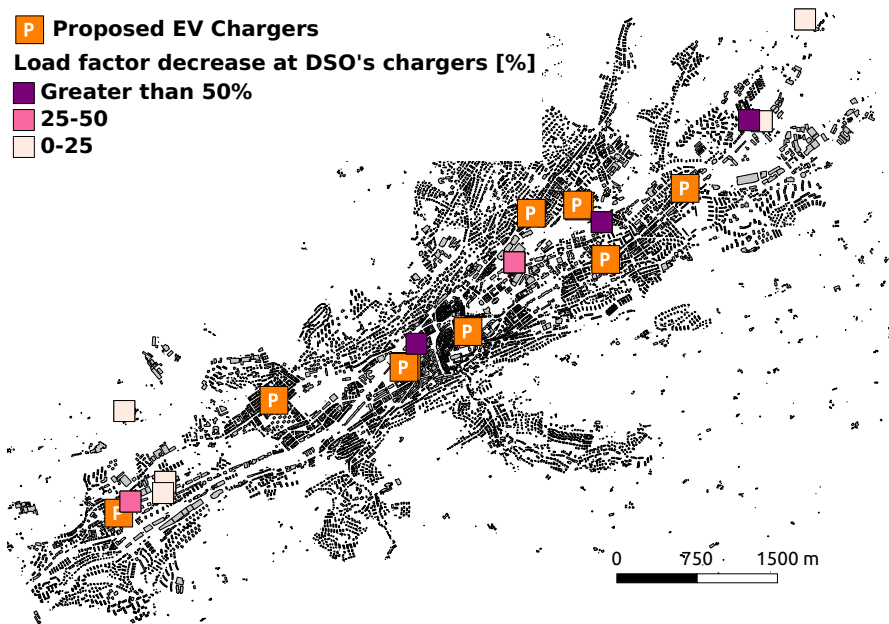


Figure 3.6: (a) Locations of 10 proposed privately owned public chargers and their impact on the load factors at the DSO's existing public chargers

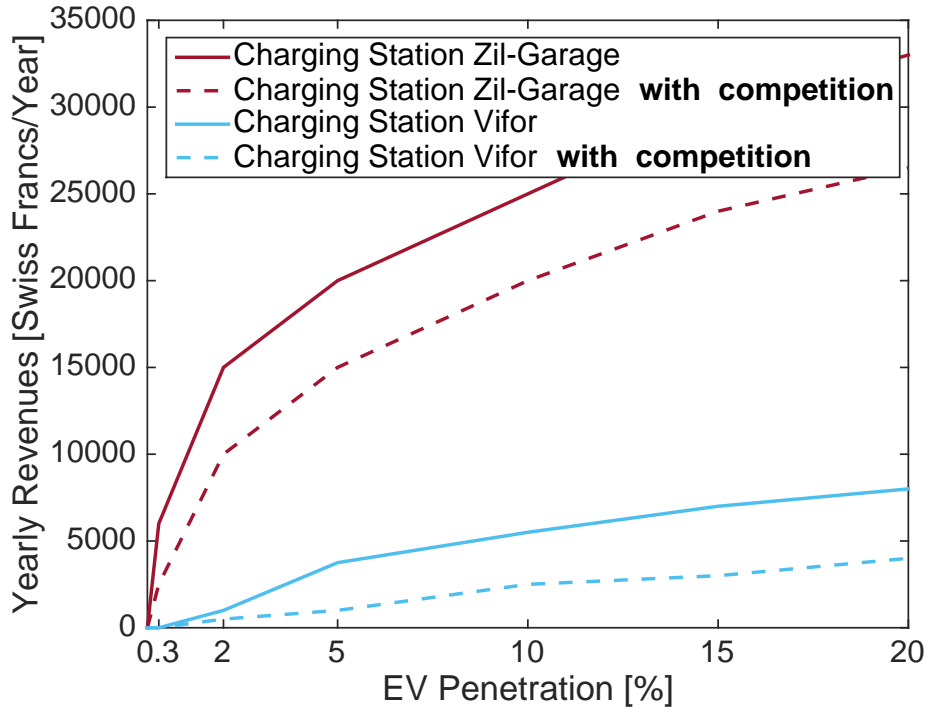


Figure 3.6: (b) Comparison of revenue, at two of the DSO's public charging stations, without and with competition from the privately owned public chargers.

3.3.3 Techno-economic consequences of increasing electric vehicle penetration

Economic consequences

This section assesses scenarios in which the city's EV infrastructure of public charging stations was expanded as the EV penetration increased. Figure 3.7 shows the optimized placement and number of public charging stations for EV penetrations of 2% (Figure 3.7 [a]), 10% (Figure 3.7 [b]), and 20% (Figure 3.7 [c]). These optimized placements ensure both that sufficient EV charging is available to all EV users and that the load factor of the public chargers is maximized. The revenues from EV charging were based on parking duration, a mixed behavior of the EV users was assumed, and different preferences of EV users – *i.e.*, leaving the parking lot immediately after charging; leaving 30, 60, 120, 240, or 480 minutes after charging; and leaving at the end of the EV user's workday – were assessed. As can be seen in Figure 3.7, and as summarized in Table 3.6, the

median number of required chargers increased with EV penetration. It is noteworthy that at busy locations, to minimize the queuing time of EV users, DC fast chargers were deployed in place of AC chargers. As a guideline, a ratio of 10 public chargers to 100 EVs has been targeted in Europe [30]. For an EV penetration of 10%, the simulations showed that this target was reached, while the number of public chargers exceeded the target for lower EV penetrations. As there are varying preferences of EV users in terms of when the EV user leaves the EV charger, there was an uncertainty in the median number of required chargers; Table 3.6 shows that the uncertainty in the median number of required chargers increased with increased EV penetration.

Table 3.6: Summary of the impact of EV penetration on optimized public EV charging infrastructure.

EV Penetration [%]	Median Number of Required Public Chargers	Ratio of Median Number of Public Chargers to 100 EVs	Uncertainty in Median Number of Public Chargers
2	146	12	34
5	402	13	83
10	552	9	109
20	824	7	127

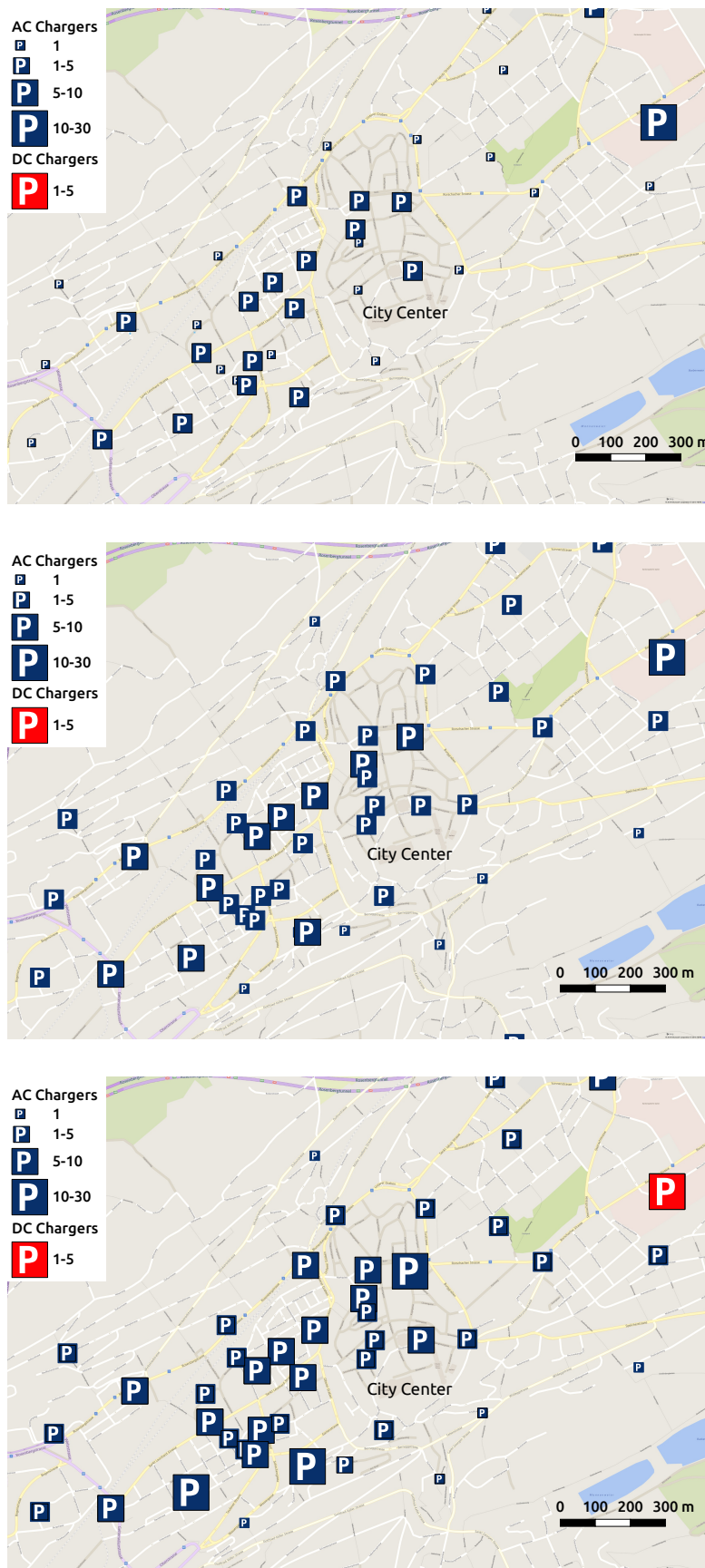


Figure 3.7: Optimized placements of public EV charging infrastructure for EV penetrations of (a) 2%, (b) 10%, and (c) 20%. The size of the symbols is indicative of the number of chargers.

For an EV penetration of 2%, the effect of elasticity in demand on the DSO's revenue for EV charging and the time to break even for the EV charging infrastructure are compared in Figure 3.8. Both the DSO's total (that is, from charging at home, work, and public chargers) revenue and the revenue from public chargers alone are shown in Figures 3.8 – 3.9. Thus, as shown in Figure 3.8 and Figure 3.9, the revenue was normalized relative to the total revenue based on power sales at the reference price (of 3.5 Swiss Francs with power sales and 2 Swiss Francs with parking fees). For each option, different charging behaviors of EV users – price-driven behavior and comfort-driven behavior – were examined. Furthermore, for each option, different preferences of EV users – *i.e.*, leaving the parking lot immediately after charging; leaving 30, 60, 120, 240, or 480 minutes after charging; and leaving at the end of the EV user's workday – were assessed; the impacts of these preferences of EV users are displayed as uncertainty bars in Figures 3.8 – 3.11.

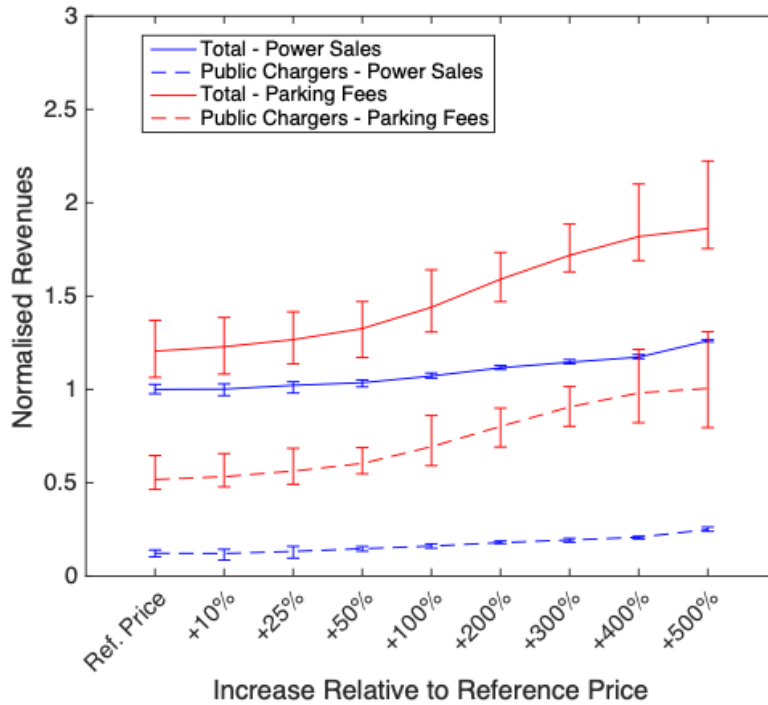


Figure 3.8: Comparison, for EV users with price-driven charging behavior, of the effect of elasticity of demand on the DSO's revenue for EV charging based on power sales and parking duration. The total revenue is from charging at home, work, and public chargers. The revenue is normalized relative to the total revenue based on power sales at the reference price. The EV penetration is 2%. The vertical bars show the uncertainty due to the preference of when EV users leave.

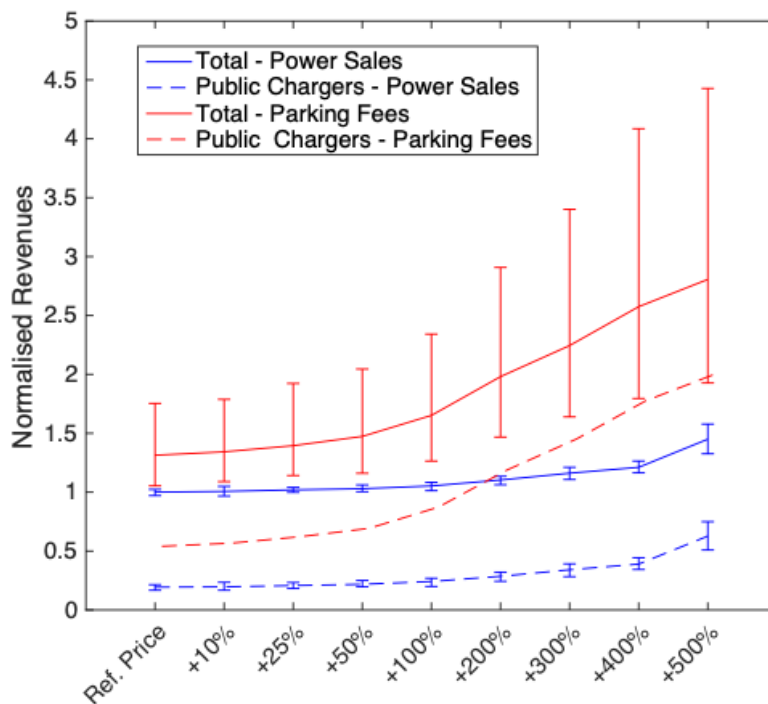


Figure 3.9: Comparison, for EV users with comfort-driven charging behavior, of the effect of elasticity of demand on the DSO's revenue for EV charging based on power sales and parking duration. The total revenue is from charging at home, work, and public chargers. The revenue is normalized relative to the total revenue based on power sales at the reference price. The EV penetration is 2%. The vertical bars, not shown for public charger parking fees for the sake of clarity, represent the uncertainty due to the preference of when EV users leave.

It can be seen that, similar to the case of an unchanged EV public charging infrastructure, as the public charging infrastructure was expanded, the DSO's revenue from parking fees was always greater than the revenue from power sales, both for price-driven (Figure 3.8) and comfort-driven (Figure 3.9) charging behaviors. Furthermore, for both charging behaviors of EV users, the DSO's revenue was less sensitive to changes in price, as EV users that were price driven tended to charge even more at home as the price of charging was increased. Even though a business model based on parking fees rather than power sales would generate greater revenue, it can be seen that in the uncertainty in revenue, for public chargers in the case of price-driven charging behavior (Figure 3.8) and for both total and public charging revenue in the case of comfort-driven charging behavior (Figure 3.9), increased with increased prices. This increase in uncertainty occurred as EV users with a comfort-driven charging behavior tended not to adapt their charging

behavior, as their behavior was more driven by comfort and less so by price.

Figure 3.10 shows the effect of elasticity of demand on the time to break even of the whole EV charging infrastructure. As the time to break even accounts for the revenues, the investment costs, and the operation and maintenance costs, the time to break even, rather than the generated revenue, was considered a more robust assessment of the profitability of business models. Despite the increased uncertainty in revenue for a business model that is based on parking fees, a business model based on parking fees is preferable to a business model based on power sales, as the latter business model only broke even if the price of charging was five times the market price for EV charging in the city; even then, the time to break even was substantially larger than for the power sales business model. It is noteworthy that while the business model based on parking fees did not break even with sales at the reference price (which was the city's current market price for the parking of traditional vehicles), with prices of 10% or more above the reference price, the business model broke even, and the time to break even decreased as the sales price increased.

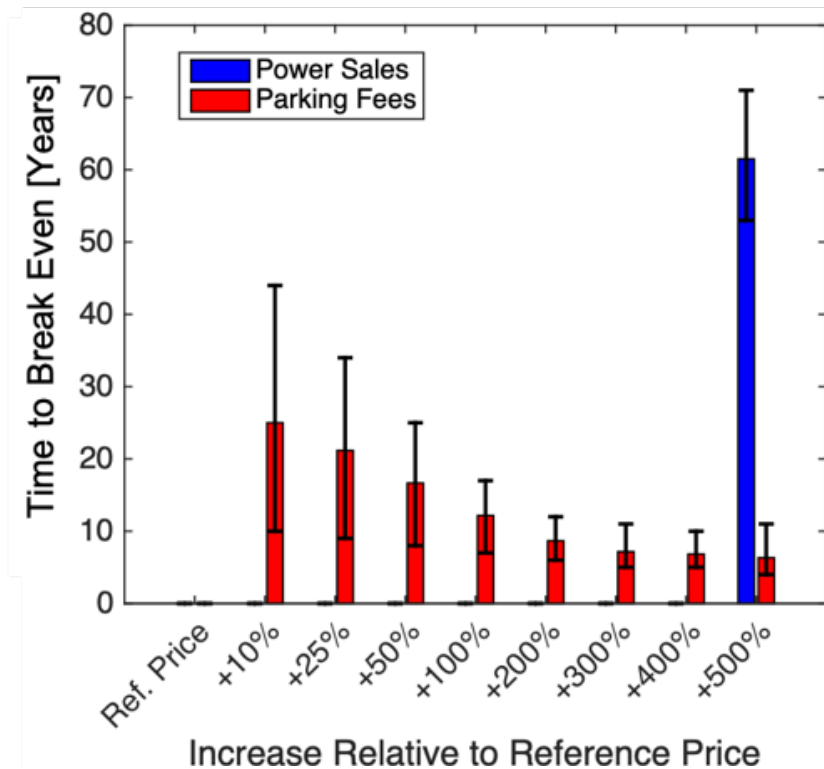


Figure 3.10: Comparison of the effect of elasticity of demand on the time to break even of the EV charging infrastructure for EV charging based on power sales and parking duration. The EV penetration is 2%. The vertical bars represent the uncertainty due to the preference of when EV users leave.

Figure 3.11 compares the impact of EV penetration on the time to break even, for the business model based on parking fees, for both the price-driven and comfort-driven charging behaviors. This business model has been identified above as the most profitable. However, with sales at the city's prevailing market price for the parking of traditional vehicles, at the current EV penetration of 0.3%, no break even was possible for either price-driven or comfort-driven charging behaviors of EV users. At an EV penetration of 2%, this business model was profitable only if the EV users exhibited comfort-driven charging behavior. Thus, even though revenue increased with increased EV penetration, early entrants into the EV charging marketplace had substantial financial exposure if knowledge of the charging behavior of EV users was unknown. Only for EV penetrations of 10% or larger was the financial exposure due to the charging behavior of EV users reduced and was the uncertainty due to the preference of when EV users leave a parking lot smaller.

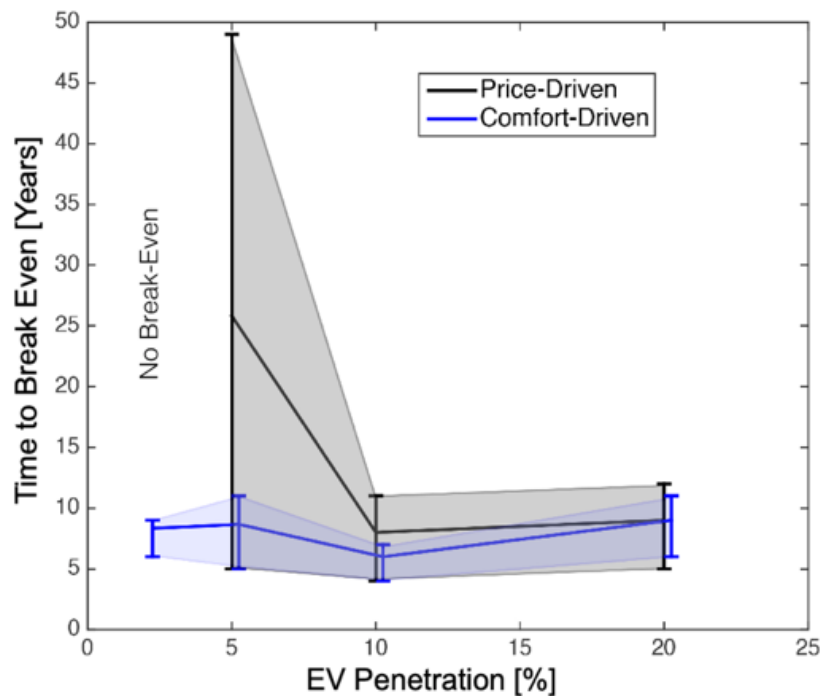


Figure 3.11: Comparison, for the business model based on parking fees, of the impact of EV penetration on the time to break even for both the price-driven and comfort-driven charging behaviors. The vertical bars represent the uncertainty due to the preference of when EV users leave.

Technical consequences

In this section, the results of the electric mobility demand model were used to assess the technical consequences of an increasing EV penetration. When assessing the impact of EV demand on grid load, the additional electric demand was aggregated at low-voltage transformers and compared to the predicted demand derived from power flow simulations without EVs.

Figure 3.12 quantifies, by source, the additional electricity demand that arises from EV charging. The EV penetrations were 2% (Figure 3.12 [a]), 10% (Figure 3.12 [b]), and 20% (Figure 3.12 [c]), and a business model based on parking fees was used for EV users with mixed behavior. The time series, with 1-minute temporal resolution, covered the duration of a week. It is evident that the characteristics of charging at work, home, and public chargers were different. While charging at work and at public chargers showed sharp peaks in electricity demand at morning peak hours, the time series of charging at home had less distinctive peaks and had maxima during evenings. Over the range of EV penetrations that have been assessed, charging at home was the largest source of the additional electricity demand, and, quantitatively, charging at home, work, and public chargers accounted for 47%, 45%, and 8% of the total additional electricity demand due to EV charging. It can also be seen in Figure 3.12 that as our agent-based simulation framework differentiates between the activities of all individuals in the population, the trends in the additional demand differed between workdays and weekends.

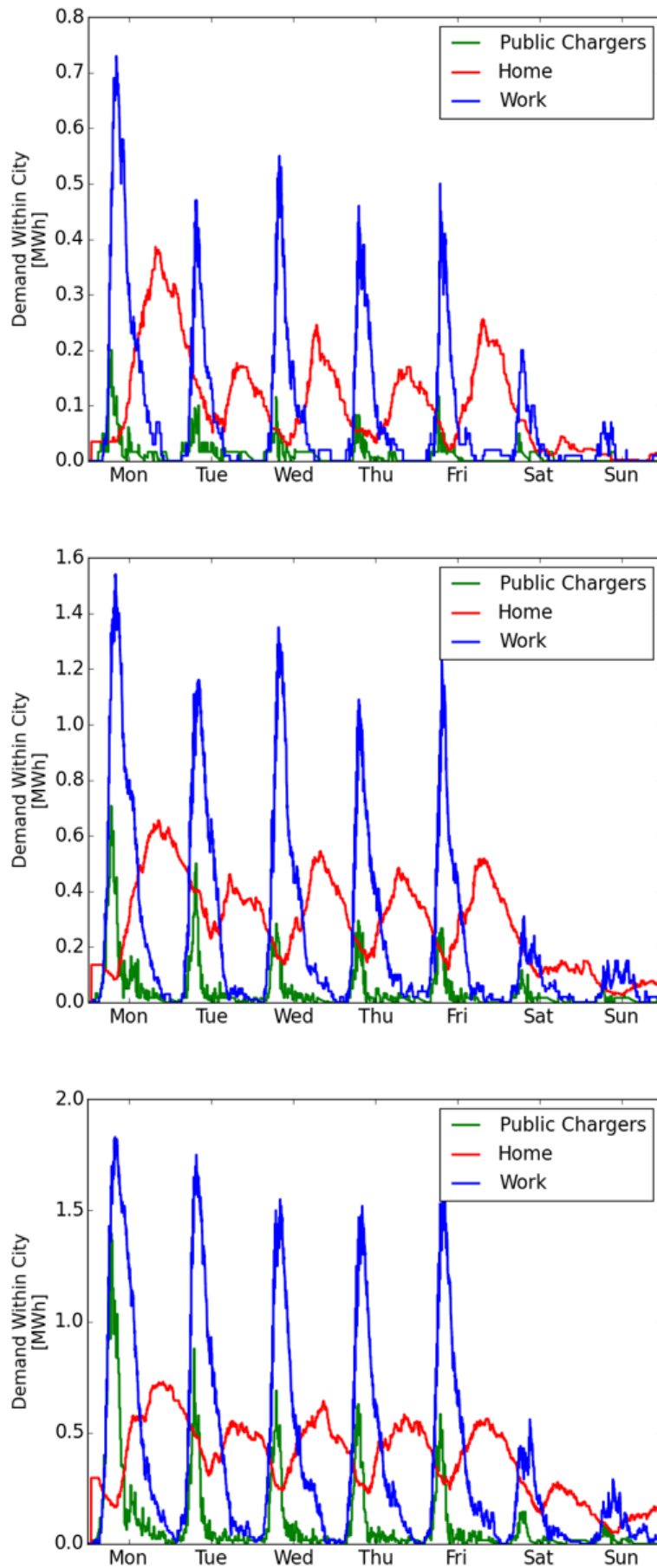
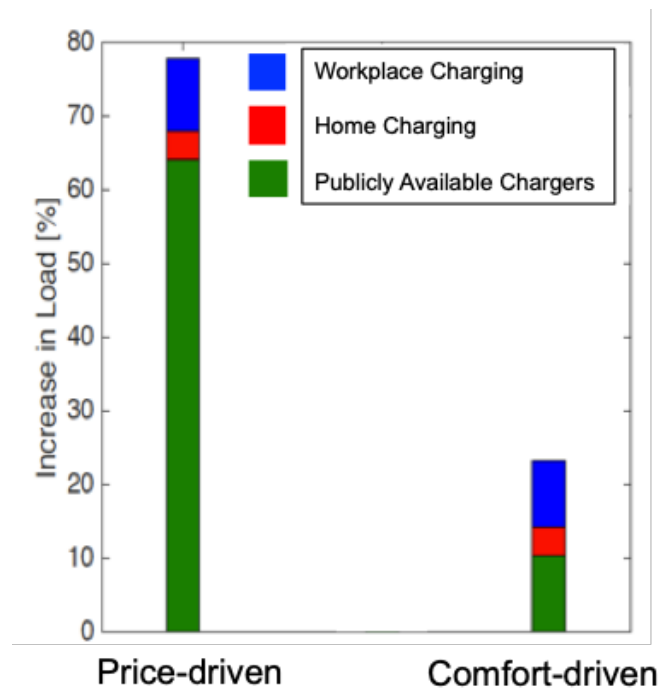


Figure 3.12: Comparison of the sources of the additional electricity demand due to EV charging, for EV penetrations of 2% (a), 10% (b), and 20% (c).

For a 20% EV penetration, the maximum increase in load at the city's low-voltage transformers is shown in Figure 3.12 . The increase was determined at the time of the largest hourly increase in load and for the transformer that had the largest increase in load. It is evident that the largest hourly increase occurred in the case of price-driven behavior, which had an increase of approximately 78% compared to 22% for the case of comfort-driven behavior. This larger increase occurred as more EV users charged in the city in the case of price-driven behavior. It can also be seen in Figure 3.12 (a) that in the case of the price-driven behavior, public chargers accounted for 80% of the hourly increase in load, whereas in the case of the comfort-driven behavior, charging at work and public chargers were approximately equal, each accounting for 40% of the maximum hourly increase in load. In Figure 3.12 (b), the load increase averaged over the city at the hour of the maximum increase in load is shown. It is useful to highlight three observations. First, it can be seen that the city-averaged increase in load of 6.1% was less than the local increase in load that is shown in Figure 3.12 (a). Furthermore, averaged over the city, it is evident that EV users charging at work accounted for the largest increase in load, as both residents of the city and external commuters were considered. Lastly, in comparison to the case of local load increases, there was little difference averaged over the city due to the different behaviors of EV users. Overall, Figure 3.12 highlights the importance of using a digital twin of the actual built infrastructure, as bottlenecks in the grid could then be reliably identified.



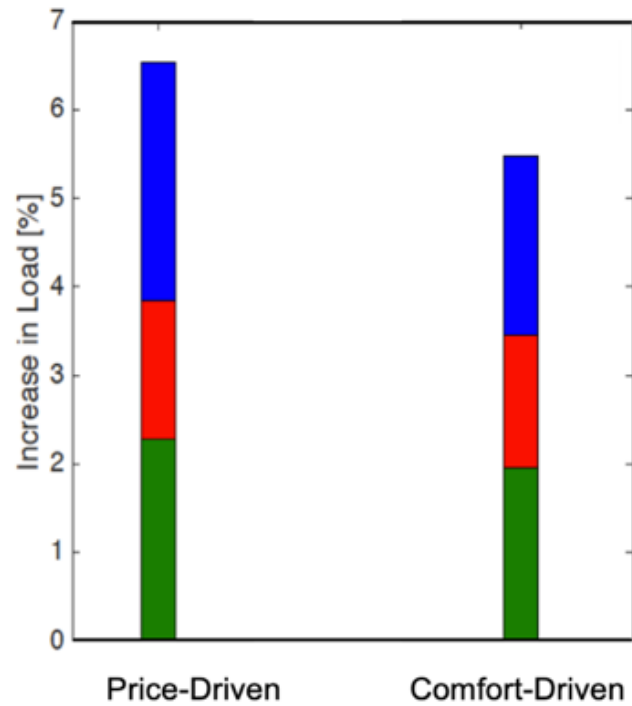


Figure 3.12: (a) Comparison of the maximum increase in the peak load due to EV charging across the city. (b) Comparison of the increase in peak load at peak hour due to EV charging averaged over the city.

Chapter 4

Case Study: Heat

The existing DH network of the test-case city supplies DH to 2,210 buildings, mostly located in central areas of the city. The energy concept EnK³ envisages that, by 2050, the valley area of the city will mainly be supplied with DH from waste-to-energy plants. The connection rate of buildings to the extended DH network shall reach 90% in the longer term. Buildings outside of the DH areas will be heated with heat pumps. Figure 4.1 illustrates the consequences of these plans on the city's heat demand until 2050 for different heat sources.

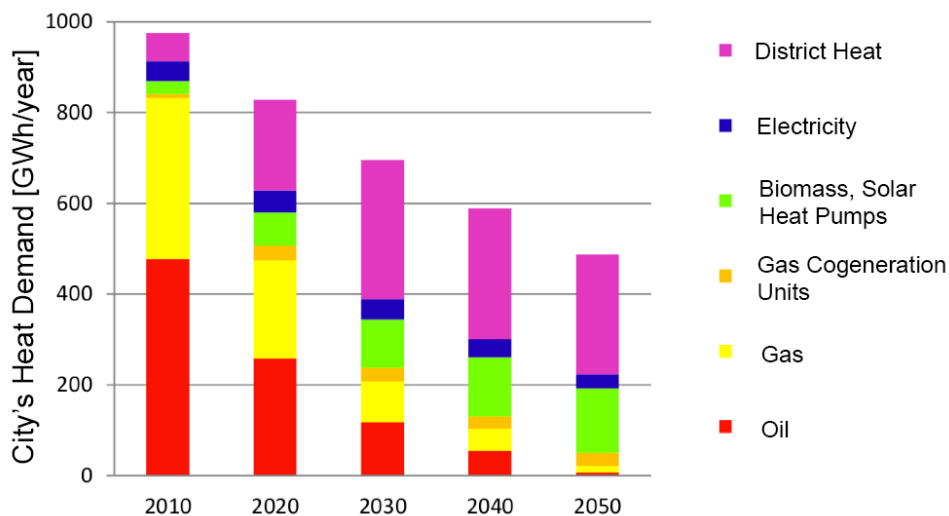


Figure 4.1: Evolution of heat demand in the city of St. Gallen according to EnK³ by energy source. Elaborated from: [18]

The DH network extension is associated with large investment (65.5 million Swiss Francs)

and political risks, as there is no obligation for building owners to connect to the extended network. The following questions need to be answered:

- Does the business plan pay off?
- Which property owners will connect to the network?
- What is the optimal layout of the future DH network?
- What are the main arguments to convince the population of the necessity of new expenditures?

To answer these questions, the extension of the DH network in the city of St. Gallen and the decarbonization of the building stock were assessed with the developed agent-based simulation framework. The following newly developed agent-based, bottom-up models were integrated into *EnerPol*: (i) an agent-based heat demand model that accounts for the characteristics and behavior of the building occupants; (ii) a predictive model that quantifies, based on the characteristics of the building, the likelihood of the building being connected to a DH network; and (iii) a routing model that determines the optimal least-cost path for the pipeline of an expanded DH network. The overall approach is illustrated in Figure 4.2.

The results indicate that accounting for building occupants' behavior substantially improves the quantitative prediction of the heat demand. Furthermore, by means of a predictive model, possible extensions of the local DH network of the test-case city were identified, and it is shown how the profitability of the DH infrastructure can be enhanced by using the model. The findings of this case study have been used to increase the social acceptance of new investments in the DH network, and in 2017, the city's inhabitants approved a credit of 65.5 million Swiss Francs to extend the DH network [54]. Moreover, the model was delivered to the multi-utility *sgsw* and installed on their servers for use by the DH sales department.

4.1 Methodology

The methodology section first presents the development of the bottom-up heat demand model (Sections 4.1.1, 4.1.2, and 4.1.3) and then the development of the DH predictive and routing model (Sections 4.1.4 and 4.1.5). The two models were coupled together as illustrated in Figure 4.2.

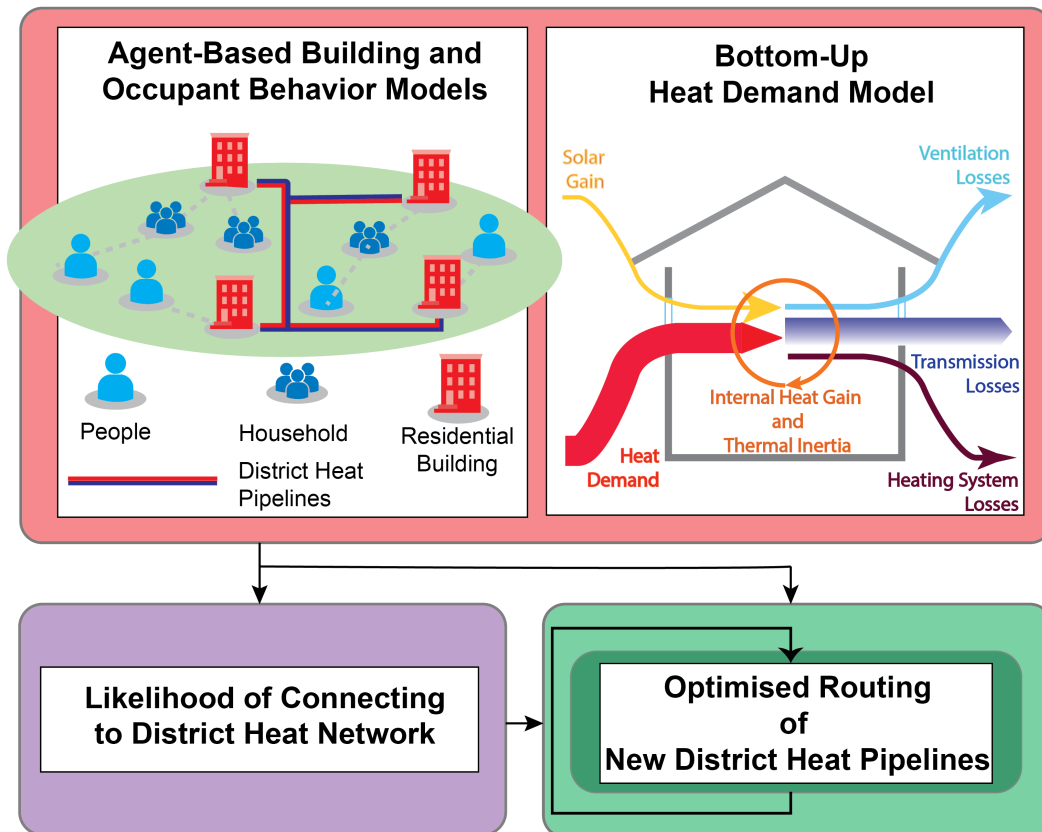


Figure 4.2: Process flow diagram of heat case study, coupling agent-based building and occupant behavior models with a bottom-up heat demand model and a predictive model of the likelihood of buildings to connect to the DH network to optimize the routing of new DH pipelines.

4.1.1 Characterization of agents

The modeling approach of the heat demand model combines large-scale ABMs of both population and building stock with a fully bottom-up thermodynamic heat demand

model. A detailed synthetic population was generated for an entire country, and the daily activities of each person, household, and dwelling were modeled. Both the occupants of buildings and buildings were modeled as agents. The characteristics of the building occupants and the buildings are summarized in Table 4.1 and Table 4.2, respectively.

Characterization of building occupants

The characteristics of occupants of buildings were generated in the agent-based population model (2.4.1); those relevant for the heat demand model are reported in the following table.

Table 4.1: Outcomes of agent-based population model used to characterize the occupants of buildings in the heat demand model

Agent	Characteristic
Person	Age, sex, employment status, location, job location, number of kids
Household	Members, number of kids, incomes
Dwelling	Size, number of rooms

The characteristics of buildings were extracted from the digital twin of the built infrastructure (2.3.1); those relevant for the heat demand model are reported in the following table.

Table 4.2: Characteristics of buildings used by the heat demand model

Category	Sub-category	Characteristic
History		Build year, renovation year, installation year of heating system
End-Use	Sector	Residential, commercial, industrial
	Archetype	Single-family, multi-family, mix-use
Ownership		Public, private, housing cooperative, social housing
Geometry	Internal	Perimeter, height, surfaces of building envelope (areas of roof, wall, and windows)
	External	Energy-consuming area
Heat demand	Build-year dependent	Thermal resistances of walls, roofs, and floors; ventilation rate, type of SH system, type of DHW system
	Non-build-year dependent	Domestic hot water consumption, heat gain from occupants, heat gain from electrical appliances, installation year of heating system
Weather		Hourly external temperature, wind speed, solar radiation

Characterization of buildings

The topographic landscape model of Switzerland, *swissTLM3D*, developed by the Swiss Federal Office of Topography, was used to derive the geometric characteristics of each building [101]. The energy-consuming area was calculated as a share of the total floor area in a building to account for the fact that not the entire building may be heated and that some buildings are not for solely residential purposes. SIA architectural norms were used to model numerous components of the total heat demand, such as the consumption of domestic hot water and heat gains from solar radiation, building occupants, and electrical appliances. For the heat demand model, the following norms were used: *Norm 380/1: Thermische Energie im Hochbau* [102], *Norm 2024: Raumnutzungsdaten für die Energie- und Gebäudetechnik* [103] and *Norm 2044: klimatisierte Gebäude - Standard Berechnungsverfahren für den Leistungs- und Energiebedarf* [104].

Other components of the building heat demand were modeled as a function of the building build or renovation year. In particular, the thermal resistances of walls, roof, and ground and the ventilation rates to model mechanically ventilated buildings were given in [55]. Ventilation rates for ventilation through windows and infiltration were given in [105]. Lastly, the weather data were either simulated using the Weather Research and Forecasting Model [106], which is integrated into the *EnerPol* framework, or were from actual measurements obtained from the data portal for teaching and research of *MeteoSwiss* [107]. A WRF full-year simulation at 10km x 10km resolution was conducted to obtain the hourly solar irradiance at ground level, the hourly wind speeds at heights of 20 meters above the ground, and the ambient temperature. From the research portal of *MeteoSwiss*, 15-minute solar irradiance at ground level and ambient temperature were obtained; in calibration and validation scenarios, only real weather data were used.

4.1.2 Agent-based model of building occupants' behavior

The population of building occupants was generated in *EnerPol*'s agent-based population model. Additionally, the agent-based daily activity model was used to simulate the daily routines of the building occupants, with a temporal resolution of 15 minutes, to determine where an agent was at each time of the day; in particular, whether he/she was at home. Subsequently, the time and duration of building occupants' activities that have an impact on heat demand, such as sleeping, waking up, showering, and cooking, were simulated. These occupants' activities were modeled as in the electricity demand model.

Each demographic of the population has a preferred ambient comfort temperature, as reported in [108] (elderly people) and [109] (males and females); stochastic perturbations in the preferred comfort temperature were introduced through a normal probability distribution of comfort temperatures, centered on the preferred comfort temperature of

each demographic. Thus, based on the mix of building occupants, the ambient comfort temperature, as well as the nighttime setback of ambient temperature for comfort and environmental reasons [110], of each dwelling were determined. Thereby, the timing and duration of showering were also determined for each building occupant. The daily household consumption of domestic hot water was taken as 45 liters per occupant for single-household buildings, and 40 liters per occupant for residential buildings with multiple dwellings and other typologies of households [111]. The characteristics and behavior of the building occupants were subsequently used in the modeling of the time-varying heat demand in each residential building.

4.1.3 Agent-based heat demand model

Space heating, Q_u^{SH} , and heating of domestic hot water, Q_u^{DHW} , constituted the hourly total heat demand of a residential building, Q_f^{SH+DHW} . The thermal efficiencies of the space heating (η_{SH}) and the domestic hot water systems (η_{DHW}), in Equation (4.1), were specified as a function of the type of heating system and the build year of the building. The hourly space heating demands, Q_u^{SH} and Q_u^{DHW} , were calculated by solving a heat balance equation where various heat fluxes inside and across building boundaries were modeled as heat sources or sinks of heat, as shown in Figure 4.3.

$$Q_f^{SH+DHW} = \frac{Q_u^{SH}}{\eta_{SH}} + \frac{Q_u^{DHW}}{\eta_{DHW}} \quad (4.1)$$

Thereby, the approach described in [102, 103, 104] was adapted to account for the agent-based modeling of the occupants of buildings and of the buildings themselves. Therefore, the heat transfer across building surfaces – that is roof, walls, and windows –, Q_T , the ventilation losses, Q_V , the heat gain from solar radiation through windows, Q_S , the heat gain from electrical appliances, Q_E , and the heat gain from building occupants, Q_p , were modeled as a function of buildings' occupants.

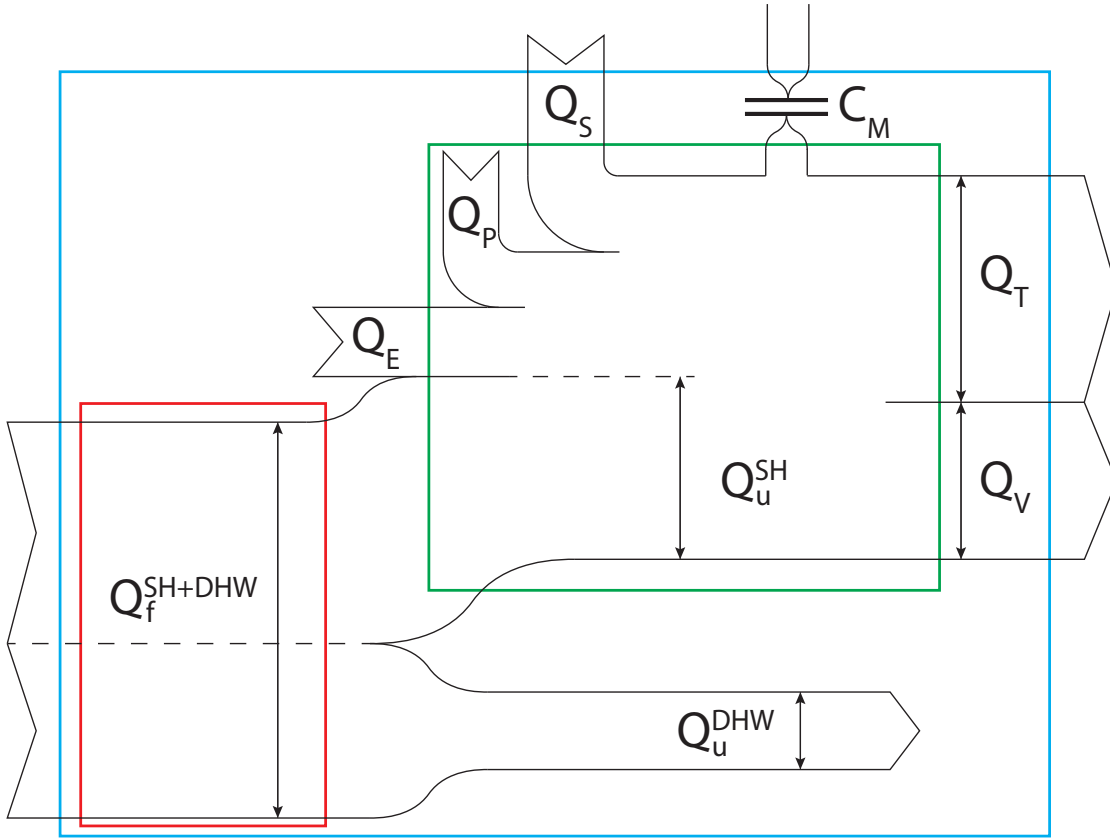


Figure 4.3: Modeled heat fluxes, inside the building, and across system boundaries (green: building heated area; red: space heating and hot water system; blue: building boundaries). The thermal inertia of the building is accounted for using the capacitance in an electrical analog circuit (based on [102]).

The heat transfer Q_T accounted for the conduction, convection, and radiation that arise across building surfaces due to the difference between the ambient temperature inside a building and the temperature external to the building. The overall heat transfer coefficient of a building surface was given by

$$U = \frac{1}{\frac{1}{h_{in}} + R + \frac{1}{h_{out}}} \quad (4.2)$$

The conduction resistance, R , was specified as a function of the building's build year and the type of wall [55]; typical conduction resistances are shown in Table 4.3. The internal convection and radiation coefficient h_{in} and external radiation coefficient $h_{out, radiation}$

were assumed to be constant (respectively, $9.1 \text{ W}/(\text{m}^2 \cdot \text{K})$ and $5 \text{ W}/(\text{m}^2 \cdot \text{K})$ [102]), whereas the external convection coefficient, $h_{out,convection}$, was evaluated as a function of the local wind speed and the terrain surrounding the building [57].

$$h_{out} = h_{out,convection} + h_{out,radiation} = 3 \cdot u_{w,local} + 2.8 + h_{out,radiation} \quad (4.3)$$

$$\text{where } u_{w,local} = u_{w,20m} \cdot \beta \cdot \left(\frac{z}{20}\right)^\alpha$$

In Equation (4.3), the local wind $u_{w,local}$ speed at the half-height of the building was extrapolated from the predicted wind speed at 20 meters above ground level, where α and β were coefficients related to the surrounding terrain and z is the building's half-height.

Table 4.3: Example conduction resistances used in the agent-based heat demand model [55]

Build Year	Type of Wall	Conduction resistance [$\text{m}^2\text{K}/\text{W}$]		
		R_{env}	R_{roof}	R_{win}
Before 1918	Rough stone	0.90	1.84	0.34
1919-1945		0.89	2.34	0.34
1961-1970	Insulated,	0.81	1.26	0.34
2001-2010	armed concrete	1.80	2.06	0.42

The ventilation losses, Q_V were given by the product of the hourly ventilation rate, the energy-consuming area, the heat capacity of air, and the density of air at the altitude of the building. The ventilation rate, Equation (4.4), accounted for the ventilation behavior of building occupants; the ventilation share of each member of the household, f_{share} ; the build year; and infiltration ($n_{V,infiltration} = 0.1 \cdot 10^{-3} \frac{\text{m}^3}{\text{m}^2\text{s}}$). The ventilation behavior of building occupants was established based on survey data [112], some outcomes of which are summarized in Table 4.4. For building occupants who ventilate more than once a day, two to five 10-minute-long ventilation events were assigned; the probability of the occurrence of a ventilation event was uniform over the day; and, thus, the durations of the ventilation events, T_{window} , were defined.

$$n_{V,total} = \sum_i^{Household} (n_{V,infiltration} + n_{V>window} \cdot f_{share}) \quad (4.4)$$

with $n_{V, window} = 0$ *if* $t \notin T_{window}$
and $n_{V, window} = 5.7 \cdot 10^{-3} \frac{m^3}{m^2s}$ *if* $t \in T_{window}$

Based on survey data, 10% of buildings were assumed to have a mechanical ventilation system, and for these buildings, the ventilation rate was assumed to be independent of the behavior of building occupants. Further, as the quality of insulation has improved over time (Figure 4.4), the ventilation rate in mechanically ventilated buildings was specified as a function of the building's build year [55].

The archetype of the building was accounted for in the determination of the heat gain from solar radiation through windows, Q_S . Specifically, depending on the measured solar gains of typical Swiss archetypes [113] the measured or predicted solar radiation was scaled up or down.

The heat gain from electrical appliances, Q_E , Equation (4.5), varied as the appliances were used by each building occupant.

$$Q_E = \sum_i^{Household} load_{t,i} \cdot Q_{E,max} \cdot f_{share} \cdot f_{correction} \cdot A_{eca} \quad (4.5)$$

Following [102], the maximum heat gain from electrical appliances ($Q_{E,max}$) was 8 W/m. To model the temporal variability of the heat gain, an hourly load profile, $load_t$, that ranged from 0.1 to 1 was specified; the amplitude of this profile was randomly applied to each member of the household, whose presence in or absence from the building was

Table 4.4: Shares of buildings relative to the behavior of building occupants [112].

Behavior	Share of buildings [%]	Behavior	Share of buildings [%]
Occupants ventilate once a day	47	Occupants ventilate before sleeping	52
Occupants ventilate more than once a day	53	Occupants do not ventilate before sleeping	48

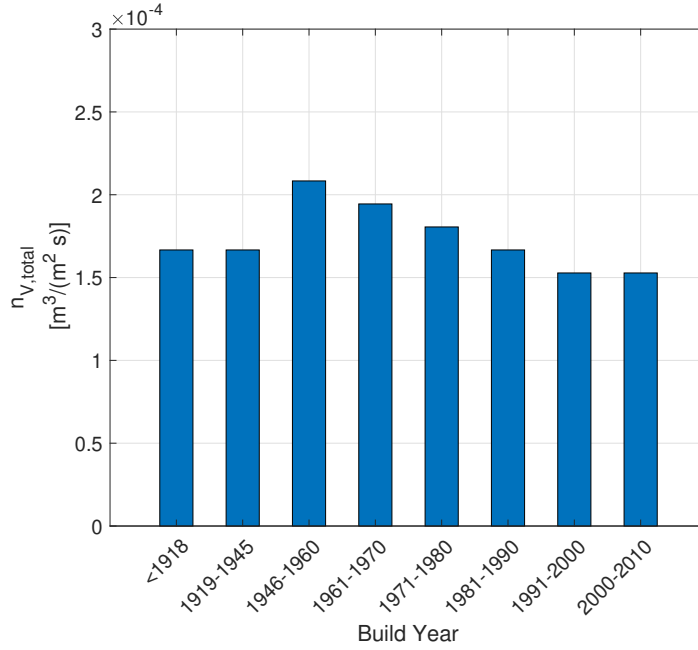


Figure 4.4: Modeled hourly ventilation rate as a function of build year for mechanically ventilated buildings [55].

denoted by f_{share} . To ensure that the annual time history of the heat gain was equal to the data reported in [102], a correction factor $f_{correction}$ was applied.

The heat gain from building occupants, Q_p , was specified as 70W per person [102].

In the heat balance equation, the thermal inertia of the buildings was accounted for by using an electrical analog circuit, in which the thermal capacity of the building was represented by the capacitance C_m , as schematically represented in Figure 4.3. The building was modeled as a simplified resistor-capacitor circuit as described in SIA norm 2044 [104] and accordingly sketched in Figure 4.5. In the figure, different building components are represented as circuit nodes and are characterized by different temperatures, whereby T_{air} was the indoor air temperature; $T_{air}^{external}$ was the outdoor air temperature; $T_{central}$ and $T_{central}^{external}$ combined air temperature, mass temperature, and surface temperatures of light building parts (windows) inside and outside of the buildings, respectively; $T_{thermal\ mass}$ and $T_{thermal\ mass}^{external}$ were temperature of heavy building parts (walls and roof) inside and outside of the buildings, respectively. $H_{ventilation}$, $H_{transmission}$, H_1 , and H_2 were heat transfer coefficients between nodes that were recalculated at each time step. The heat gains toward air, light building parts, and heavy building parts were symbolized by Q_{air}^{gain} , $Q_{central}^{gain}$, $Q_{thermal\ mass}^{gain}$. C_m and A_m were the building heat capacity and its associated area.

The nodes were connected by five resistances; these represented building materials and systems whose heat transfer coefficients were derived from previously described building properties and re-calculated at each time step, as described in detail in [114]. The solar heat gains and internal heat gains were distributed among the indoor nodes. Finally, the building mass area (A_m) and internal heat capacity (C_m) were modeled as a function of the energy-consuming area, according to [104]. Thereby, it was assumed that all buildings were thermally medium-heavy, and the air stream temperature accounted for infiltration [104]. Once all parameters were quantified, a numerical finite difference method (*Crank-Nicholson* scheme) was applied at each hourly time step to calculate all temperatures of Figure 4.5 and to find Q_i^{SH} such that T_{air} was equal to the indoor comfort temperature.

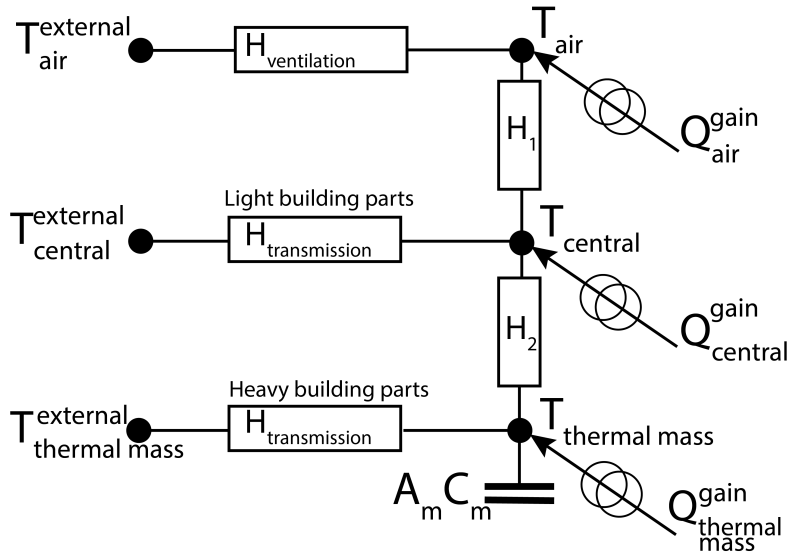


Figure 4.5: Resistor-capacitor circuit model used to account for the thermal inertia of buildings in the heat demand model; adapted from architectural norm [104].

The heating of domestic hot water, Q_u^{DHW} , was given as

$$Q_u^{DHW} = \sum_i^{Household} (V_{shower,t,i} + V_{other\ draws,t,i}) \cdot \Delta T \cdot c_p \cdot f_{share} \quad (4.6)$$

with $V_{shower,t,i} = 0$ *if* $t \notin T_{shower}$

whereby showering and smaller draws of water were differentiated, and the presence or absence of building occupants was accounted for. The shares of the daily consumption of domestic hot water were based on [115] and are summarized in Table 4.5. The annual consumption of domestic hot water in each household was based on the average daily consumption of the household members as previously discussed; to account for the seasonal variation in the consumption of domestic hot water, the daily consumption over a year had a sinusoidal variation that was maximum in mid-winter. Lastly, as domestic hot water is usually stored in a hot water tank, a water heater, for which the maximum power was defined such that the daily consumption of domestic hot water could be supplied with 16 hours of full-load operation, was implemented to account for the difference between the time when energy was used to heat the water and the time when the hot water was consumed.

Table 4.5: Summary of type and share daily consumption of domestic hot water. Source: [115]

Type of draw		Share of daily usage [%]
Shower		50
Other draws	Kitchen	29
	Bathroom	21

4.1.4 District heat predictive model

Figure 4.6 illustrates a schematic of the workflow process that couples the agent-based heat demand model, the predictive agent-based building model, and the routing of the extended DH network.

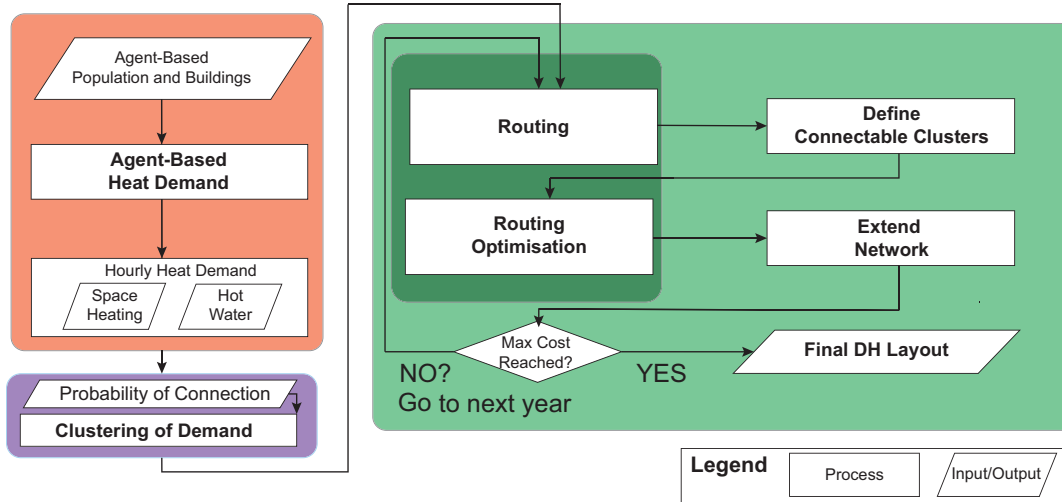


Figure 4.6: Schematic of the workflow process, coupling the agent-based heat demand model (red), the predictive agent-based building model (purple), and the routing of the extended DH network (green), that is integrated into the *EnerPol* framework.

The likelihood of a building being connected to a DH network was described on the basis of a logistic regression model. Such models are well suited for problems in which one needs to find the probability of any event occurring/not occurring or being true/false. Moreover, in logistic regression models, categorical predictors, such as the characteristics of a building (*e.g.*, the type of heating system) may be used. In this work, residential buildings were differentiated by their characteristics, which are summarized in Table 4.2; therefore, in areas where the DH network was operational, a relationship between the characteristics of the buildings and the buildings connection or non-connection to the DH network was sought. The initial dataset comprised 2,210 buildings (that is, all buildings located in zones where DH was already operational). After filtering out buildings with incomplete information, the regression matrixes were built upon 1,123 building entries, which was considered an adequate sample size.

Thus, a stepwise approach was used, whereby from an initial step in which all characteristics of the buildings were considered, in subsequent steps the relevance of a characteristic in the evaluation of the probability of connection was determined. Thus, the

logistic regression model yielded a relationship of the form

$$p(x_1, x_2, \dots) = \frac{1}{1 + e^{B_1x_1 + B_2x_2 + \dots}} \quad (4.7)$$

where p was the probability of connecting to the DH network, and the coefficients B_i were the regression coefficients.

To guarantee statistically meaningful results, the following conditions were verified:

- Predictors were expressed as intervals; categorical predictors were converted into numeric variables by defining dummy numerical intervals;
- Predictors were independent of one another; therefore, covariance between regression coefficients was verified;
- The sample size was adequate (> 50 records per predictor); and
- The statistical significance of the determined regression coefficient was evaluated by calculating the p-value associated with each coefficient; the null hypothesis was discarded if a p-value was smaller than 0.05.

4.1.5 District heat routing model

A routing algorithm was developed to optimally extend the existing DH network. The routing of the extended DH network was obtained with a Dijkstra-based algorithm. The nodes of the Dijkstra graph were the centroids of clusters which comprised the residential buildings on each 50-meter-long road segment. The edges of the Dijkstra graph were the road segments between the centroids (Figure 4.7).

Thus, the current practice of laying DH pipelines under roads was captured in the routing. The weights of the edges were formulated as shown in Equation 4.8, such that the potential revenues of the DH that was going to be supplied were more favorable and that CAPEX and OPEX (C_{Inv} and C_{Maint}) and the renovation of recently installed or upgraded road and gas infrastructure were less favorable.

$$Weight = -C_{Inv} - C_{Maint} + Revenues \pm Factor_{Roads} \pm Factor_{Gas} \quad (4.8)$$

In the extension of the DH network, short-path extensions were limited to a length of 2 km; subsequent new clusters were connected to the existing network, and unprofitable clusters were discarded.

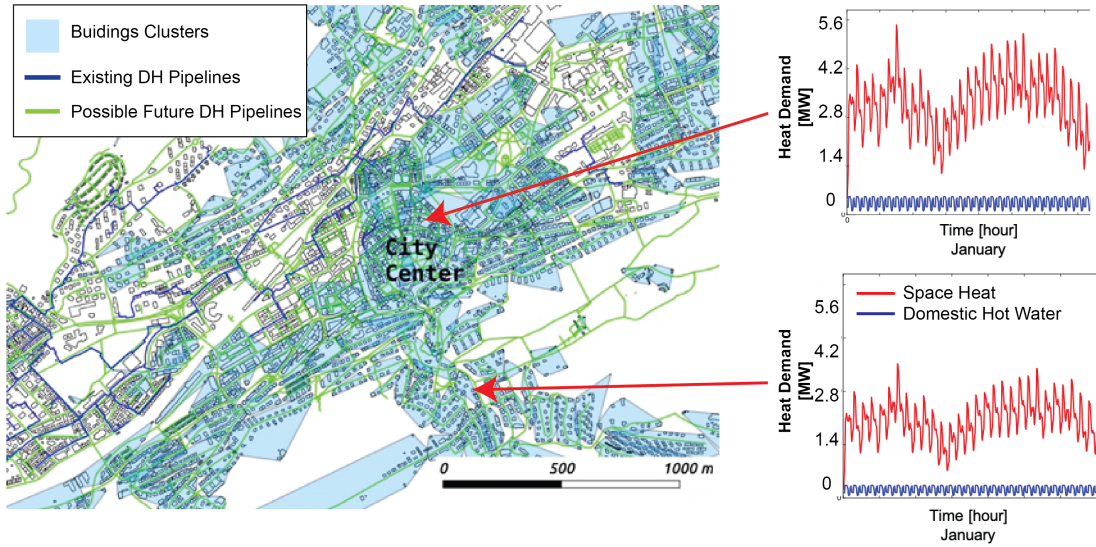


Figure 4.7: Examples of residential building clusters and representative profiles of space heating and heating of domestic hot water.

4.2 Scenarios

Two different scenarios were assessed, whereby the DH pipeline routing model was run by setting different goals.

1. *Demand-driven* scenario: The extended DH network was routed such that all buildings within a cluster and within 30 meters of future DH pipelines could connect to the DH network.
2. *Predicted-demand-driven* scenario: The extended network was routed such that only buildings with a connection probability of more than 50% and within 30 meters of future DH pipelines connected to the DH network.

It is worth noting that, in the former scenario, only buildings with more than 50% probability of connection did connect to the extended network; thus, it is these buildings that were considered in the assessment of the profitability of network extension in the demand-driven scenario. The extension of the DH network was considered over a five-year period.

4.3 Results

The results section is structured as follows: In the first section, the model predictions are compared with data on the actual DH production profile in the investigated city. In the second section, the outcome of the predictive model is analyzed and the probability of connection to future DH pipelines quantified. In the third section, the results of the DH extension scenarios (*demand-driven* and *predicted-demand-driven*) are illustrated.

4.3.1 Impact of individual behaviors on heat demand prediction

Figure 4.8 compares the actual and predicted hourly heat demand in the city for the year 2017. It can be seen that there is good qualitative agreement between the predictions and measurements, and the predictions captured well the trends that are seen in the measurements. Quantitatively, the predictions had over- and under-shoots compared to the measurements; the mean difference between the predictions and measurements over the year was -4.8%.

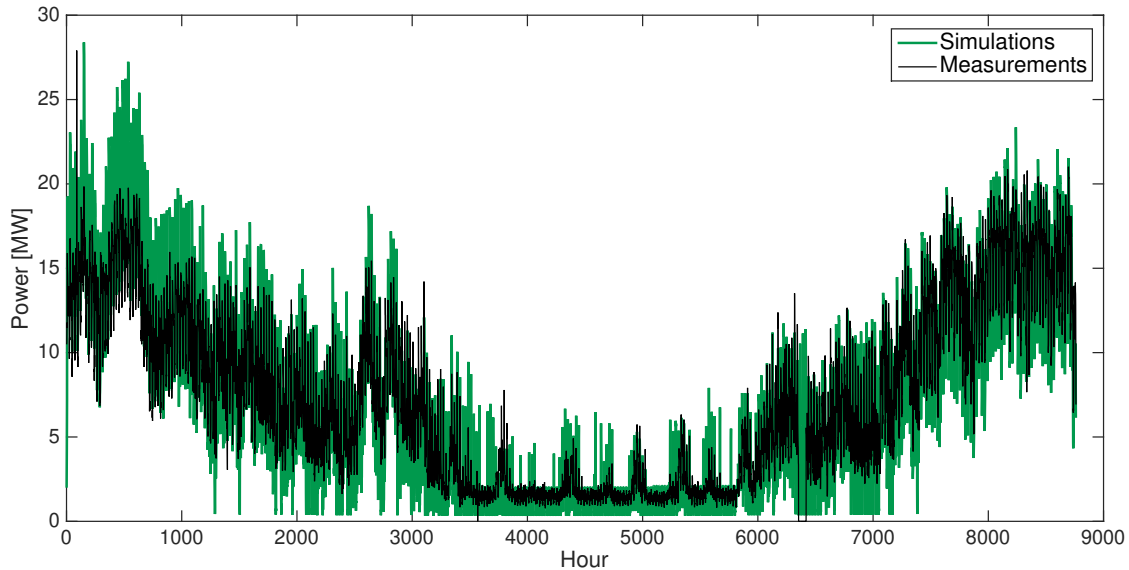


Figure 4.8: Comparison of the actual and predicted hourly heat demand in the city for the year 2017.

Figure 4.9 compares, for a three-day period in winter 2017, the actual and predicted hourly heat demand in the city. The predictions from three variants of the heat demand model:

- *without agent-based modeling (NA)*: in this scenario, only weather data varied over time, while heat fluxes that depended on occupants behavior were constant over time and only a seasonal trend was applied on DHW demand;
- *with modeling behavior of occupants (OB)*: in this scenario, the impact of occupants behavior on the heat fluxes was modeled; no storage of DHW was modeled; and
- *with OB and storage of domestic hot water (DHWS)*

are shown. Also highlighted in Figure 4.9 are the overnight decrease in heat demand and the morning peak in heat demand, which are respectively indicated by the arrows numbered 1 and 2. It is evident from the comparison that, while the heat demand model without agent-based modeling (NA) did account for the time-varying weather conditions, this variant of modeling heat demand did not capture as well the variations in actual heat demand that were due to the behavior of the occupants of buildings. On the other hand, the heat demand models OB and DHWS did capture these variations better. Indeed, the overnight minima in heat demand, highlighted by arrow 1, that were observed in the measurements were qualitatively captured by both ABMs. However, quantitatively, both models overestimated the magnitude of the minima. It is thought the overestimation arose as, in newer buildings with better insulation, a nighttime setback temperature need not to be used, whereas in the present work 80% of all buildings were assumed to use a nighttime setback temperature. The increase in heat demand due to the morning ablutions of the occupants of buildings, highlighted by arrow 2, was captured by the ABMs. The quantitative agreement in the magnitude of this morning heat demand was substantially improved when the storage of domestic hot water was accounted for.

Hence, accounting for the behavior of building occupants improved predicted heat demand; the ABMs were better able to capture the evening peak in demand, when building occupants return home.

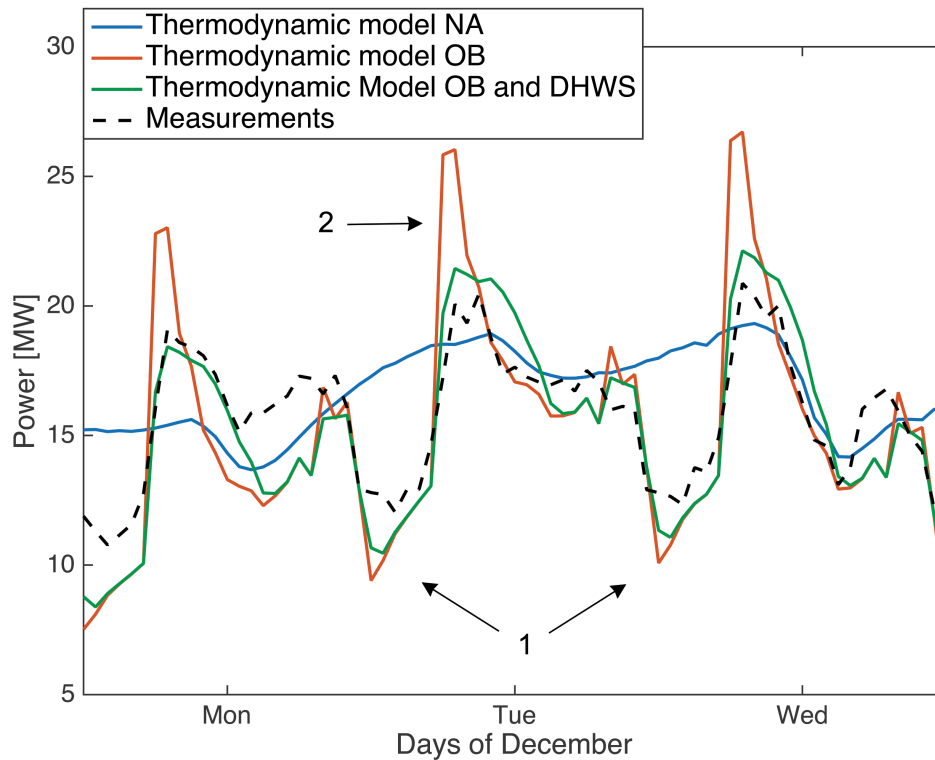


Figure 4.9: Comparison of the actual and predicted hourly heat demand in the city for a winter week in 2017. Predictions from three variants of the heat demand model are shown: without agent-based modeling (NA); with behavior of occupants (OB); and with behavior of occupants and storage of domestic hot water (OB and DHWS). Arrows 1 and 2 indicate the overnight decrease in heat demand and the morning peak in heat demand, respectively.

Table 4.6 summarizes the test statistics of the three variants of the heat demand model in terms of the root mean square deviation, the Pearson's correlation coefficient, and the mean relative error. The root mean square deviation, which was normalized by the range of the measured data, and the correlation coefficient were reported for each season, whereas the mean relative error was reported for the whole year. The correlation coefficients showed that, for all seasons, the ABMs yielded a more precise representation of the dynamics of the heat demand. Indeed, the ABM that accounted for both the behavior of occupants and storage of domestic hot water had correlation coefficients greater than 82% for spring, fall, and winter. As less space heating is required in the summer, the correlation coefficient of 53%, while larger than for the ABM that accounted only for the behavior of occupants, indicated that the modeling of the demand for

domestic hot water in the summer can be further improved. One possible improvement is to account for the fact that less domestic hot water is required in summer. The root mean square deviations quantified that the ABMs more accurately simulated the hourly heat demand. This improved modeling was most evident in spring, fall, and winter, which accounted for 94% of the annual heat demand. Overall, it can be seen that the magnitude of the annual mean relative error of -4.8% in the ABM that accounted for both the behavior of occupants and storage of domestic hot water was a 25% improvement over the heat demand model without agent-based modeling.

Table 4.6: Comparison of the test statistics of the three variants of the heat demand model: without agent-based modeling (NA); with occupants' behavior (OB); and with behavior of occupants and storage of domestic hot water (OB and DHWS).

	Annual Mean Relative Error [%]	Normalized Root Mean Square Deviation [%]				Pearson's correlation coefficient [-]			
		Spring	Summer	Fall	Winter	Spring	Summer	Fall	Winter
NA	6.5	16.2	13.2	13.9	15.6	0.73	0.42	0.81	0.60
OB	-4.8	18.8	25.8	16.1	14.3	0.80	0.44	0.84	0.78
OB and DHWS	-4.8	15.6	14.3	13.3	11.3	0.82	0.53	0.89	0.84

Furthermore, the -4.8% annual mean relative error of the ABM that accounted for both the behavior of occupants and storage of domestic hot water was substantially smaller than the errors in the range of 7% to 21% for other urban building energy models [116]. The good qualitative and quantitative agreement between predictions and measurements that are presented above validate our novel agent-based simulation methodology.

4.3.2 Findings on likelihood of connection of buildings to district heat network

As shown in Table 4.7, based on the characteristics of buildings in the city, the build year, the building's type of heating system, the installation year of the heating system, and the ownership of the building were identified as being the most relevant explanatory variables that quantified the likelihood of a building being connected to the DH network. These most relevant characteristics were identified using the predictive agent-based building model, with exclusion criteria of p-value and covariance being respectively greater than 5% and 0.5 being used in each step of the model.

In a first step, all characteristics of buildings included in the digital twin (Table 4.2) were considered to be potentially relevant and evaluated in the regression. Besides properties that were directly related to heat demand calculation (*i.e.*, building type, build year, and heated surface), data on multi-utility customers (*i.e.*, annual heat consumption, heating system type, and installation year of the heating system) and on building ownership were included in the regression. Despite the expected redundancy of some parameters (for instance, building heated surface and annual heat demand), the approach chosen was to let the regression model confirm or deny the unsuitability of these parameters in forecasting a future connection. This was achieved by running a stepwise regression where, in each step, a predictive variable was (re-)considered for addition or elimination from the set of considered predictive variables. The characteristics of buildings excluded from the regression are reported in Table 4.7 as well.

Table 4.7: Candidate and most relevant explanatory variables used and identified in the predictive agent-based building model.

Variable	First Step			Last Step		
	Bi	p-value [%]	Covariant	Bi	p-value [%]	Covariant
Building type, X1	-1.15	1	None	Removed		
Build year, X2	-2.35	<0.01	None	2.58	<0.01	None
Heated surface, X3	2.16	<0.01	B4	Removed		
Annual heat demand, X4	-1.55	0.01	B3	Removed		
Type of heating system, X5	1.76	<0.01	None	1.60	<0.01	None
Installation year of heating system, X6	-2.76	<0.01	None	-2.50	<0.01	None
Ownership of building, X7	-1.55	<0.01	None	-1.31	<0.01	None

The most relevant explanatory variables were used to quantify the likelihood of each building in the city being connected to an expanded DH network. Figure 4.10 shows an example of the probability of connection for buildings in a part of the city. The probabilities varied as a function of the characteristics of the buildings. For example, in Figure 4.10, Building A had a 100% probability of connection, as this publicly owned building had a 35-year-old heating system. On the other hand, the privately-owned, residential Building B that had a 5-year-old heat pump had a 0% probability of connection.

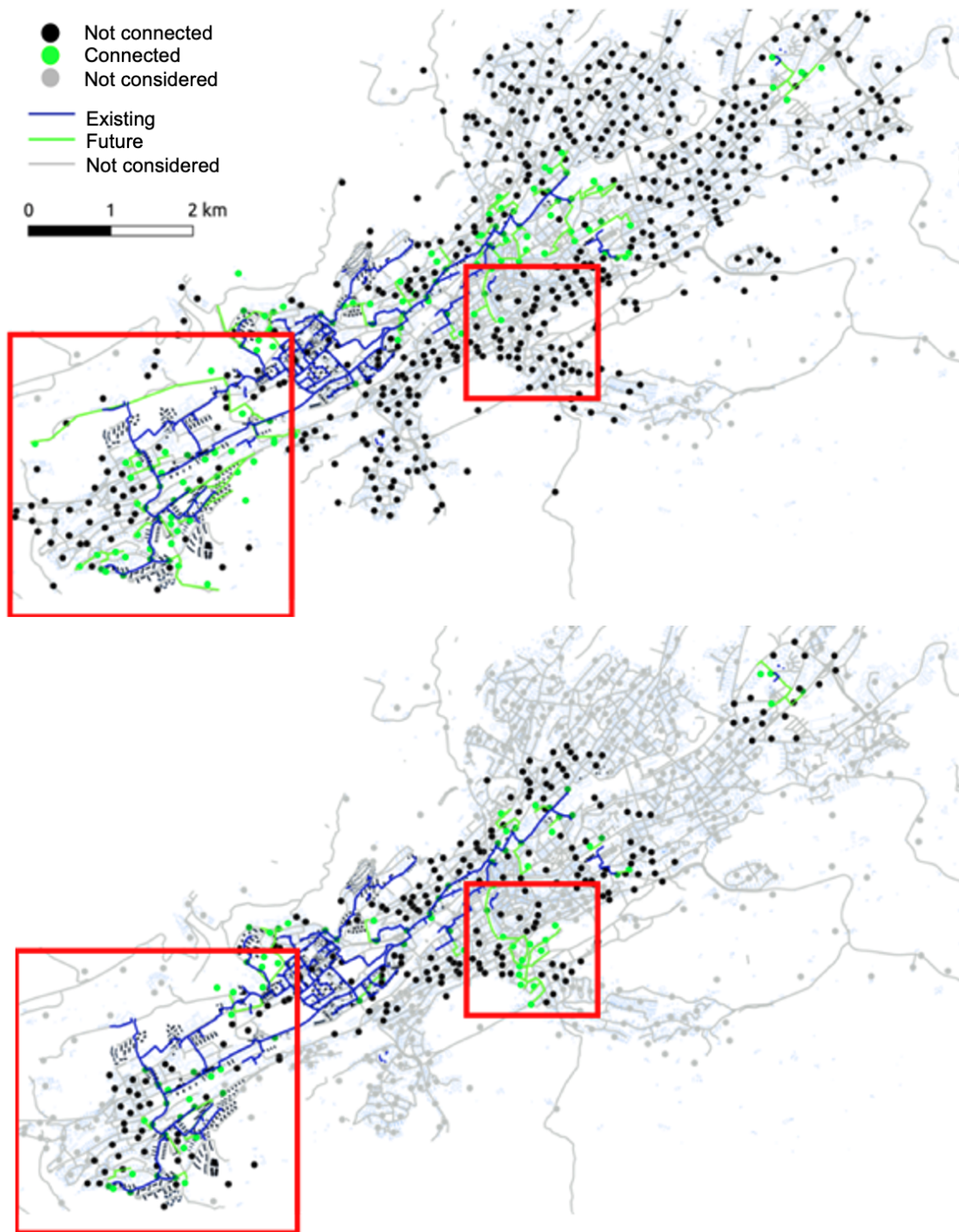


Figure 4.11: Comparison of the expanded DH network in the demand-driven scenario (upper plot) and the predicted-demand-driven scenario (lower plot). The red squares highlight the areas where the expanded DH networks are substantially different.

The CAPEX and OPEX costs associated with the network expansion are summarized in Figure 4.12. It can be seen that the more extended network of the demand-driven scenario did not always generate larger CAPEX costs than the less extended network of the predicted-demand-driven scenario. This is because the CAPEX accounted both for the length of the installed DH pipelines and the type of road under which the pipelines were laid. Moreover, the CAPEX costs increased in relation to the distance from the DH plant, because larger drops in pressure must be overcome. Since OPEX costs depended on the amount of DH that was supplied, the predicted demand-driven scenario generally had larger OPEX costs. The larger OPEX costs did not necessarily imply lower profitability, as the expected larger revenues of the predicted demand-driven scenario could compensate for the larger OPEX costs.

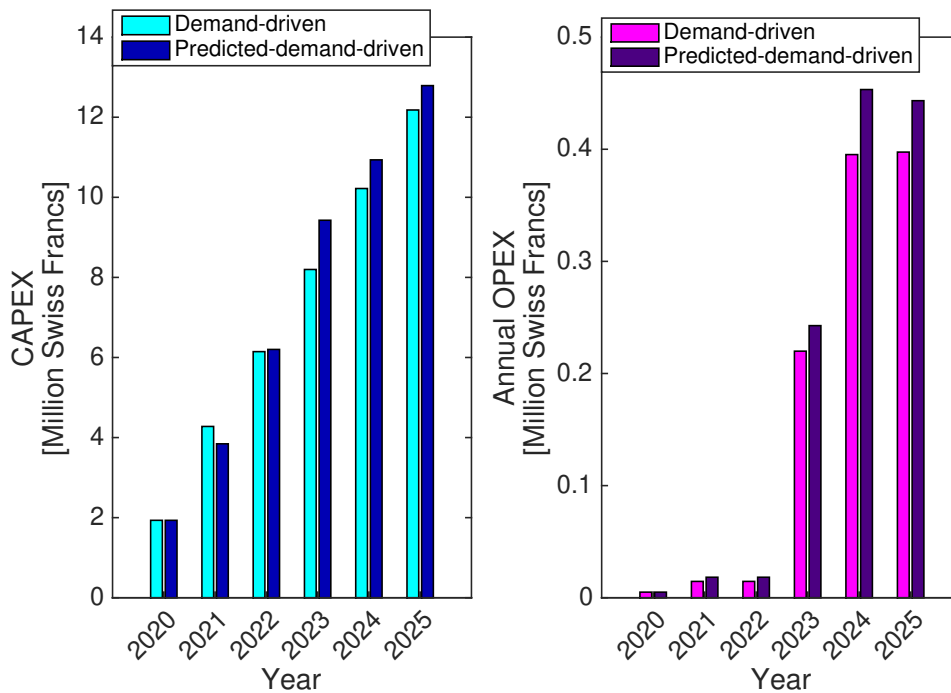


Figure 4.12: Comparison of the annual CAPEX and OPEX for the expanded DH networks in the demand-driven and predicted-demand-driven scenarios.

Figure 4.13 compares the annual profits and IRR of the DH networks in the demand-driven and predicted-demand-driven scenarios. Negative IRRs are not shown in Figure 4.3. In the assessment of profitability, the new network was considered; moreover, as is common for infrastructure projects, the financial metrics were evaluated over a 50-year time horizon. For the demand-driven and predicted-demand-driven scenarios, the annual profits increased from 0.01 million Swiss Francs in 2020 to respectively 1.03 and 1.18

million Swiss Francs in 2025. The maximum IRRs were respectively 5.3% and 6.7%, and the IRRs were positive from 2023 and 2021, respectively. The lower IRR in the former scenario could be explained as follows: In the demand-driven scenario, the DH network was expanded to buildings that were theoretically profitable, but possibly expensive, to reach; however, the investment costs were less compensated by the revenues, as the buildings did not necessarily get connected to the expanded DH network. On the other hand, in the predicted-demand-driven scenario, the DH network was expanded to buildings that were likely to be connected; therefore, the revenues compensated for the investment costs. Thus, the predicted-demand-driven scenario provided a more compelling business case, as the expanded DH network was more profitable and yielded a 25% higher return on investment.

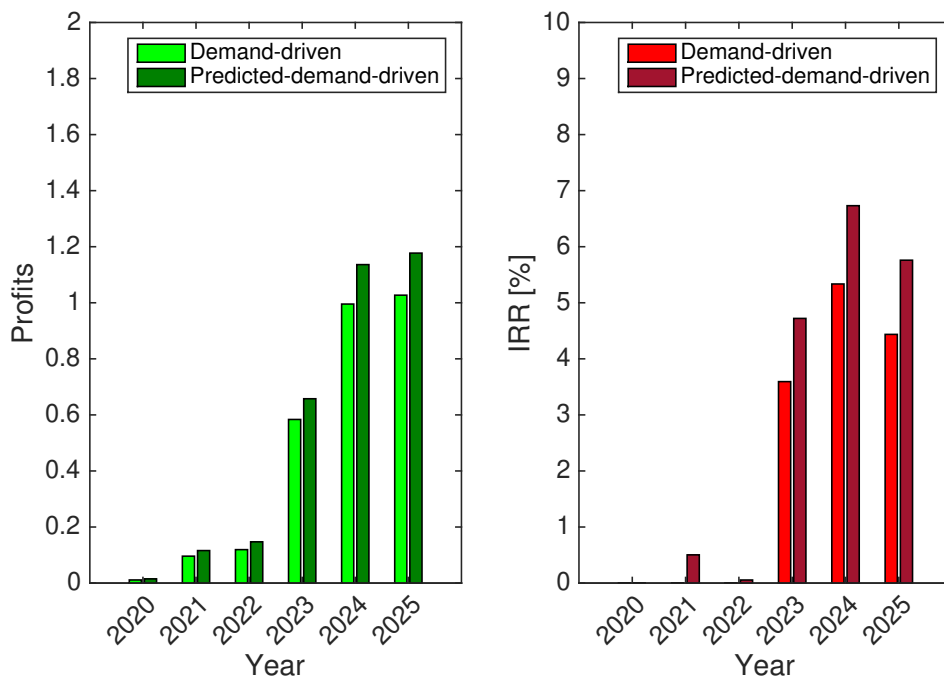


Figure 4.13: Comparison of the annual profits (left) and IRR (right) of the DH network in the demand-driven and the predicted-demand-driven scenarios.

Chapter 5

Case Study: Electricity

The increased penetration of e-mobility and the decarbonization of the building stock through the usage of heat pumps will have a direct impact on the distribution grid. Moreover, future population dynamics and urban transformations, such as an increasing and aging population and the creation of new one-person dwellings, will entail changes in the electricity demand, both in magnitude and in time. To ensure a stable operation of the network, power flow simulations can determine whether the current distribution grid layout will be able to cope with these changes in the future.

A bottom-up electricity demand model, in combination with the developed bottom-up heat and e-mobility demand models, has been developed and used to assess future scenarios. The motivation for its development was twofold: (i) such a model gives the necessary spatial and temporal resolution to quantify the increase in load at the neighborhood level and its impact on the local distribution grid, and (ii) the usage of ABMs allows the integration of behavioral and cultural patterns that, upon calibration, could deliver more realistic results compared to an approach only based on architectural norms and standards.

The results indicate that the implementation of location-specific behavioral patterns improves the overall demand predictions and that a bottom-up ABM is more suitable to assess the impact of the energy transition compared to a top-down-based approach. The results also identify areas of the city where the distribution grid experiences the largest increases in load.

The methodology of the electricity demand model was partly developed by the present author and partly developed by D. Haegel during a semester project supervised by the present author, as reported in Chapter “Student Projects Supervised”.

5.1 Methodology

Similarly to the case of the heat demand model, the outcomes of the ABMs were used as the main inputs of the electricity demand model. Likewise, elements of the digital twin of the built infrastructure were used to further characterize the electricity demand of buildings. An overview is presented in Table 5.1. Moreover, the outcome of the agent-based daily activities model was extended by a set of activities taking place at home, such as sleeping, cooking, and washing. Their implementation is detailed below.

Table 5.1: Outcomes of agent-based and elements of digital twin used by the electricity demand model

Source	Attributes
Agent-based population model	Households' size, structure, and household members' ages Job, workplace location
Agent-based daily activities model	Agents' presence time at home and at the workplace, as well as characterization of other daily activities (leisure, education, shopping, or business)
Digital twin of built infrastructure	3D building model, building end-use, energy-consuming area Electricity distribution grid

The electricity demand of a building was obtained by modeling its base and peak (or activated) load. The base load is the electricity consumption produced by electrical appliances and building services with automated control systems, such as fridges, and was therefore independent of building occupants' behavior. The variable load is electricity consumption caused by devices that are actively switched on by occupants, such as electric stoves, and was therefore dependent on occupants' behavior.

The approach chosen to model the activated load in the electricity demand model is twofold:

- For residential and office buildings, the electricity demand was mainly modeled using an agent-based physical approach – that is, the daily activities of the agents were directly converted into electricity demand. The correlations between agent daily activities and electricity demand were believed to be clearer for residential [117] and office buildings [118] than for other building types. Moreover, the demand patterns across residential and office buildings were assumed to be more homogeneous. Therefore, physical models have been developed and tested for these two building categories.
- For other building types, the results of the smart meter data analysis – in particular, the typical normalized power demand profiles and the distributions of base

load demand reported in Section 2.3.3 – were utilized together with standard values from architectural norms to estimate the electricity demand.

The final result was the electricity demand of each building with a quarter-hourly time resolution.

It is worth noting that the electricity demand for residential buildings alone accounts for 33% of the Swiss [119] and 29% of the EU's [120] electricity demand. The service sector accounts for 27% of the Swiss [119] and 27% of the EU's electricity demand [120], with office buildings covering one of the largest shares of it [121]. The electricity demand breakdown for residential and office buildings located in Switzerland is presented in Figure 5.1 and Figure 5.2, respectively. The agent-based modeling of the different energy end-uses in residential and office buildings is explained in detail in Sections 5.1.1 and 5.1.2, respectively.

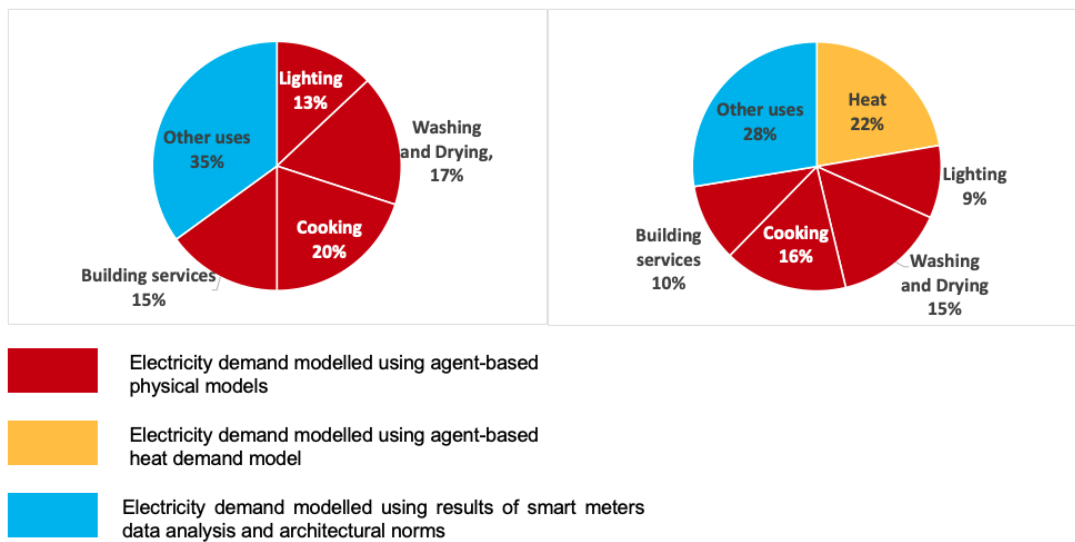


Figure 5.1: Percentage breakdown by end-use of electricity demand in a multi-family residential building in Switzerland – without (left) and with (right) electric space and hot water heating system. Source: [122]

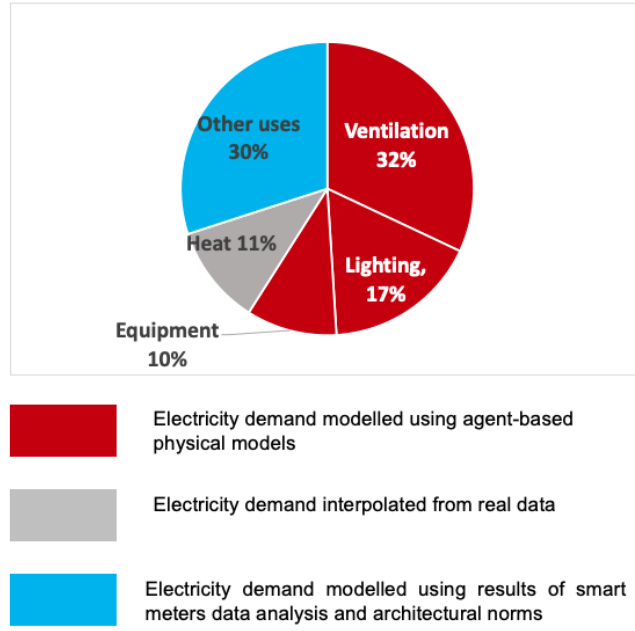


Figure 5.2: Percentage breakdown by end-use of electricity demand in an office building with electric space and hot water heating system. Source: [123]

5.1.1 Agent-based model of electricity demand of residential buildings

The electricity demand of a single-family or multi-family residential building was computed according to Equation (5.1). The demand for lighting, cooking, washing & drying, other uses, and heat depended on the occupant's behavior and included ABMs and was, therefore, time dependent. The demand for building services was solely dependent on the number of dwellings of a building (30W/dwelling [122]).

$$P^{Residential}(t) = \sum_{Dwellings} \left(P_{light,dwelling}(t) + P_{cooking,dwelling}(t) + P_{washing-drying,dwelling}(t) + P_{other\ uses,dwelling}(t) \right) + P_{Heat}(t) + P_{Base} \quad (5.1)$$

The modeling of P_{light} , $P_{cooking}$, and $P_{washing-drying}$ is detailed below. $P_{other\ uses}$ accounted for the electricity consumption of various appliances, such as entertainment devices, laptops and phone chargers, computers, vacuum cleaners, and hair dryers. It was modeled by linearly scaling a standard variable load of 1.0 W per square meter of energy-demanding area [103] by the share of household members at home and awake.

For residential buildings with electric SH or DHW system, P_{Heat} was obtained from the heat demand model (Section 4.1).

Demand for lighting in residential buildings

The activation of artificial lighting inside a residential building depended on the indoor natural light intensity (ELI), which was measured in lux. The external solar radiation, obtained from the WRF model [106], was converted into indoor natural light intensity using Equation (5.2) (Igawa's luminous efficiency model [124]), which accounted for the photosensitivity of the human eye to different light wavelengths. In Equation (5.2), h is the time- and location-dependent solar zenithal angle, Irr is the external solar radiation in W/m^2 , and DH is a factor that accounts for the number of windows and the cardinal direction of rooms. DH was assumed to be 5% for all buildings [125].

$$ELI = ((9 \cdot h + 210) \cdot Irr^{0.9} + (-11 \cdot h^4 + 54 \cdot h^3 - 102 \cdot h^2 + 90 \cdot h - 29) \cdot Irr^{1.1}) \cdot DH \quad (5.2)$$

Artificial lighting was required when ELI dropped below a threshold of 400 lux [126, 127]. For the increase in demand for lighting to gradually decrease with ELI , the factor f_{light} was introduced (Equation (5.3))

$$f_{light}(t) = CDF \left(\left(3 - \frac{6}{100} \right) \cdot (ELI(t) - 400) \right) \quad (5.3)$$

where CDF is the standard normal cumulative distribution function.

The demand for lighting was the multiplication of the averaged installed lighting capacity of a building ($0.8 W/m^2$ [126, 127]) by a factor related to the building occupancy at a given time ($f_{occupancy}$), times factor f_{light} , Equation (5.4).

$$P_{light,dwelling}(t) = f_{light}(t) \cdot f_{occupancy}(t) \cdot 0.8 \frac{W}{m^2} \cdot A_{eca} \quad (5.4)$$

Figure 5.3 illustrates the relation between the external solar radiation Irr and factor f_{light} for two different geographic locations.

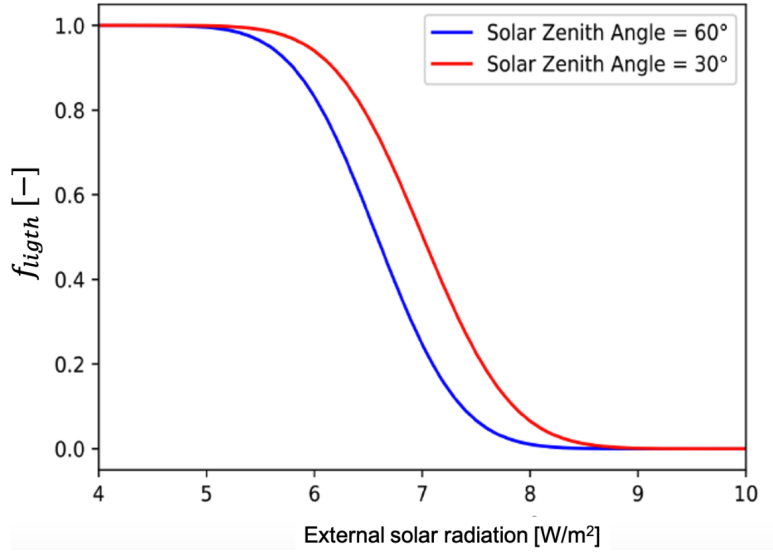


Figure 5.3: Relation between external solar radiation and factor f_{light} for two geographic locations with different azimuth angles. Source: [128]

Demand for cooking in residential buildings Electricity demand for cooking in residential buildings accounts, on average, for about 20% of building demand (16% if the building has an electric heating system) and is responsible for demand peaks around noon and in the evening, even though its relative importance on the overall residential demand is decreasing [128]. In the modeling of demand for cooking, the following assumptions were made:

- The entire household cooked daily, at maximum, once for lunch and once for dinner. For European households, this assumption was justified [129].
- Cooking demand only accounted for occupants' behavior and not for building properties [130].
- The average power of an electric stove, which is the most widely used cooking device in Europe [131], was 1300 W [132].

The building's total demand for cooking was calculated by accounting for the behavior of the occupants of each dwelling, according to Equation (5.5):

$$P_{cooking,dwelling}(t) = 1300 \text{ W} \cdot cooking_{AF, dwelling}(t) \quad (5.5)$$

In Equation (5.5), $cooking_{AF, dwelling}$ is a binary activation factor for cooking demand that modeled the behavior of the different dwellings of a building. Its value was 1 if all

conditions of Table 5.2 were true; otherwise, it was 0. The probabilities of eating at a restaurant or of eating a cold dish were taken from surveys [133].

Table 5.2: List of conditions that need to be true for the activation of electricity demand for cooking

Condition	From agent-based daily activities	From statistics	From electricity demand model
Lunch or dinner time		•	
No lunch or dinner before			•
At least an adult at home	•		
No meal at restaurant	•	•	
No cold dish		•	

If all conditions were true, a time window for cooking was opened. Its duration was set according to the daily activities of the adults living at the simulated dwelling, or randomly between conventional meal times if the agents were at home for the entire day. Once cooking had started, electricity was supplied for 30 minutes [135].

Demand for washing and drying in residential buildings

Washing machines and tumblers account, on average, for about 17% of building demand (13% if the building has an electric heating system). Due to their high electricity consumption, a dedicated model for washing and drying demand has been developed. In the modeling of demand for washing and drying, the following assumptions were made:

- Washing and drying demand only accounted for occupants' behavior and not for building properties, like cooking.
- The average power of a washing machine (EU energy label from A+++ to A) was set to 910 W [130]; the average power of a tumbler was set to 2800 W (EU energy label A and B) [130].

The building's total demand for washing and drying was calculated by accounting for the behavior of the occupants of each dwelling, according to Equation (5.6)

$$P_{washing-drying,dwelling}(t) = 910 \text{ W} \cdot washing_{AF, dwelling}(t) + 2800 \text{ W} \cdot drying_{AF, dwelling}(t) \quad (5.6)$$

In Equation (5.6), $washing_{AF, dwelling}$ and $drying_{AF, dwelling}$ are binary activation fac-

tors for washing and drying demand, respectively, that modeled the behavior of the different dwellings of a building. The value of $washing_{AF, dwelling}$ is was 1 if all conditions of Table 5.3 are were true; otherwise, it is was 0.

The first condition accounted for the fact that, in Swiss multi-family houses, washing is generally not allowed during nighttime. The reservoir-based control variable gradually increased over time with a rate that was dependent on the household size. Once washing had started, electricity was supplied for 1 hour and 45 minutes [134]. Of all EU households, 20.6% use a tumbler to dry the laundry [135]. For these households, the value of $drying_{AF, dwelling}$ turned to 1 after $washing_{AF, dwelling}$ went back to zero. Once drying had started, electricity was supplied for 30 minutes [136].

5.1.2 Agent-based model of electricity demand of office buildings

The electricity demand of office buildings was computed according to Equation (5.7).

$$P^{Office}(t) = P_{Lighting}(t) + P_{Equipment}(t) + P_{Heat}(t) + P_{Base} + P_{Ventilation} + P_{AC} \quad (5.7)$$

As for electricity demand for residential buildings, the relations between occupants' activities and electricity demand follow relatively clear patterns. Therefore, the demand for ventilation, AC, lighting, and equipment was modeled by including ABMs and it was, therefore, time dependent. For office buildings, no agent-based heat demand model had been developed. P_{Heat} was obtained from yearly measurements and scaled with the ambient temperature at a simulated point in time ($P_{Heat}(t) \sim T_{ext}(t)$).

Electric demand due to ventilation ($P_{Ventilation}$) and AC systems (P_{AC}) were modeled using normed standard values that referred to the energy-demanding area: namely, 0.4 W/m² for ventilation and 1.5 W/m² for AC, as specified in architectural norms [103]. The base load (P_{Base}) of office buildings was set to 1.9 W/m² [126].

Table 5.3: List of conditions that need to be true for the activation of electricity demand for washing

Condition	From agent-based daily activities	From statistics	From electricity demand model
Not nighttime			•
At least an adult at home	•		
Reservoir-based control variable is full			•

Demand for lighting in office buildings

The modeling of demand for lighting in office buildings was similar to that of residential buildings. The differences were as follows:

- Artificial lighting was required when ELI dropped below a threshold of 500 lux instead of 400 lx [127, 126], meaning that, in offices, lights are turned on earlier in the evening.
- The averaged installed lighting capacity of a building was increased to 2.5 W/m² [126].
- Factor $f_{occupancy,office}$, related to the building occupancy at a given time, was hereby defined as the ratio of employees at work divided by the total number of employees, according to agent-based daily activities.

These changes resulted in the adapted Equation (5.8)

$$f_{light,office}(t) = CDF((3 - 6/100) \cdot (ELI(t) - 500)) \quad (5.8)$$

$$P_{light,office}(t) = f_{light,office}(t) \cdot f_{occupancy,office}(t) \cdot 2.5 \text{ W/m}^2 \cdot A_{eca}$$

Demand for equipment in office buildings

This electricity demand is caused by the usage of several electric appliances, such as computers, screens and printers, coffee machines, and other kitchen appliances. The power rating of the equipment items in a standard European office building, according to Menezes *et al.* [137], is reported in Table 5.4. The number of appliances available was estimated based on the number of employees.

Table 5.4: Power rating and number of electric appliances per employee in an office building. Source: [137]

Appliance	$\frac{n_{appliances}}{n_{employees}}$	$P_{appliance} [W]$
PC	1	45
Screen	1	30
Printer	0.03	220
Coffee machine	0.02	350

Hence, $P_{Equipment}$ could be calculated according to Equation (5.9):

$$P_{Equipment}(t) = f_{occupancy,office}(t) \cdot n_{employees} \cdot 88.6W \quad (5.9)$$

5.1.3 Smart meter- and norms-based model of electricity demand of other building types

The electricity demand of buildings that were neither residential nor office buildings was not modeled using agent-based simulations. Instead, this demand was modeled using the outcomes of the smart meter data analysis (Section 2.3.3). The typical profile of the normalized power demand of a certain building type (nDF) was combined with the average electricity consumption value from architectural norms ($p_{building}$), reported in Table 5.5 for different building types.

Table 5.5: Average electricity consumption in W/m^2 by building type according to architectural norms [126, 127]

Building type	Average electricity consumption [W/m^2]
Education	1.17
Wholesale, Retail	1.77
Health	2.40
Accommodation	1.61
Traffic	1.32
Manufacturing/Industrial	10.6
Entertainment, Recreation, Arts	3.40

The second outcome of the smart meter data analysis, which was the distribution of base load demand normalized to surface area in m^2 , was used to improve the calibration of the model.

Hence, the time-dependent demand of this third category of buildings was calculated according to Equation (5.10).

$$P^{Building}(t) = nDF(t) \cdot p_{building} \cdot ECA \quad (5.10)$$

5.2 Energy Transition Scenario

The impact of the energy transition was assessed by comparing two full-year simulations of the electricity demand in the city and by assessing the impact on the grid of the change

in demand through power flow simulations. The two scenarios were defined according to Table 5.6. Data reported for the year 2030 were the outcomes of the agent-based population and mobility simulations.

Table 5.6: Summary of attributes of scenarios "Base-case" (2019) and "Energy transition" (2030) assessed applying the electric mobility, heat, and electricity demand models

Scenario Name	Year	City population	Residents' average age	Households	Average household size
Base-case	2019	80,079	41.1	38,315	2.07
Energy transition	2030	87,890	43.3	43,228	2.03

Scenario Name	Year	EV penetration [%]	SH and DHW heating systems
Base-case	2019	0.3	As they are
Energy transition	2030	20	Complete replacement of oil-fired heating systems and electric ohmic systems through DH (where available) and heat pumps where DH is not available

To simulate the technological development, an increase in the efficiency of EVs, EV chargers, and SH and DHW systems, as well as the renovation of older buildings, was implemented.

5.3 Results

The first part of the results section analyses the outcomes of the calibration and validation of the electricity demand model. Based on the results of power flow simulations (Section 2.3.4), two representative low-voltage transformers were selected to calibrate the model and four transformers to validate the calibrated model. To ensure that the model is able to model various electricity demand patterns, the selection of the calibration and validation transformers was based on the characteristics of the set of buildings that each transformer supplied.

Table 5.7: Characterization of yearly electricity demand, according to power flow simulation of low-voltage grid, at 6 low-voltage transformers (2 calibration and 4 validation transformers)

Prevailing building end-use	Transformer	Number of buildings supplied	Demand [MWh/year]		
			[Share of transformer total demand]		
			Residential	Office	Third Largest Demand Sector
Residential	Calibration <i>Gellerstrasse</i>	270	2400 (86%)	232 (8%)	Culture 96 (3%)
	Validation <i>Rotmonten</i>	302	3074 (85%)	174 (5%)	School 327 (9%)
Office	Calibration <i>Turnhalle</i>	30	135 (3%)	3216 (74%)	Culture 420 (10%)
	Validation <i>Mövenweg</i>	47	142 (3%)	1194 (27%)	Industrial 3051 (69%)
	Validation <i>Waaghaus</i>	79	922 (15%)	4651 (78%)	Other 288 (5%)
Mixed-Use	Validation <i>Spelteriniplatz</i>	44	527 (40%)	352 (27%)	Education 296 (23%)

The selected transformers and the characterization of the supplied electricity demand by building end-use are reported in Table 5.7.

For each transformer, the calibration process was executed by assessing an average winter¹ week from 2019 to account for the impact of SH and DHW heat demand on the total demand. Thereby, heat demand for residential and non-residential buildings was calculated by using temperature measurements from 2019. In the validation process, an average winter week and an average summer² week were assessed.

The second part of the results section presents the assessments of the “Base-case” and “Energy transition” scenarios and draws conclusions on the impact of the energy transition on the distribution grid infrastructure.

¹December-March

²May-September

5.3.1 Impact of individual behaviors on electricity demand prediction

Demand of residential buildings

Figure 5.4 illustrates a comparison between the predictions of the electricity demand model and the measurement data at transformer *Gellerstrasse*, which was used as the calibration transformer for residential buildings' electricity demand. The results shown for an average winter day were obtained by simulating 120 winter days (December–March) in 2019.

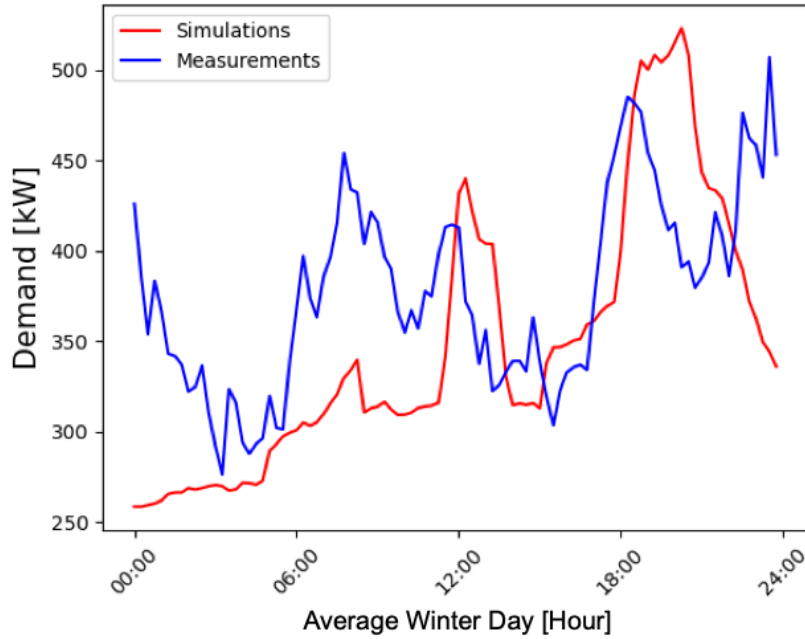


Figure 5.4: Comparison between measurements and uncalibrated bottom-up electricity demand model at transformer *Gellerstrasse* (residential buildings) for an average winter day.

The results demonstrate that the uncalibrated model can predict results within the order of magnitude of the measurements. Moreover, the night peak in demand is captured by the model. The error quantification, also reported in Table 5.8, resulted in a mean absolute error of 15.0 kWh (over a day), a normalized root mean square deviation of 20%, and a correlation coefficient of 0.52.

It is clear from Figure 5.4 that the nighttime electricity consumption that peaks at midnight and gradually decreases until the early morning was not captured by the model. It was assumed that the offset is due to the hot water preparation during the night, which, in Switzerland, involves heating by an electric boiler, regardless of the SH technology used.

Table 5.8: Comparison of the error metrics of the calibration process for electricity demand in residential buildings (transformer *Gellerstrasse*)

	Transformer Gellerstrasse	
	Before Calibration	After Calibration
Mean Absolute Error [kWh]	15.0	9.42
Normalized RMSD [%]	20	11.7
Correlation Coefficient [-]	0.52	0.70

The following location-specific calibrations, which are related to the behavior of buildings' occupants, have been implemented to improve the modeling of residential demand:

- An improved model for DHW preparation and storage was integrated into the heat demand model. Hot water for morning showers and other draws was prepared up to five hours in advance. The hot water temperature was set to 60°C in multi-family houses and 50°C in single-family houses. These limits were set due to hygiene regulations. The external water temperature was assumed to be constant as it is drawn from a large reservoir.
- To reduce the amplitude of the evening peak, the practice of many real estate administrations to prohibit the use of washing machines and dryers starting at 22:00 has been considered. Moreover, the share of households using a tumbler was increased from the EU average (20.6%) to the CH average (33%).

The applied base load values for residential buildings, presented in Section 5.1.1, underwent a calibration process. Thereby, two different base load values, for single- and multi-family buildings, respectively, were introduced. A reduction factor for electricity demand for cooking, to account for the lower propensity of urban households to cook elaborate dishes at lunch, was also assessed. 350 permutations of these factors were run; the permutation that yielded the best agreement with measurements is reported in Table 5.9. In Table 5.9, the results of the smart meter data analysis are also reported: The calibrated values are more in line with smart meters data than the initial values taken from norms.

Figure 5.5 presents a comparison between the predictions of the electricity demand model after calibration and the measurement data at transformer Gellerstrasse for an average winter day and an average winter week.

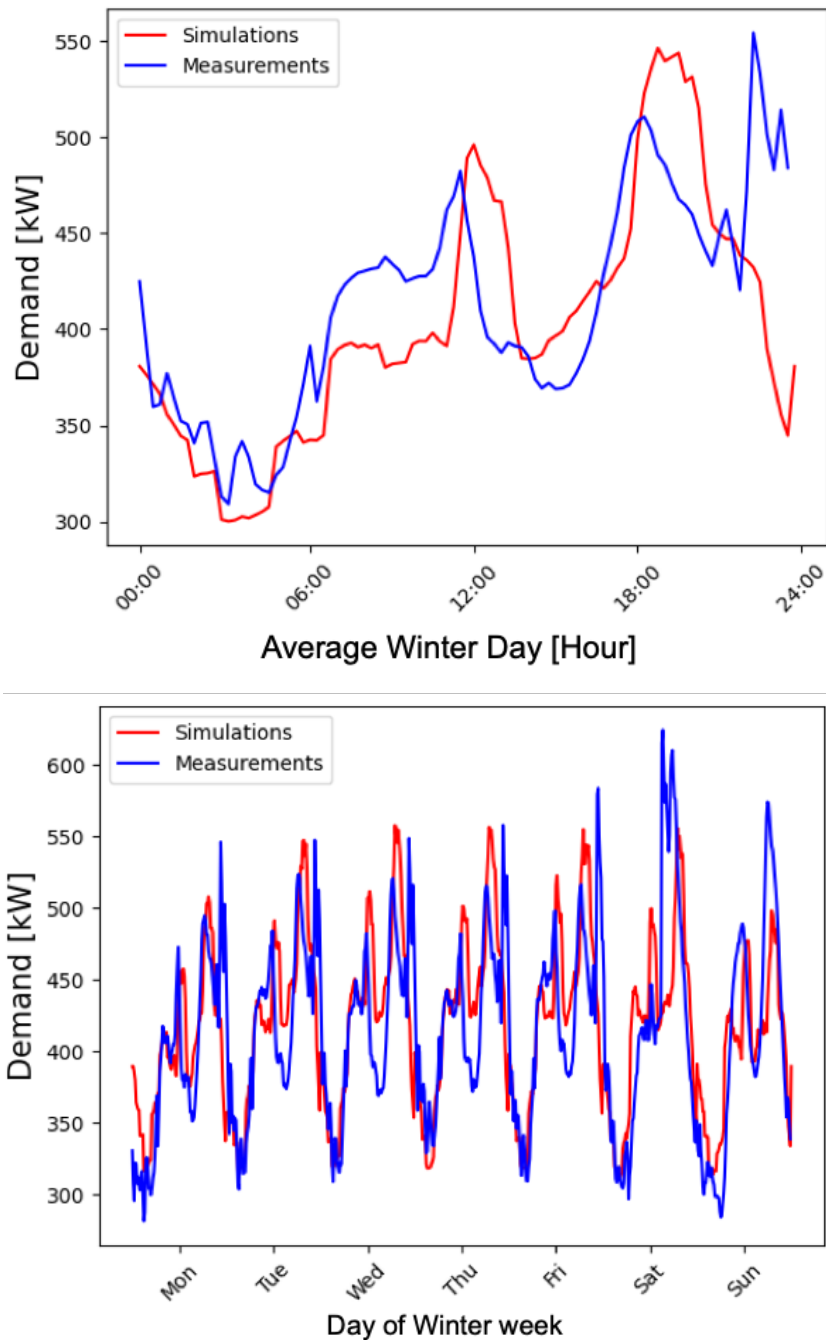


Figure 5.5: Comparison between measurements and results of the bottom-up electricity demand model at transformer *Gellerstrasse* (residential buildings) for an average winter day (above) and an average winter week (below) after the calibration of demand base loads and the integration of behavioral patterns.

Table 5.9: : Results of the calibration of base load values and of a reduction factor for demand for cooking for residential demand (transformer *Gellerstrasse*)

		Transformer <i>Gellerstrasse</i>		
		Before Calibration	After Calibration	Smart Meters
Base load residential	single-family buildings	1	1.35	1.4 - 2.3
	[W/m ²]			
Base load residential	multi-family buildings	1	2.5	1.4 - 2.3
	[W/m ²]			
Reduction factor for demand for cooking		0%	-25%	-

Figure 5.6 illustrates a comparison between the predictions of the calibrated electricity demand model and the measurement data at validation transformer *Rotmonten* for an average winter week. The mean absolute error over the week was 10.3 kWh, the normalized root mean square deviation was 12.3%, and the correlation coefficient was 0.51. The simulated trend follows the magnitude and the dynamics of the measurements; an overshooting of demand in the evening, as well as an undershooting of demand for some days, were found. Table 5.10 reports the error metrics evaluated over the week for both transformers, *Gellerstrasse* and *Rotmonten*; for the sake of completeness, error metrics are also reported for an average summer week.

Table 5.10: Comparison of the error metrics of the calibration and validation process for electricity demand in residential buildings (transformers *Gellerstrasse* and *Rotmonten*)

	<i>Gellerstrasse</i>		<i>Rotmonten</i>	
	(Calibration)		(Validation)	
	Winter Week	Summer Week	Winter Week	Summer Week
Mean Absolute Error [kWh]	9.42	12.0	10.3	18.0
Normalized RMSD [%]	11.7	18.1	12.3	30
Correlation Coefficient [-]	0.70	0.62	0.51	0.52

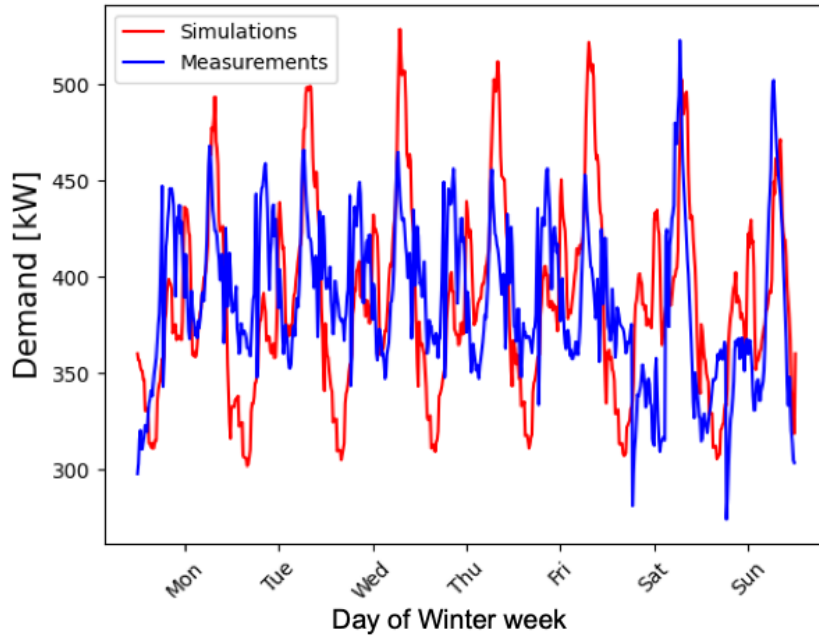


Figure 5.6: Comparison between measurements and bottom-up electricity demand model at transformer *Rotmonten* (residential buildings) for an average winter week as validation of the electricity demand model for residential buildings.

Demand of office buildings

Figure 5.7 presents a comparison between the predictions of the electricity demand model and the measurement data at transformer *Turnhalle St. Leonhard*, which was used as the calibration transformer for office buildings' electricity demand.

It is evident from Figure 5.7 that the model was able to simulate the right order of magnitude of demand of office buildings and that the day-to-day pattern was also correctly captured, with peak demand reached during office working hours. However, the model significantly underestimated the peak-to-base ratio. Moreover, the demand drop over weekends was not captured.

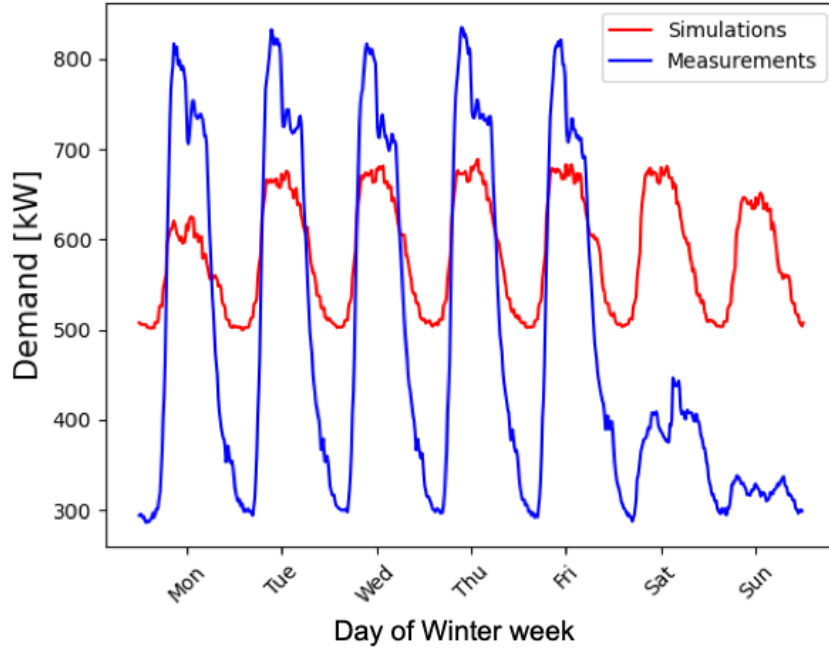


Figure 5.7: Comparison between measurements and uncalibrated bottom-up electricity demand model at transformer *Turnhalle St. Leonhard* (office buildings) for an average winter day.

The following calibrations, which are related to the behavior of office building occupants, have been implemented to improve the modeling of demand:

- A share of the base load demand and of demand for ventilation/AC in offices was implemented as a function of office opening hours. The opening hours were inferred from the daily activities of agents who worked in such buildings; when more than 7% of the workforce was physically present in the building, the office was considered open.
- The applied base loads were differentiated between weekdays and weekends.

The demand base load values for office buildings, presented in Section 5.1.2, underwent a calibration process. Thereby, two different base load values (for weekdays and weekends, respectively), as well as opening-hours activated shares of base demand and demand for lighting and ventilation, were assessed. Additionally, as demand for equipment is believed to be highly location specific, an increase factor for demand for equipment was also calibrated. 2,133 permutations of these factors were run; the permutation that yielded the best agreement with measurements is reported in Table 5.11.

Table 5.11: Results of the calibration of base load values, of opening-hours activated shares of demand for base, lighting, and ventilation demand, and of an increase factor for demand for equipment (transformer *Turnhalle St. Leonhard*)

	Transformer <i>Turnhalle St. Leonhard</i>	
	Before Calibration	After Calibration
Base load on weekdays [W/m ²]	1.9	0.4
Base load on weekends [W/m ²]	1.9	0.2
Base load for weekdays during opening hours [W/m ²]	0	1.4
Base load for weekends during opening hours [W/m ²]	0	0.4
Base demand for lighting [W/m ²]	2.5	0.3
Base demand for lighting during opening hours [W/m ²]	0	1.4
Base demand for ventilation [W/m ²]	0.4	0.8
Base demand for ventilation during opening hours [W/m ²]	0	1.9
Increase factor for demand for equipment	0%	+90%

From Table 5.11, it appears that demand for equipment and for ventilation were underestimated and demand for lighting overestimated in the uncalibrated model based on norms. These findings are consistent with the percentage breakdown by end-use of electricity demand in an office building (Figure 5.2).

Figure 5.8 presents a comparison between the predictions of the electricity demand model after calibration and the measurement data at transformer *Turnhalle St. Leonhard* for an average winter week. Besides the overall better agreement, particularly during weekends, the peak-to-base ratio of $2.8/1$ is more consistent with the results of the smart meter data analysis ($3.4/1$ according to Table 2.7).

Figure 5.9 illustrates a comparison between the predictions of the calibrated electricity demand model and the measurement data at validation transformer *Mövenweg* for an average winter week. The mean absolute error over the week was 15.9 kWh, the normalized root mean square deviation was 17.1%, and the correlation coefficient 0.93. The simulated trend closely follows the magnitude and the dynamics of the measurements.

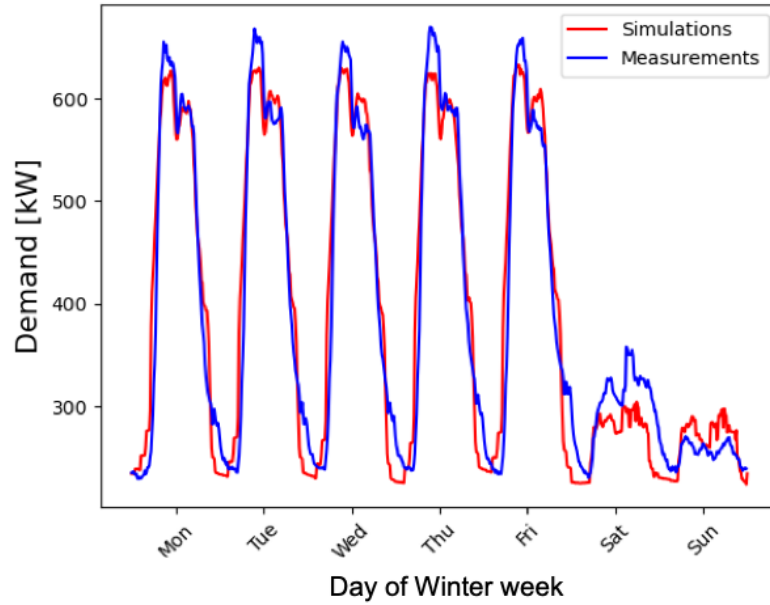


Figure 5.8: Comparison between measurements and results of the bottom-up electricity demand model at transformer *Turnhalle St. Leonhard* (office buildings) for an average winter week after the calibration of demand loads and the integration of behavioral patterns.

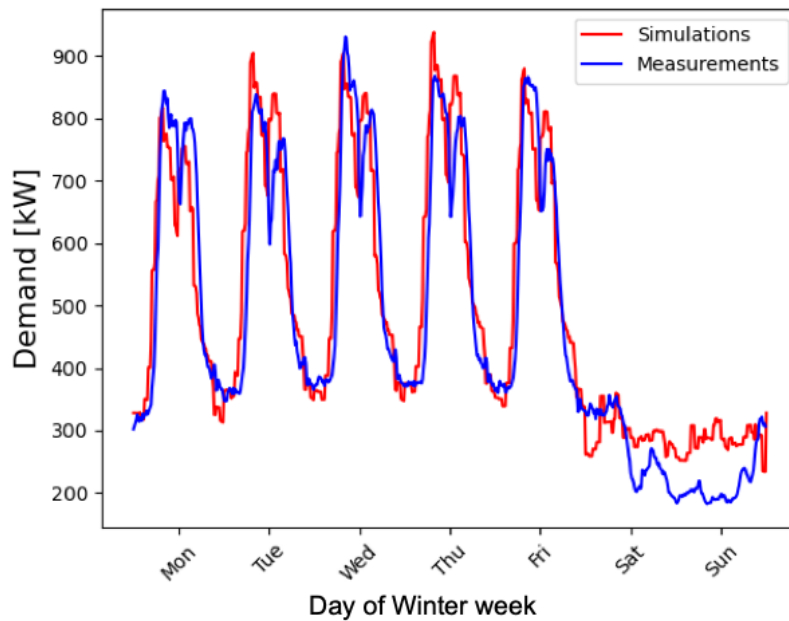


Figure 5.9: Comparison between measurements and results of the bottom-up electricity demand model at transformer *Mövenweg* (office buildings) for an average winter week as validation of the electricity demand model for office buildings.

The model was also tested in a central area of the city, at validation transformer *Waaghaus* (Figure 5.10). By observing the considerable demand underestimation of the model compared to measurements, it appears clear that something peculiar characterizes the demand at this transformer. The transformer is located in the historic city center, where many office buildings have shops and restaurants on the ground floor. These energy-intensive economic activities are not sufficiently considered by the model, which models their energy consumption as if they were offices. This finding reiterates the importance of a realistic and highly resolved digital twin.

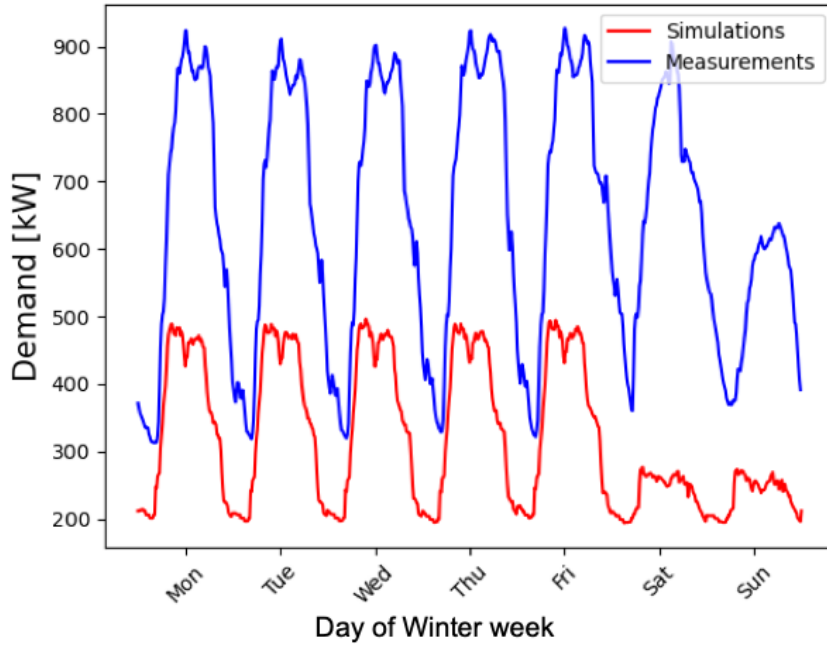


Figure 5.10: Comparison between measurements and results of the bottom-up electricity demand model at transformer *Waaghaus* (office buildings in the city center) for an average winter week as validation of the electricity demand model for office buildings.

Table 5.12 reports the error metrics evaluated over the week for transformers *Turnhalle*, *St. Leonhard*, *Mövenweg*, and *Waaghaus*; for the sake of completeness, error metrics are also reported for an average summer week.

Table 5.12: Comparison of the error metrics of the calibration and validation process for electricity demand in office buildings (transformers *Turnhalle St. Leonhard*, *Mövenweg*, and *Waaghaus*)

	<i>Turnhalle St. Leonhard</i>		<i>Mövenweg</i>		<i>Waaghaus</i>	
	(Calibration)		(Validation)		(Validation)	
	Winter Week	Summer Week	Winter Week	Summer Week	Winter Week	Summer Week
Mean Absolute Error [kWh]	10.5	12.5	15.9	34.1	82.6	75.1
Normalized RMSD [%]	11.5	13.6	17.1	36.8	55.1	55.1
Correlation Coefficient [-]	0.96	0.94	0.93	0.64	0.77	0.80

Finally, Figure 5.11 illustrates a comparison between the predictions of the calibrated electricity demand model and the measurement data at validation transformer *Spelsteriniplatz* for an average summer week. Thereby, the ability of the model to simulate the electricity demand in a mixed-use area is verified: The mean absolute error was 5.79 kWh, the normalized root mean square deviation 16%, and the correlation coefficient 0.83.

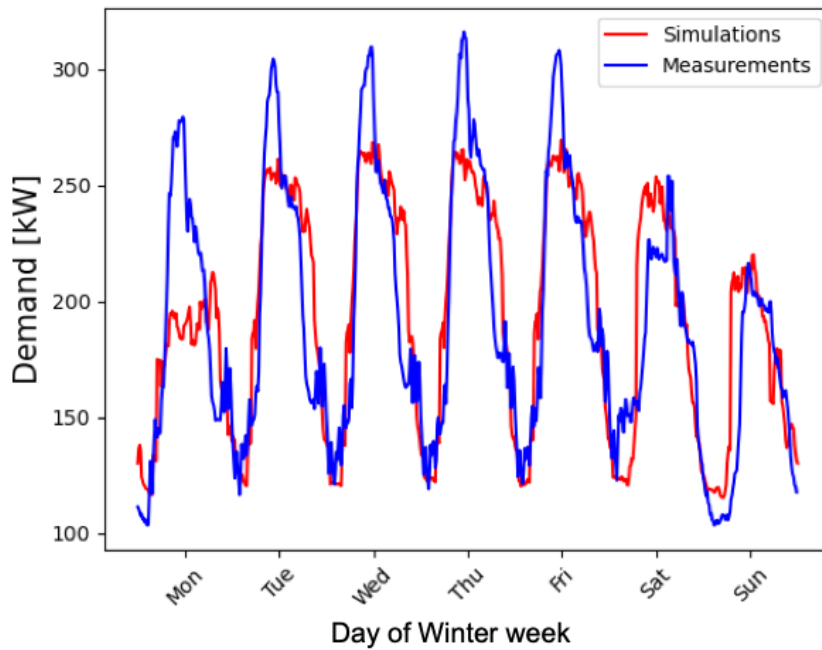


Figure 5.11: Comparison between measurements and results of the bottom-up electricity demand model at transformer *Spelsteriniplatz* (mixed-used area) for an average summer week as validation of the electricity demand model mixed-used buildings.

Bottom-up calculation vs. top-down distributions

Figure 5.12 compares the bottom-up electricity demand model with measurements at transformer *Spelterniplatz* for an average week in 2019. In the same graphics, the demand profiles that were obtained by a top-down allocation of 2019 electricity demand in Switzerland to the supply area of transformer *Spelterniplatz* are also included. In one approach, the demand was allocated according to the number of agents and jobs located in the supply area, according to agent-based population simulations, divided by the total number of agents and jobs in Switzerland. In the second approach, the demand was allocated according to the surface areas of residential, office, and industrial buildings, according to *Open Street Maps*, located in the supply area and divided by the aggregated surface sizes at the country level. This second approach was previously the *EnerPol* demand modeling approach prior to this work.

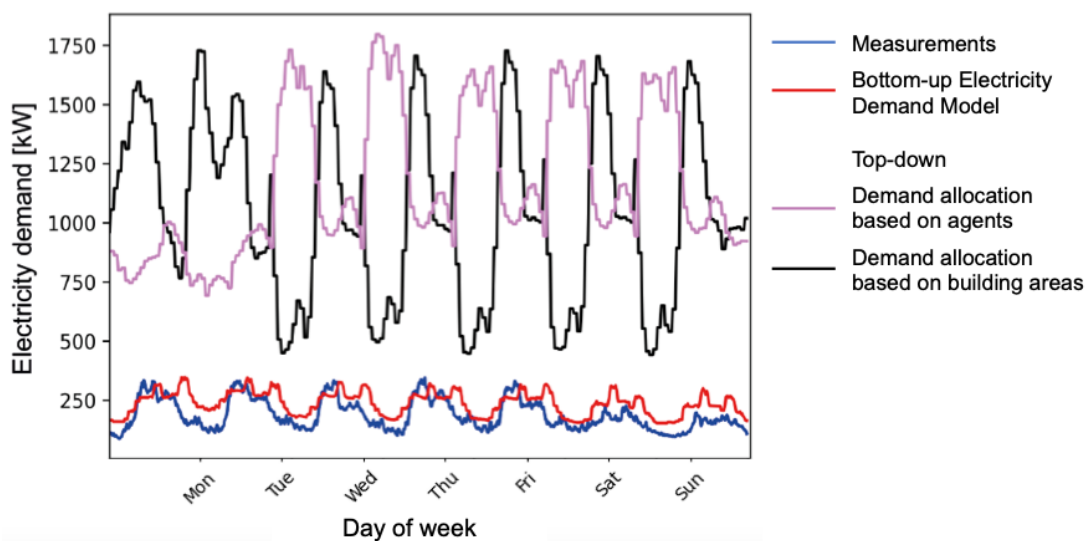


Figure 5.12: Comparison between measurements, results of the bottom-up electricity demand model, and demand distribution according to two top-down models at transformer Spelterniplatz (mixed-used area). Source: [128]

It is clear from Figure 5.12 that top-down approaches do not provide the necessary spatial and temporal resolution to carry out assessments of the distribution grid and, more generally, of energy transitions at a city level. The behavioral patterns of building occupants, the characteristics of agents, and the granularity of the built infrastructure are not well captured by the tested top-down approaches.

5.3.2 Impact of energy transition on distribution grid

Figure 5.13 displays the electricity demand of the entire city for an average winter week of 2019, as predicted by the electricity demand model. The predicted average demand was 44.6 MW, the base load 29.4 MW, and the maximum peak demand 58 MW. If extrapolated over the full year, this gives a predicted electricity consumption of 390 GWh/year. This value includes all electricity demand related to the building stock and does not, for example, include electricity demand for transport.

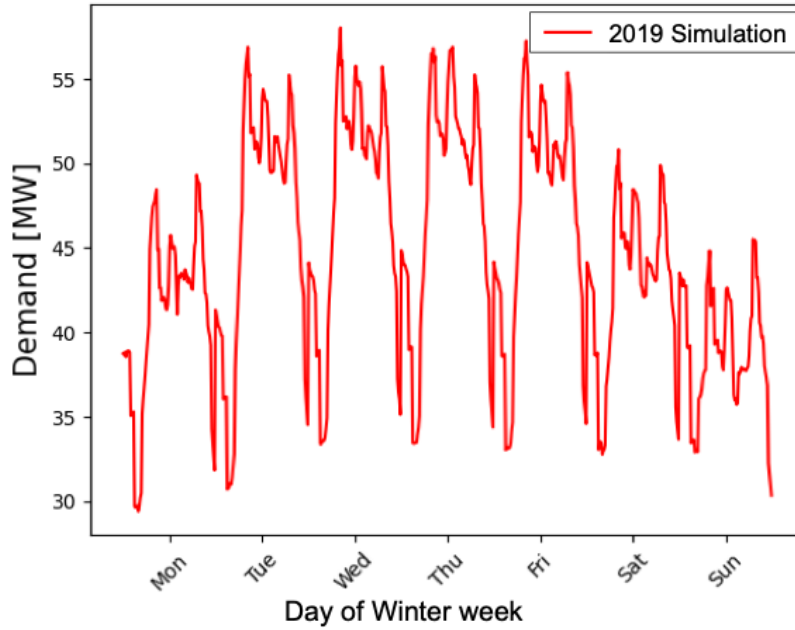


Figure 5.13: Electricity demand of the entire city as predicted by the electricity demand model for an average winter week in 2019.

For the sake of completeness, the breakdown of electricity consumption by building end-use is provided in Figure 5.14. From the figure, it is evident that the smaller demand on Mondays compared to the other weekdays can be attributed to the industrial sector.

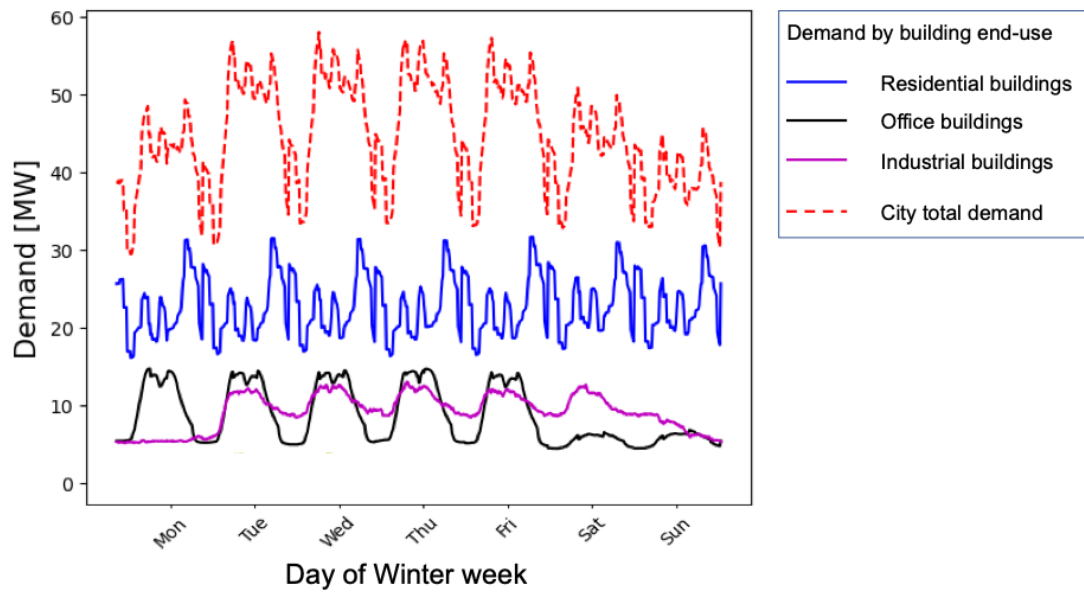


Figure 5.14: Breakdown of by end-use of the electricity demand of the entire city as predicted by the demand model for an average winter week in 2019.

Figure 5.15 shows the electricity demand of the entire city for an average winter week in 2019 for the base-case scenario and in 2030 for the energy transition scenario, as predicted by the electricity demand model. The general increase in electricity demand due to the electrification of mobility, the decarbonization of the building stock, and the increasing population outnumbers the efficiency improvements. For the energy transition scenario, the predicted average demand was 52.1 MW (+16.8%), the base load 37.1 MW (+26.2%), and the maximum peak demand 67 MW (+15.5%). If extrapolated over the full year, this gives a predicted electricity consumption of 455 GWh/year (+11.7%).

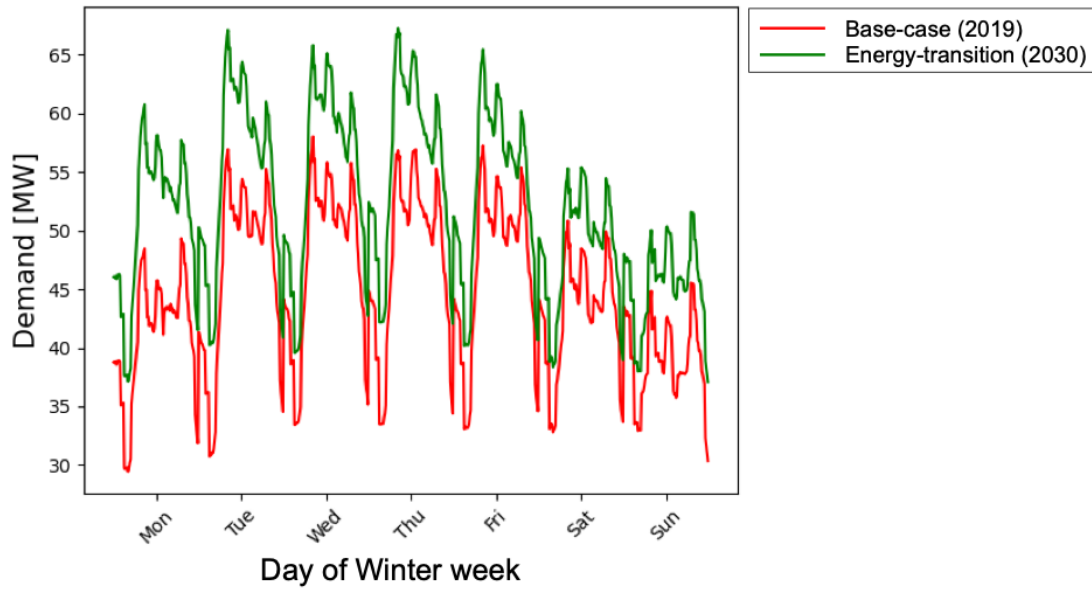


Figure 5.15: Electricity demand of the entire city as predicted by the electricity demand model for the scenarios “Base-case” and “Energy transition”.

The impact of the electricity demand on the distribution grid was assessed by running power flow simulations of the low-voltage distribution grid. The results are visualized in Figure 5.16 for 2019 and 2030, respectively. The line load, normalized with the maximum line capacity, is depicted for the entire city domain at 12:00 on a weekday.

Because of the increase in electricity demand due to the energy transition, the number of lines whose line load exceeds 50% increased from 1 line in 2019 to 20 lines in 2030. The lines that experienced an increase in load are mainly located in the city center and in the northern city districts. If grid upgrades are needed, they are likely to happen in these areas of the city.

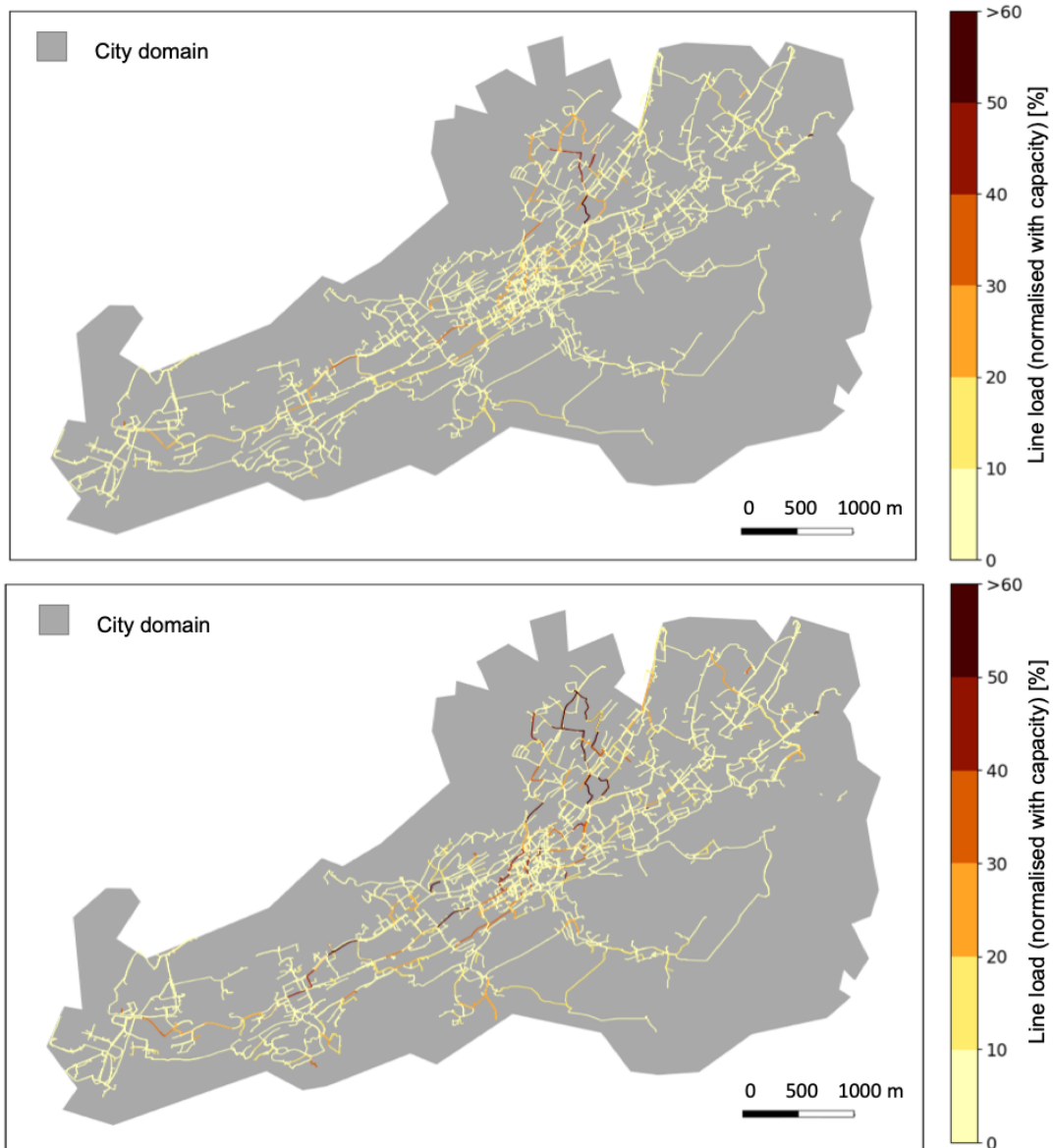


Figure 5.16: Line loading as % of the maximum line thermal limit in the city low-voltage distribution grid at 12:00 on a weekday in 2019 (above) and 2030 (below).

Chapter 6

Conclusions

6.1 Concluding Remarks

In this work, the integrated bottom-up simulation framework *EnerPol* has been extended, improved, and applied to assess the role of individuals in a city-scale energy transition. The major contribution of this work is the development of three comprehensive demand models that simulate electricity, heat, and electric mobility demand. All three models are bottom-up, integrated, and based on physical principles. This work's main novelty is the inclusion of individuals' behavioral patterns in all developed models by making extensive use of large-scale agent-based simulations.

These extensions allowed the author to simulate the consequences of an energy transition for a city, setting a particular focus on the role of individuals. Thereby, the newly developed models have been assessed in terms of their accuracy and performance compared to previous models.

Three case studies have shown how real-scale bottom-up agent-based models (ABMs) are superior to other approaches and how important the inclusion of individuals' characteristics (such as behavioral models and cultural patterns) is in the assessments.

Due to the use of ABMs, the novel simulation approach has several advantages over prior studies. First, the ABMs distinguish the characteristics and behaviors of all individuals in the population. Second, the ABMs can account for the interactions between agents, between agents and the infrastructure, and between agents and the environment. Finally, unlike models based on past statistical data, which do not account for future changes, future changes can modify agents' behaviors in the agent-based framework.

Moreover, the demand models have been integrated into a developed comprehensive digital twin of urban infrastructure – that is, a real digital twin of a city, with a level of

detail that has never before been applied in *EnerPol*. The integration of all models into a single framework enabled a holistic interpretation of the results that converged into a final scenario, where the impact of the decarbonization of both the building stock and private mobility on the low-voltage distribution grid was assessed.

The presented results have been used by the multi-utility to support their decision-making process, improve business models, increase social acceptance of future investments, and improve their practice with databases and enhance their data quality. For example, the multi-utility company has already been using the heat case study results to write a business plan to extend the local DH network. This business plan was used to provide arguments for approving the credit for the district heating network extension in a popular referendum held in November 2017 [54]. This real-world application of this work's outcomes demonstrates the suitability of such data-based predictive models for increasing the social acceptance of future infrastructural projects related to an energy transition.

6.2 Summary of Accomplishments

The main **contributions** of the **electric mobility** case study are as follows:

- Agent-based population and mobility models are used to simulate, respectively, the activities of individual agents and the agents' travel between his/her locations of activity.
- *A priori*, for current and future EV penetrations, the users of EVs are most often unknown. We have developed a stochastic model of EV users, such that realistically plausible distributions of EVs in a population can be generated, and, therefore, uncertainties related to EV adoption can be accurately assessed. Thus, even in the absence of EV use or EV ownership surveys, or in locations where there is not yet penetration of EVs, our novel simulation approach may be used to plan EV charging infrastructure.
- Human patterns of EV charging behavior are stochastically modeled. Thus, by running multiple simulations while varying charging behavior, both the average impact and the uncertainties due to specific behavioral patterns can be established.
- To accurately assess the population and mobility, all individuals in the country's population, including the city's inhabitants and commuters, are modeled using agent-based simulations. For the first time, using a recently developed GPU mobility simulator, large-scale agent-based simulations are combined with the high-

resolution digital twin of a DSO's infrastructure to assess the technological and financial impacts of the deployment of EVs from the perspective of a DSO, with a focus on the consequences of varied customer behavior. Furthermore, this novel methodology has been validated using measurement data.

The main **findings** of the **electric mobility** case study are as follows:

- For a DSO that plans to deploy public chargers, the revenue from parking fees is greater than the revenue from power sales. Thus, a business model based on revenue from parking fees has a much shorter time to break even. However, revenue from parking fees is more sensitive to EV users' charging behavior and preferences.
- For the investigated case study, at today's EV penetration of 0.3%, the break-even of the existing public charger infrastructure of the DSO is, at best, 10 years, when the business unit manages all charging infrastructure (that is, from charging at home, work, and public chargers). Otherwise, break-even can only be reached if the EV penetration is 4% or greater. Moreover, competition in the public charging marketplace can substantially decrease revenue, up to a 35% decrease in load factor at an EV penetration of 2% in the present test case. Thus, participants in the marketplace have substantial financial exposure when penetrations of EVs are low.
- Charging at home and at work are the largest sources of additional electricity demand due to EV charging. While charging at work is characterized by sharp peaks in electricity demand at morning peak hours, charging at home has less distinctive peaks with maxima during evenings.
- For a 20% EV penetration, local increases in the grid loads may reach 78% during peak hours, whereas the increase in grid load averaged over the city may be only 6%. Thus, to reliably identify what particular upgrades are required in the distribution grid, it is essential to use a digital twin of the existing built infrastructure.

The main **contributions** of the **heat** case study are as follows:

- For the first time, large-scale ABMs of both population and building stock are combined with a fully bottom-up heat demand model. A detailed synthetic population is generated for an entire country, and the daily activities of each person, household, and dwelling are modeled. The simulated daily activities allow for the

modeling of the occupancy and activities of the occupants of the buildings. Furthermore, the heat demand is determined for each household, ensuring that the model captures the spatial and temporal differences in the heat demand across the building stock.

- A physical bottom-up thermodynamic demand model was developed and used to calculate the hourly building heat demand over a year-long period. The model uses the characteristics of individual buildings and dwellings to quantify the heat fluxes across each building, as well as each building's thermal inertia. The predicted heat demand is validated with measurements.
- In a novel holistic approach, the extension of the DH network of a mid-sized city in Switzerland has been evaluated. District heat pipelines should be built in city areas where buildings have both large heat demand and a good likelihood of connecting to the future network and generating revenues to guarantee economic sustainability. Therefore, the agent-based heat demand simulation framework has been coupled with (i) a predictive model to determine the likelihood of a building connecting to the extended network and (ii) a routing model that optimally connects new buildings to the existing DH network.

The main **findings** of the **heat** case study are as follows:

- Accounting for building occupants' behavior through ABMs improves the quantitative prediction of the magnitude and dynamics of the time-resolved heat demand; this improves the model predictions, which yield an annual error less than the magnitude of error in other urban building energy models.
- In quantifying the likelihood that a building would connect to an extended DH network, the building characteristics of build year, type of heating system, installation year of heating system, and building ownership were found to be the most statistically relevant.
- In assessing the extension of a DH network, a novel holistic approach that accounts both for the likelihood of a building being connected to the extended network and that the heat demand of the building will be profitable is considered. For the test case of a mid-sized city in eastern Switzerland, these considerations yielded a maximum internal rate of return of the infrastructure that was 25% higher than if such considerations were not made.

The main **contributions** of the **electricity** case study are as follows:

- A physical bottom-up electricity demand model was developed and used to calculate the quarter-hourly building electricity demand of the entire building stock. The characteristics of individual buildings and households were used to quantify the electricity demand at the resolution of individual buildings. The predicted electricity demand was calibrated and validated with measurements.
- Demand at residential and office buildings was modeled applying a purely agent-based approach; smart meter measurements were used to model and calibrate the demand predictions. A sensitivity analysis on the normed values of electricity consumption reported in architectural standards indicated which demand components varied the most from norms.
- Power flow simulations of the low-voltage grid were run for the first time in the investigated city to assess the impact on the electricity distribution grid of the mobility and the building sector's decarbonization; population dynamics were thereby taken into account.

The main **findings** of the **electricity** case study are as follows:

- Accounting for the behavior of building occupants, through the usage of agent-based simulations, and for cultural patterns in the modeling of electricity demand improved the predictions of both the magnitude and the dynamics of the time-resolved electricity demand. In mixed-use areas, the model predicted the electricity consumption with a normalized root mean square deviation of 16% and a correlation coefficient of 0.83.
- The accuracy of the predictions of the developed bottom-up model is superior to those of the previously applied top-down approaches, as these do not sufficiently capture the granularity of the built infrastructure and the building occupants' behavior and are, therefore, not suitable for modeling the energy transition at the distribution grid level.
- The impact of the energy transition on the electricity demand has been quantified. The predicted electricity consumption for 2030 is 11.7% larger than today's demand; in particular, the baseload demand increases by +26.2%.

6.3 Other Accomplishments

In the development of the digital twin, the following achievements were made, which were of great importance for the multi-utility *sgsw* regarding their practice with the database:

- Automatic processing programs were developed such that future updates can be automatically implemented into *EnerPol*, assuring data quality.
- Links between GIS and SQL database were established, which improved *sgsw* data quality. For historical reasons, these links were previously missing.
- Deficiencies in GIS features or inconsistencies in *sgsw* databases were identified.

The developed models are fully integrated into the *EnerPol* framework and coupled with previously existing and newly developed models. Notably, the methodology developed in this work is applicable to any geographic location. The robustness of the developed framework has been proven and enhanced by applying the framework to a range of different geographical domains.

6.4 Future Work

In this work, the *EnerPol* has been applied on a city-scale dimension for the first time. The bottom-up agent-based approach has proved to enable an assessment of the future impact of ongoing trends on the infrastructure. In a bottom-up physical framework, the assessments' quality and correctness are strongly related to the available amount of infrastructure and customers' personal data. Since the developed methodologies are based on agent-based mobility, population, heat, and electric demand simulations, highly detailed data and high-performance computing resources are required. In future work, the capabilities and the performance of the developed models can be enhanced by working on the four pillars of *EnerPol* (Section 2.1).

6.4.1 Database improvement

High-quality and highly resolved data lay the foundation of bottom-up models. ABMs require even more data because each individual entity (*e.g.*, people, buildings, vehicles) needs to be characterized. Sensitive data on energy consumption or buildings' financial parameters are particularly precious and generally not accessible to a broad audience. In this project, a large proprietary database was made accessible, extended with data from open-source databases, and integrated into the *EnerPol* database. In the future, the

possibility to access new or more complete datasets would further validate and improve the developed models and the conducted assessments (here in order of importance):

- *Smart meter data:* A considerable share of smart meter time series needed to be discarded due to quality issues, which significantly reduced the number of available measurements for private households. Households' consumption patterns present a large variance because of different family structures, daily routines, or installed electric appliances. Smart meter measurements could be geo-referenced and linked to a specific building but, due to privacy policy, not to a specific dwelling, resulting in reference load profiles that might not capture the exact dwelling's demand dynamics. Access to a more detailed and accurate classification of smart meter measurements and generally higher data quality would enable better capturing of different demand dynamics. Additionally, if available, smart meter measurements of heat, gas, or EV demand would allow for further development of the respective models (any sensor able to measure an individual item with a temporal resolution of at least a quarter of an hour can be considered a smart meter).
- *Data for district heat routing algorithm:* When running the routing algorithm for future DH pipelines, the infrastructure along which the new district heating pipelines will be installed should be known in detail. In particular, recent or imminent planned work on the road surface must be considered. In this work, this information was assumed, as data on road quality was not shared.
- *Data on usage of electric vehicle public chargers:* At the time of writing, EVs were not widespread in the investigated city. Given that most EV drivers prefer to charge at home, the usage of public chargers is limited. Therefore, more available datasets would guarantee better statistical representativity, particularly when deducing charging patterns and preferences.
- *Distribution grid data:* To run power flow simulations, the network topography needs to be univocally defined. In practice, the connections between the different elements of the network must be parameterized. The parametrization was accomplished by extensively pre-processing the available data, which came from different sources and were not necessarily interconnected. However, because databases are often not aligned, some grid elements could not be identified and subsequently characterized. These issues should be carefully addressed and clarified in future work to ensure that the project's time efficiency is not affected.
- *Historical data on real estate:* When training the predictive model that determines

the building's probability of connection to future DH pipelines, historical data regarding the development of the real estate, which has already been connected to the DH network, is needed. Each building's history was not made available, which may have impaired the model's prediction capability. For future work, the importance of complete traceability of a building's history is crucial.

6.4.2 Model improvement

The *EnerPol* framework was extended by new models and digital tools. All presented models were developed in this project and represent a paradigm shift compared to the previous top-down approach of *EnerPol*. The following three extensions of the models for electricity, heat, and mobility demand are suggested:

- *Electricity network simulations*: The power flow simulations presented in this work start from middle voltage substations, which feed the whole city and go down to low-voltage distribution boxes and low-voltage branches. Cables connecting distribution boxes or direct house connections are assumed to be continuous. In reality, many low-voltage wires lead off from the main power line and connect to individual buildings. The wire is not continuous at these locations and should be modeled accordingly to correctly simulate the voltage drop along the cables.
- *Heat demand model*: The developed heat demand model simulates the heat demand of the residential sector. The demand for industrial and commercial buildings is not simulated, but rather extracted from customer databases; this partially undermines the work's bottom-up nature. Attempts to simulate the heat demand for such buildings in a bottom-up manner have been carried out. Nevertheless, a clear link between agent-based simulation and the associated heat demand has not been established (e.g., in an office building). It remains clear that a complete bottom-up extension of the heat demand model is yet to be implemented.
- *Electric mobility demand model*: In the developed model, EV users decide whether to charge or not charge their vehicle each time they finish one of their modeled daily activities. That means that charging "on the way", such as while driving to work, is not modeled. This limitation does not, for example, capture the demand of long-distance drivers or tourists. Moreover, the choice of the public charger location (e.g., a parking lot or a supermarket) should be modeled considering the vehicle and driver characteristics. In future work, the model should be extended accordingly.

6.4.3 Suggested scenarios

- *Business model:* The “*what-if*” scenario assessments and optimizations presented in this work always addressed both the technical and economic consequences of the energy transition. The results of the economic assessments were often presented as calculations of net present value or internal rate of returns, which were generally quantified by modeling CAPEX, yearly OPEX, and yearly revenues over a certain number of years. However, the decision of whether an investment must be done or not should consider other financial aspects and suggest an investment strategy and an investment timeline. In future work, a business model should be integrated into the developed models by default.

Acknowledgements

I wish to acknowledge the support of my supervisors, colleagues, friends, and family, who made this work possible.

First of all, I would like to thank my supervisor, Professor Dr. Reza S. Abhari, for believing in the project and in me. I am grateful to Professor Abhari for the opportunity to work on an important, challenging, and innovative project, for the responsibility of representing *EnerPol* outside LEC, for the autonomy granted to me, and for his valuable feedback. I am sure that what I learn over the years will serve me well in life. In particular, he taught me the importance of challenging assumptions and critical thinking. A special thanks to Dr. Ndaona Chokani, who has always been at the forefront in overseeing my doctoral work. His prompt feedback, the countless reviews of my scientific production, and the spur to disseminate the work outcomes have made it possible to finish this project. Dr. Chokani taught me to have self-esteem and present my skills to the best of my ability - this is one of the most important teachings of my doctorate. I am further extending my gratitude to Prof. Saraiva, who kindly evaluated this work as a co-examiner.

This study has been supported by St. Galler Stadtwerke (*sgsw*), St. Gallen, Switzerland, within the scope of a collaboration between the Laboratory of Energy Conversion of ETH, Zurich, Switzerland and St. Galler Stadtwerke. I would like to thank the *sgsw* management that strongly believed in this project: Dr. Ivo Schillig and Mr. Marco Letta, former and current CEO of *sgsw*. I would like to acknowledge the support of the City Council of St. Gallen, particularly City Counsellor Peter Hans (Direktion Technische Betriebe der Stadt St. Gallen) and Mr. Andreas Flückiger (Chief of Staff of Direktion Technische Betriebe der Stadt St. Gallen).

A heartfelt thanks to Mr. Wolfgang Korosec, Head of IT/CIO at *sgsw*, for his support, guidance, opinion exchanges, motivation, and determination in carrying out the project. Without him, this project would not have been born, and the successful results would not have been possible. Besides, I would like to thank all the technical staff of *sgsw* and the city of St. Gallen with whom I dealt during the project.

I thank Marlene Hegner for her organizational help and her efforts to oversee and ensure the seamless continuation of the project. I would also like to thank Marlene for the enjoyable afternoon conversations and commitment to supporting a social life at the institute. Also, I would like to thank Dr. Anna Gawlikowska for the exciting discussions and collaborations.

Working in the *EnerPol* group at LEC, I got to know and work with some special people. Thanks to Marcello, who has been the best office mate, especially for the patience and availability in helping me with my codes and my countless doubts. Thanks to Aleksandr for always reminding me how important it is to code properly. Thanks to Patrick P., for supporting me with the power flow simulations and for bringing shape and structure into *EnerPol*. Thanks to Patrick E., for introducing me to *EnerPol* and explain different concepts to me in a kind and effective way. Thanks to Annika, for bringing positivity, friendliness, freshness, and much biological knowledge into our team. Thanks to Chris, for the interesting conversations and help. Furthermore, thanks to Michael, Dominic, Asad, Carsten, Janis, Antriksh, and all LEC members: it was a pleasure to meet you and work with you.

Beyond the working environment, I would like to acknowledge the support I received from my dear ones: my friends from Switzerland and Germany and, particularly, Tania, Federico, and Valeryia, who, in the first person, shared with me the good and not so good moments. A special thanks to Giorgia, who always managed to give me strength and hope from far away. Finally, my family, that showed great sympathy and understanding during these years. Grazie mille.

List of Publications

Journal Publications

- M. Pagani, W. Korosec, N. Chokani, R. S. Abhari, “User behavior and electric vehicle charging infrastructure: An agent-based model assessment”, *Applied Energy*, Vol. 254, 113680, 2019
- M. Pagani, P. Maire, W. Korosec, N. Chokani, R. S. Abhari, “District heat network extension to decarbonize building stock: A bottom-up agent-based approach”, *Applied Energy*, Vol. 272, 115177, 2020

Conference Contributions

- M. Pagani, W. Korosec, N. Chokani, R.S. Abhari, “Agent-based Model Assessment of EV Charging Infrastructure in St. Gallen”, *Energieforschungsgespräche*, 2019
- M. Pagani, W. Korosec, N. Chokani, R. S. Abhari, “Techno-Economic Optimization of EV Charging Infrastructure Incorporating Customer Behavior”, *15th International Conference on the European Energy Market EEM*, 2018

Student Projects Supervised

The following student projects were developed and subsequently supervised by the present author throughout this doctorate. Where indicated in previous chapters, the methodologies developed and the results obtained in these student projects have contributed to the present dissertation.

Bachelor Thesis

- B. Hilpisch, “Assessing Transformation of the German Power System with Aid of a Population Model”, Laboratory for Energy Conversion, ETH Zurich, 2018
- N. Y. Aka, “Development of Physical Bottom-Up Model for Heating Demand Calculation of Commercial and Industrial Buildings”, Laboratory for Energy Conversion, ETH Zurich, 2019

Semester Projects

- P. Ruffieux, “Integration of Utility-Scale Wind Farms in the United Kingdom”, Laboratory for Energy Conversion, ETH Zurich, 2017
- P. Maire, “Bottom-Up Heating Demand Model for Multi-Utility Company Optimization”, Laboratory for Energy Conversion, ETH Zurich, 2018
- D. Haegel, “Agent-Based Modelling of Electricity Demand”, Laboratory for Energy Conversion, ETH Zurich, 2019

Master Thesis

- M. Rusch, “Stochastic Simulation of Interconnected Power Systems with Integrated Renewables”, Laboratory for Energy Conversion, ETH Zurich, 2016
- T. Abächerli, “Electrification of the Transportation Sector: An Integrated Agent-Based Assessment”, Laboratory for Energy Conversion, ETH Zurich, 2020

Curriculum Vitae

Of Marco Ambrogio Pagani, born 03.01.1989 in Switzerland.

Professional Experience

- Ph.D. candidate, Laboratory for Energy Conversion, Institute of Energy Technology, ETH Zurich, 2016–2021
- Engineering intern, EMPA – Swiss Federal Laboratories for Materials Science and Technology, Materials for Energy Conversion, Dübendorf (CH), 2015
- Intern, School of Energy Systems, Lappeenranta University of Technology, Lappeenraanta (FI), 2015
- Engineering intern, Alstom Power AG, Gas Turbine Reconditioning Network, Birr (CH), 2014
- Intern, ERI Bancaire, Banking Systems, Lugano (CH), 2009

Education

- Dr. sc., Laboratory for Energy Conversion, Institute of Energy Technology, ETH Zurich, 2016–2021
- M.Sc. in Mechanical Engineering, ETH Zurich, 2012–2015
- B.Sc. in Mechanical Engineering, ETH Zurich, 2009–2012

List of Figures

- 1.1 Gross electricity generation in Germany by energy source from 2000 to 2020 (in TWh/year). Elaborated from: [2] (*: values for 2020 are preliminary) 2
- 1.2 Share of renewable energy sources in German gross electricity generation and amount of EEG levy (surcharge for end consumers) for household electricity. Elaborated from: [3] 3
- 1.3 Levelized cost of energy for renewable energies and conventional power plants in Germany in the years 2013 (above) and 2018 (below). Elaborated from: [4] 4
- 1.4 Forecast of global greenhouse gas emissions as a function of implemented policy and the resulting increase in world average temperature (width of the curve indicates inaccuracy). Source: [9] 6
- 1.5 Share of electricity from renewable sources in the EU member states in 2018. Source: [11] 7
- 1.6 Ongoing technological, planning, and financial trends to support city-scale energy transition, classified according to the three pillars of the energy concept EnK³ – electricity, heat, and mobility. Elaborated from: [18] 8
- 1.7 Energy flows for the city of St. Gallen in 2010 (above) and elaborated in energy concept EnK³ 2050 (below). Source: [18] 10
- 1.8 Schematic of an agent-based simulation environment. Source: [27] 14

- 2.1 Schematic of *EnerPol*'s four pillars on which the *EnerPol* framework is based. 26
- 2.2 Detail of the digital twin with elements of the energy and the urban infrastructure 28
- 2.3 Map of low-voltage transformers with indication of power flow measurement availability. 32

2.4	Annual aggregated power demand at a low-voltage transformer in a residential area in grid level 7 with a time resolution of 15 minutes (source: Power Quality System of <i>sgsw</i>).	33
2.5	Example of low-voltage network topography around a low-voltage transformer (brown circle) as it is modeled in the digital twin; blue circles are network nodes placed at a lower hierarchical level in the network.	34
2.6	Normalized power demand factor over an average year for customers belonging to "Education" category calculated from smart meter measurements.	37
2.7	Normalized power demand factor over an average week for industrial customers (left) and customers belonging to "Education" category (right) calculated from smart meter measurements.	38
2.8	Normalized power demand factor over an average week for households calculated from smart meter measurements.	38
2.9	Distribution of base loads normalized with energy-consuming area for customers belonging to category "Education" (left) and category "Retail" (right) calculated from smart meter measurements with indication of average value and standard deviation.	41
2.10	Day-averaged line loading as % of the line thermal limit in the city's low-voltage distribution grid.	44
3.1	Current trend of EV penetration in the city of St. Gallen versus mid- and long-term goals of the EnK ³	47
3.2	Schematic of iterative sequence of placement and mobility simulations that is integrated into the <i>EnerPol</i> framework.	53
3.3	Locations (upper) and comparison of predicted and actual monthly charging cycles (lower) in 2017 at the four most widely used public charging stations of the city.	57
3.4	Comparison, for EV users with price-driven and comfort-driven charging behaviors, of the effect of EV penetration on the DSO's revenue for EV charging based on parking duration (solid lines) and power sales (dotted lines).	58
3.5	Comparison of time to break even for the cases when revenue comes from all EV charging infrastructure and for when revenue comes only from public EV chargers are considered. The revenue comes from parking fees, and the EV users have price-driven charging behavior.	59
3.6	(a) Locations of 10 proposed privately owned public chargers and their impact on the load factors at the DSO's existing public chargers	60
3.6	(b) Comparison of revenue, at two of the DSO's public charging stations, without and with competition from the privately owned public chargers.	61

3.7	Optimized placements of public EV charging infrastructure for EV penetrations of (a) 2%, (b) 10%, and (c) 20%. The size of the symbols is indicative of the number of chargers.	63
3.8	Comparison, for EV users with price-driven charging behavior, of the effect of elasticity of demand on the DSO's revenue for EV charging based on power sales and parking duration. The total revenue is from charging at home, work, and public chargers. The revenue is normalized relative to the total revenue based on power sales at the reference price. The EV penetration is 2%. The vertical bars show the uncertainty due to the preference of when EV users leave.	64
3.9	Comparison, for EV users with comfort-driven charging behavior, of the effect of elasticity of demand on the DSO's revenue for EV charging based on power sales and parking duration. The total revenue is from charging at home, work, and public chargers. The revenue is normalized relative to the total revenue based on power sales at the reference price. The EV penetration is 2%. The vertical bars, not shown for public charger parking fees for the sake of clarity, represent the uncertainty due to the preference of when EV users leave.	65
3.10	Comparison of the effect of elasticity of demand on the time to break even of the EV charging infrastructure for EV charging based on power sales and parking duration. The EV penetration is 2%. The vertical bars represent the uncertainty due to the preference of when EV users leave.	66
3.11	Comparison, for the business model based on parking fees, of the impact of EV penetration on the time to break even for both the price-driven and comfort-driven charging behaviors. The vertical bars represent the uncertainty due to the preference of when EV users leave.	67
3.12	Comparison of the sources of the additional electricity demand due to EV charging, for EV penetrations of 2% (a), 10% (b), and 20% (c).	69
3.12	(a) Comparison of the maximum increase in the peak load due to EV charging across the city. (b) Comparison of the increase in peak load at peak hour due to EV charging averaged over the city.	71
4.1	Evolution of heat demand in the city of St. Gallen according to EnK ³ by energy source. Elaborated from: [18]	72
4.2	Process flow diagram of heat case study, coupling agent-based building and occupant behavior models with a bottom-up heat demand model and a predictive model of the likelihood of buildings to connect to the DH network to optimize the routing of new DH pipelines.	74

4.3	Modeled heat fluxes, inside the building, and across system boundaries (green: building heated area; red: space heating and hot water system; blue: building boundaries). The thermal inertia of the building is accounted for using the capacitance in an electrical analog circuit (based on [102]).	78
4.4	Modeled hourly ventilation rate as a function of build year for mechanically ventilated buildings [55].	81
4.5	Resistor-capacitor circuit model used to account for the thermal inertia of buildings in the heat demand model; adapted from architectural norm [104].	82
4.6	Schematic of the workflow process, coupling the agent-based heat demand model (red), the predictive agent-based building model (purple), and the routing of the extended DH network (green), that is integrated into the <i>EnerPol</i> framework.	84
4.7	Examples of residential building clusters and representative profiles of space heating and heating of domestic hot water.	86
4.8	Comparison of the actual and predicted hourly heat demand in the city for the year 2017.	87
4.9	Comparison of the actual and predicted hourly heat demand in the city for a winter week in 2017. Predictions from three variants of the heat demand model are shown: without agent-based modeling (NA); with behavior of occupants (OB); and with behavior of occupants and storage of domestic hot water (OB and DHWS). Arrows 1 and 2 indicate the overnight decrease in heat demand and the morning peak in heat demand, respectively.	89
4.10	Distribution of predicted probabilities of connecting a building to an expanded DH network of the city.	92
4.11	Comparison of the expanded DH network in the demand-driven scenario (upper plot) and the predicted-demand-driven scenario (lower plot). The red squares highlight the areas where the expanded DH networks are substantially different.	93
4.12	Comparison of the annual CAPEX and OPEX for the expanded DH networks in the demand-driven and predicted-demand-driven scenarios. . . .	94
4.13	Comparison of the annual profits (left) and IRR (right) of the DH network in the demand-driven and the predicted-demand-driven scenarios.	95
5.1	Percentage breakdown by end-use of electricity demand in a multi-family residential building in Switzerland – without (left) and with (right) electric space and hot water heating system. Source: [122]	98
5.2	Percentage breakdown by end-use of electricity demand in an office building with electric space and hot water heating system. Source: [123]	99

5.3	Relation between external solar radiation and factor f_{light} for two geographic locations with different azimuth angles. Source: [128]	101
5.4	Comparison between measurements and uncalibrated bottom-up electricity demand model at transformer <i>Gellerstrasse</i> (residential buildings) for an average winter day.	108
5.5	Comparison between measurements and results of the bottom-up electricity demand model at transformer <i>Gellerstrasse</i> (residential buildings) for an average winter day (above) and an average winter week (below) after the calibration of demand base loads and the integration of behavioral patterns.	110
5.6	Comparison between measurements and bottom-up electricity demand model at transformer <i>Rotmonten</i> (residential buildings) for an average winter week as validation of the electricity demand model for residential buildings.	112
5.7	Comparison between measurements and uncalibrated bottom-up electricity demand model at transformer <i>Turnhalle St. Leonhard</i> (office buildings) for an average winter day.	113
5.8	Comparison between measurements and results of the bottom-up electricity demand model at transformer <i>Turnhalle St. Leonhard</i> (office buildings) for an average winter week after the calibration of demand loads and the integration of behavioral patterns.	115
5.9	Comparison between measurements and results of the bottom-up electricity demand model at transformer <i>Mövenweg</i> (office buildings) for an average winter week as validation of the electricity demand model for office buildings.	115
5.10	Comparison between measurements and results of the bottom-up electricity demand model at transformer <i>Waaghaus</i> (office buildings in the city center) for an average winter week as validation of the electricity demand model for office buildings.	116
5.11	Comparison between measurements and results of the bottom-up electricity demand model at transformer <i>Spelterinipplatz</i> (mixed-used area) for an average summer week as validation of the electricity demand model mixed-used buildings.	117
5.12	Comparison between measurements, results of the bottom-up electricity demand model, and demand distribution according to two top-down models at transformer <i>Spelterinipplatz</i> (mixed-used area). Source: [128]	118
5.13	Electricity demand of the entire city as predicted by the electricity demand model for an average winter week in 2019.	119

5.14 Breakdown of by end-use of the electricity demand of the entire city as predicted by the demand model for an average winter week in 2019. . . . 120

5.15 Electricity demand of the entire city as predicted by the electricity demand model for the scenarios “Base-case” and “Energy transition”. 121

5.16 Line loading as % of the maximum line thermal limit in the city low-voltage distribution grid at 12:00 on a weekday in 2019 (above) and 2030 (below). 122

List of Tables

- 2.1 Description of the geo-referenced database included in the digital twin of the investigated city to model the city’s real estate 30
- 2.2 Description of the geo-referenced database included in the digital twin of the investigated city to model the city’s mobility infrastructure 30
- 2.3 Description of the geo-referenced database included in the digital twin of the investigated city to model the city’s electricity infrastructure 31
- 2.4 Description of the geo-referenced database included in the digital twin of the investigated city to model the city’s DH infrastructure 31
- 2.5 Categorization and quality assessment of smart meter data delivered by St. Gallen and EKZ. 36
- 2.6 Assessment of representativity of typical normalized power demand profiles obtained from smart meter data analysis – by customer category . . . 40
- 2.7 Results of the analysis of smart meter measurements: (i) Peak-to-base ratios for weekdays and weekends, and (ii) baseload distribution’s mean and standard deviation values for customers categories whose typical power demand load profiles have been implemented in the electricity demand model 42

- 3.1 Outcomes of agent-based and elements of digital twin used by the electric mobility demand model 49
- 3.2 Summary of probabilities of charging at home, work, or public chargers when an agent with comfort-driven behavior has an opportunity to charge his/her EV. k is scaling factor. 50
- 3.3 Modeled charging elements and associated investment and maintenance costs. 52
- 3.4 Characteristics of electric vehicles. Sources: [92, 93] 55

3.5	Prices for EV charging at public chargers in Switzerland for three of the main national providers (rated power at AC chargers: 22 kW; at DC chargers: 150 kW). Roaming fees and subscriptions are not included. Source: [95]	56
3.6	Summary of the impact of EV penetration on optimized public EV charging infrastructure.	62
4.1	Outcomes of agent-based population model used to characterize the occupants of buildings in the heat demand model	75
4.2	Characteristics of buildings used by the heat demand model	75
4.3	Example conduction resistances used in the agent-based heat demand model [55]	79
4.4	Shares of buildings relative to the behavior of building occupants [112].	80
4.5	Summary of type and share daily consumption of domestic hot water. Source: [115]	83
4.6	Comparison of the test statistics of the three variants of the heat demand model: without agent-based modeling (NA); with occupants' behavior (OB); and with behavior of occupants and storage of domestic hot water (OB and DHWS).	90
4.7	Candidate and most relevant explanatory variables used and identified in the predictive agent-based building model.	91
5.1	Outcomes of agent-based and elements of digital twin used by the electricity demand model	97
5.2	List of conditions that need to be true for the activation of electricity demand for cooking	102
5.3	List of conditions that need to be true for the activation of electricity demand for washing	103
5.4	Power rating and number of electric appliances per employee in an office building. Source: [137]	104
5.5	Average electricity consumption in W/m ² by building type according to architectural norms [126, 127]	105
5.6	Summary of attributes of scenarios "Base-case" (2019) and "Energy transition" (2030) assessed applying the electric mobility, heat, and electricity demand models	106
5.7	Characterization of yearly electricity demand, according to power flow simulation of low-voltage grid, at 6 low-voltage transformers (2 calibration and 4 validation transformers)	107
5.8	Comparison of the error metrics of the calibration process for electricity demand in residential buildings (transformer <i>Gellerstrasse</i>)	109

5.9	: Results of the calibration of base load values and of a reduction factor for demand for cooking for residential demand (transformer <i>Gellerstrasse</i>)	111
5.10	Comparison of the error metrics of the calibration and validation process for electricity demand in residential buildings (transformers <i>Gellerstrasse</i> and <i>Rotmonten</i>)	111
5.11	Results of the calibration of base load values, of opening-hours activated shares of demand for base, lighting, and ventilation demand, and of an increase factor for demand for equipment (transformer <i>Turnhalle St. Leonhard</i>)	114
5.12	Comparison of the error metrics of the calibration and validation process for electricity demand in office buildings (transformers <i>Turnhalle St. Leonhard</i> , <i>Mövenweg</i> , and <i>Waaghaus</i>)	117

Bibliography

- [1] United Nations. (2015) Paris Agreement. Accessed on December, 2020. [Online]. Available: <https://unfccc.int/process-and-meetings/the-paris-agreement/the-paris-agreement>
- [2] BDEW, “Bruttostromerzeugung in Deutschland nach Energieträger in den Jahren 2000 bis 2020 (in Terawattstunden),” Berlin - Germany, Statista, 2020.
- [3] H. Nier, “Die Energiewende hat ihren Preis,” *Statista*, 2016, Berlin - Germany.
- [4] Fraunhofer ISE, “Studie: Stromgestehungskosten erneuerbare Energie,” Freiburg - Germany, 2018.
- [5] European Commission. (2020) EU climate action and the European Green Deal. Accessed on December, 2020. [Online]. Available: https://ec.europa.eu/clima/policies/eu-climate-action_en
- [6] Swiss Federal Office of Energy, “Energy Strategy 2050: Chronology,” Report, 2018.
- [7] Swiss Federal Office of Energy. (2018) Totalrevision des CO₂-Gesetzes. Accessed on December, 2020. [Online]. Available: <https://www.bafu.admin.ch/bafu/de/home/themen/klima/recht/totalrevision-co2-gesetz.html>
- [8] E. Yep, “China’s long march to zero carbon,” *S&P Global*, 2020, London - United Kingdom.
- [9] M. McGrath, “Climate change: Temperature analysis shows UN goals “within reach”,” *BBC News*, 2020.
- [10] European Commission. Progress made in cutting emissions. Accessed on December, 2020. [Online]. Available: https://ec.europa.eu/clima/policies/strategies/progress_en
- [11] Eurostat, “Electricity and heat statistics,” Kirchberg - Luxembourg, 2017.

- [12] Federal Office for the Environment, “Schweiz verfehlt Klimaziel 2020,” *Schweizer Radio und Fernsehen*, 2020, Bern - Switzerland.
- [13] U.S. Environmental Protection Agency, “Inventory of U.S. Greenhouse Gas Emissions and Sinks:1990-2018,” Washington - United States, 2020.
- [14] European Commission, “Fossil CO₂ and GHG emissions of all world countries,” Brussel - Belgium, 2020.
- [15] C 40 Cities. (2021) Why Cities? Accessed on March, 2021. [Online]. Available: www.c40.org/why_cities
- [16] E. Lobsiger-Kägi, T. Weiss Sampietro, U. Eschenauer, V. Carabias-Hütter, L. Braunreiter, and A. W. Müller, “Treiber und Barrieren auf dem Weg zu einer smart city: Erkenntnisse aus Theorie und Praxis,” *ZHAW Zürcher Hochschule für Angewandte Wissenschaften (Zürich - Switzerland)*, vol. 7, pp. 3–31, 2016.
- [17] St. Galler Stadtwerke. Über uns. Accessed on November, 2020. [Online]. Available: <https://www.sgsw.ch/home/ueber-uns.html>
- [18] Stadtrat der Stadt St. Gallen, “Energiekonzept 2050 Wärme, Elektrizität, Mobilität (*EnK³*),” St. Gallen - Switzerland, 2015.
- [19] Deutsche Energie Agentur, “Dena-Projekt: Urbane Energiewende,” Berlin - Germany, 2019.
- [20] L. Steg, G. Perlaviciute, and E. van der Werff, “Understanding the human dimensions of a sustainable energy transition,” *Frontiers in Psychology*, vol. 6, p. 805, 2015.
- [21] T. Brosch, D. Sander, and M. Patel, “Editorial: Behavioral insights for a sustainable energy transition,” *Frontiers in Energy Research*, vol. 4, pp. 1–3, 2016.
- [22] Swiss Federal Office of Energy. (2017) Chronologie zur Energiestrategie 2050. [Online]. Available: <https://www.uvek.admin.ch/uvek/de/home/uvek/abstimmungen/abstimmung-zum-energiegesetz/chronologie-und-grafiken.html>
- [23] E. Ruokamo, “Household preferences of hybrid home heating systems— A choice experiment application,” *Energy Policy*, vol. 95, pp. 224–237, 2016.
- [24] F. G. Braun, “Determinants of households’ space heating type: A discrete choice analysis for German households,” *Energy Policy*, vol. 38, pp. 5493–5503, 2010.
- [25] A. Tabi, S. L. Hille, and R. Wüstenhagen, “What makes people seal the green power deal?—customer segmentation based on choice experiment in Germany,” *Ecological Economics*, vol. 107, pp. 206–215, 2014.

- [26] M. Marini, “Agent-based assessment of future demographics and impact on infrastructure transition needs,” Ph.D. dissertation, Laboratory for Energy Conversion, ETH Zurich, Switzerland, 2020.
- [27] A. Turrell, “Agent-based models: understanding the economy from the bottom up,” *Bank of England Quarterly Bulletin Q4*, pp. 173–188, 2016.
- [28] L. G. Swan and V. I. Ugursal, “Modeling of end-use energy consumption in the residential sector: A review of modeling techniques,” *Renewable and Sustainable Energy Reviews*, vol. 13, pp. 1819–1835, 2009.
- [29] R. Nouvel, A. Mastrucci, U. Leopold, O. Baume, V. Coors, and U. Eicker, “Combining gis-based statistical and engineering urban heat consumption models: Towards a new framework for multi-scale policy support,” *Energy and Buildings*, vol. 107, pp. 204–212, 2015.
- [30] International Energy Agency, “Global EV Outlook 2018,” Paris - France, 2018.
- [31] L. Goldie-Scot, “A behind the scenes take on Lithium-ion battery prices,” *BloombergNEF*, 2019.
- [32] P. Campbell, “Volkswagen sets bold targets as it steps up electric ambitions,” *Financial Times*, 2019.
- [33] H. Hall, H. Cui, and N. Lutsey, “Electric vehicle capitals: Accelerating the global transition,” *The International Council on Clean Transportation*, vol. -, pp. 1–15, 2018.
- [34] N. Anglani, F. Fattori, and G. Muliere, “Electric vehicles penetration and grid impact for local energy models,” in *2012 IEEE International Energy Conference and Exhibition (ENERGYCON)*, 2012, pp. 1009–1014.
- [35] S. Shafiee, M. Fotuhi-Firuzabad, and M. Rastegar, “Investigating the impacts of plug-in hybrid electric vehicles on power distribution systems,” *IEEE Transactions on Smart Grid*, vol. 4, pp. 1351–1360, 2013.
- [36] L. P. Fernandez, T. Gomez San Roman, R. Cossent, C. M. Domingo, and P. Frias, “Assessment of the impact of plug-in electric vehicles on distribution networks,” *IEEE Transactions on Power Systems*, vol. 26, pp. 206–213, 2010.
- [37] P. Sadeghi-Barzani, A. Rajabi-Ghahnavieh, and H. Kazemi-Karegar, “Optimal fast charging station placing and sizing,” *Applied Energy*, vol. 125, pp. 289–299, 2014.

- [38] L. Zhang, B. Shaffer, T. Brown, and G. S. Samuelsen, "The optimization of DC fast charging deployment in california," *Applied Energy*, vol. 157, pp. 111–122, 2015.
- [39] L. Luo, W. Gu, S. Zhou, H. Huang, S. Gao, J. Han, Z. Wu, and X. Dou, "Optimal planning of electric vehicle charging stations comprising multi-types of charging facilities," *Applied Energy*, vol. 226, pp. 1087–1099, 2018.
- [40] Y. Xiang, J. Liu, R. Li, F. Li, C. Gu, and S. Tang, "Economic planning of electric vehicle charging stations considering traffic constraints and load profile templates," *Applied Energy*, vol. 178, pp. 647–659, 2016.
- [41] M. A. Kazemi, M. Sedighzadeh, M. J. Mirzaei, and O. Homaei, "Optimal siting and sizing of distribution system operator owned EV parking lots," *Applied Energy*, vol. 179, pp. 1176–1184, 2016.
- [42] S. Micari, A. Polimeni, G. Napoli, L. Andaloro, and V. Antonucci, "Electric vehicle charging infrastructure planning in a road network," *Renewable and Sustainable Energy Reviews*, vol. 80, pp. 98–108, 2017.
- [43] M. Shepero and J. Munkhammar, "Spatial Markov chain model for electric vehicle charging in cities using geographical information system (GIS) data," *Applied Energy*, vol. 231, pp. 1089–1099, 2018.
- [44] O. Sundstrom and C. Binding, "Flexible charging optimization for electric vehicles considering distribution grid constraints," *IEEE Transactions on Smart Grid*, vol. 3, no. 1, pp. 26–37, 2011.
- [45] K. Clement-Nyns, E. Haesen, and J. Driesen, "The impact of charging plug-in hybrid electric vehicles on a residential distribution grid," *IEEE Transactions on Power Systems*, vol. 25, pp. 371–380, 2009.
- [46] D. Fischer, A. Harbrecht, A. Surmann, and R. McKenna, "Electric vehicles' impacts on residential electric local profiles—a stochastic modelling approach considering socio-economic, behavioural and spatial factors," *Applied Energy*, vol. 233, pp. 644–658, 2019.
- [47] A. Schroeder and T. Traber, "The economics of fast charging infrastructure for electric vehicles," *Energy Policy*, vol. 43, pp. 136–144, 2012.
- [48] P. Morrissey, P. Weldon, and M. O'Mahony, "Future standard and fast charging infrastructure planning: An analysis of electric vehicle charging behaviour," *Energy Policy*, vol. 89, pp. 257–270, 2016.

- [49] Heat Roadmap Europe 2050 (HRE4), “Heating and Cooling: facts and figures,” Copenhagen - Denmark, 2017.
- [50] Swiss Federal Office of Energy, “Gebäudepark 2050 - Vision des BFE,” Bern - Switzerland, 2018.
- [51] L. Blatter and A. Zehnder, “Öl- und Gasheizungen sind langfristig nicht günstiger,” *Schweizer Radio und Fernsehen*, 2019.
- [52] D. Connolly, H. Lund, B. V. Mathiesen, S. Werner, B. Möller, U. Persson, T. Boermans, D. Trier, P. A. Østergaard, and S. Nielsen, “Heat roadmap europe: Combining district heating with heat savings to decarbonise the EU energy system,” *Energy Policy*, vol. 65, pp. 475–489, 2014.
- [53] U. Persson and S. Werner, “District heating in sequential energy supply,” *Applied Energy*, vol. 95, pp. 123–131, 2012.
- [54] Stadtkanzlei Stadt St. Gallen. (2017) Volksabstimmung vom 26. November 2017. [Online]. Available: www.stadt.sg.ch/home/verwaltung-politik/demokratie-politik/abstimmungen-wahlen/
- [55] D. Perez, J. H. Kämpf, and J.-L. Scartezzini, “Urban area energy flow microsimulation for planning support: A calibration and verification study,” *International Journal on Advances in Systems and Measurements*, vol. 6, 2013.
- [56] P. G. Cesaratto and M. De Carli, “A measuring campaign of thermal conductance in situ and possible impacts on net energy demand in buildings,” *Energy and Buildings*, vol. 59, pp. 29–36, 2013.
- [57] M. Mirsadeghi, D. Cóstola, B. Blocken, and J. L. Hensen, “Review of external convective heat transfer coefficient models in building energy simulation programs: Implementation and uncertainty,” *Applied Thermal Engineering*, vol. 56, pp. 134–151, 2013.
- [58] J. Liu, M. Heidarinejad, S. Gracik, and J. Srebric, “The impact of exterior surface convective heat transfer coefficients on the building energy consumption in urban neighborhoods with different plan area densities,” *Energy and Buildings*, vol. 86, pp. 449–463, 2015.
- [59] S. Pfenninger, A. Hawkes, and J. Keirstead, “Energy systems modeling for twenty-first century energy challenges,” *Renewable and Sustainable Energy Reviews*, vol. 33, pp. 74–86, 2014.

- [60] E. McKenna and M. Thomson, “High-resolution stochastic integrated thermal–electrical domestic demand model,” *Applied Energy*, vol. 165, pp. 445–461, 2016.
- [61] E. McKenna, M. Krawczynski, and M. Thomson, “Four-state domestic building occupancy model for energy demand simulations,” *Energy and Buildings*, vol. 96, pp. 30–39, 2015.
- [62] M. Muratori, M. C. Roberts, R. Sioshansi, V. Marano, and G. Rizzoni, “A highly resolved modeling technique to simulate residential power demand,” *Applied Energy*, vol. 107, pp. 465–473, 2013.
- [63] R. Subbiah, K. Lum, A. Marathe, and M. Marathe, “Activity based energy demand modeling for residential buildings,” in *2013 IEEE PES Innovative Smart Grid Technologies Conference (ISGT)*. IEEE, 2013, pp. 1–6.
- [64] E. Azar and C. C. Menassa, “Agent-based modeling of occupants and their impact on energy use in commercial buildings,” *Journal of Computing in Civil Engineering*, vol. 26, pp. 506–518, 2011.
- [65] G. Bustos-Turu, K. H. van Dam, S. Acha, C. N. Markides, and N. Shah, “Simulating residential electricity and heat demand in urban areas using an agent-based modelling approach,” in *2016 IEEE International Energy Conference (ENERGYCON)*. IEEE, 2016, pp. 1–6.
- [66] F. Chingcuanco and E. J. Miller, “A microsimulation model of urban energy use: modelling residential space heating demand in ilute,” *Computers, Environment and Urban Systems*, vol. 36, pp. 186–194, 2012.
- [67] A. Singh, D. Willi, N. Chokani, and R. S. Abhari, “Optimal power flow analysis of a Switzerland’s transmission system for long-term capacity planning,” *Renewable and Sustainable Energy Reviews*, vol. 34, pp. 596–607, 2014.
- [68] P. Eser, N. Chokani, and R. Abhari, “Impact of nord stream 2 and lng on gas trade and security of supply in the european gas network of 2030,” *Applied Energy*, vol. 238, pp. 816–830, 2019.
- [69] P. Eser, A. Singh, N. Chokani, and R. S. Abhari, “Effect of increased renewables generation on operation of thermal power plants,” *Applied Energy*, vol. 164, pp. 723–732, 2016.
- [70] P. Eser, N. Chokani, and R. S. Abhari, “Impacts of battery electric vehicles on renewable integration within the 2030 European power system,” *International Journal of Energy Research*, vol. 42, pp. 4142–4156, 2018.

- [71] A. Saprykin, M. Marini, N. Chokani, and R. S. Abhari, “Holistic, integrated generation of daily-activity plans for Switzerland: from population synthesis to trip generation,” in *20th Swiss Transport Research Conference (STRC 2020)(online)*. STRC, Conference Proceedings.
- [72] M. Pagani, W. Korosec, N. Chokani, and R. S. Abhari, “User behaviour and electric vehicle charging infrastructure: An agent-based model assessment,” *Applied Energy*, vol. 254, p. 113680, 2019.
- [73] A. Saprykin, N. Chokani, and R. S. Abhari, “GEMSim: A GPU-accelerated multi-modal mobility simulator for large-scale scenarios,” *Simulation Modelling Practice and Theory*, vol. 94, pp. 199–214, 2019.
- [74] M. Marini, N. Chokani, and R. S. Abhari, “Agent-based model analysis of impact of immigration on Switzerland’s social security,” *Journal of International Migration and Integration*, vol. 20, pp. 787–808, 2018.
- [75] M. Marini, A. P. Gawlikowska, A. Rossi, N. Chokani, H. Klumpner, and R. S. Abhari, “The impact of future cities on commuting patterns: An agent-based approach,” *Environment and Planning B: Urban Analytics and City Science*, vol. 46, pp. 1079–1096, 2019.
- [76] Geomatics and Surveying Office of the City of St.Gallen. Geomatik und Vermessung. Accessed on January, 2021. [Online]. Available: <https://www.stadt.sg.ch/home/verwaltung-politik/direktionen/planung-bau/geomatik-vermessung.html>
- [77] Swiss Federal Office for Statistics, “Eidgenoessisches Gebaeude- und Wohnungsregister,” Bern - Switzerland, 2015.
- [78] —, “Switzerland’s population 2015,” Bern - Switzerland, 2016.
- [79] —, “Betriebs- und Unternehmensregister,” Bern - Switzerland, 2013.
- [80] M. M. Yagoub, “Assessment of OpenStreetMap (OSM) Data: The case of Abu Dhabi City, United Arab Emirates,” *Journal of Map & Geography Libraries*, vol. 13, pp. 300–319, 2017.
- [81] OpenStreetMap Foundation. OpenStreetMap Project. Accessed on January, 2021. [Online]. Available: <https://www.openstreetmap.org>
- [82] E. Veldman and R. A. Verzijlbergh, “Distribution grid impacts of smart electric vehicle charging from different perspectives,” *IEEE Transactions on Smart Grid*, vol. 6, pp. 333–342, 2015.
- [83] W. Axthelm, “Die Energiewende findet im Verteilnetz statt - Mehr netzdienliche Flexibilität im Verteilnetz,” in *BEE-Forum-E-world 2020*. Essen - Germany, 2020.

- [84] L. Thurner, A. Scheidler, F. Schäfer, J.-H. Menke, J. Dollichon, F. Meier, S. Meinecke, and M. Braun, “pandapower - an open source python tool for convenient modeling, analysis and optimization of electric power systems,” *IEEE Transactions on Power Systems*, vol. 33, pp. 6510–6521, 2018.
- [85] M. Marini, N. Chokani, and R. S. Abhari, “Immigration and future housing needs in Switzerland: Agent-based modelling of agglomeration Lausanne,” *Computers, Environment and Urban Systems*, vol. 78, p. 101400, 2019.
- [86] St. Galler Stadtwerke (Ernst Basler + Partner), “Elektromobilität-Ladeinfrastruktur St. Gallen,” Zollikon - Switzerland, 2015.
- [87] C. F. Chen, G. Zarazua de Rubens, L. Noel, J. Kester, and B. K. Sovacool, “Assessing the socio-demographic, technical, economic and behavioral factors of nordic electric vehicle adoption and the influence of vehicle-to-grid preferences,” *Renewable and Sustainable Energy Reviews*, vol. 121, p. 106692, 2020.
- [88] D. Eckert, “Wo Benzin weltweit am teuersten ist,” *Die Zeit*, 2016.
- [89] National Association of Convenience Stores, “Consumer behavior at the pump,” Alexandra - United States, 2019.
- [90] J. Agenbrood and B. Holland. (2015) What is the true cost of EV charging stations? [Online]. Available: www.greenbiz.com/blog/2014/05/07/rmi-whats-true-cost-evcharging-stations
- [91] S. Stadtwerke. Mobilität, “Mobilität Ost Mobil,” St. Gallen - Switzerland, 2018.
- [92] Swiss e-Mobility. (2020) Die beliebtesten Steckerfahrzeuge. Accessed on November, 2020. [Online]. Available: <https://www.swiss-emobility.ch/de/news/aktuell/meldungen/58-Neuzulassungen-2019.php>
- [93] U.S. Department of Energy. (2020) Fuel Economy. Accessed on November, 2020. [Online]. Available: www.fueleconomy.gov
- [94] Eidgenössische Elektrizitätskommission ElCom. Strompreis Elcon 2017. Accessed on October, 2017. [Online]. Available: www.strompreis.elcon.admin.ch
- [95] G. Hense, “Ladestrompreise, roamingpreise und netzwerke für das laden von e-autos,” *Carmart*, 2020.
- [96] G. Gligorijevic. (2016) IKEA Schweiz lanciert Ladestationen für Elektroautos. Accessed November, 2020. [Online]. Available: <https://media.ikea.ch/pressrelease/ikea-schweiz-lanciert-ladestationen-fur-elektroautos/2804/>
- [97] Ampnet-DMM, “E-auto bei LIDL & Co. kostenfrei laden,” Tech. Rep., 2019.

- [98] K. Korosec, “Tesla brings back free unlimited supercharging for the Model S and X,” *Techcrunch*, 2019.
- [99] T. Habegger, “Plug@work - Das Laden von Elektroautos ist so simpel wie nie zuvor,” *News rund um die BKW*, 2019.
- [100] SAK Medienstelle. (2017) Die E-Mobilität rollt: SAK und die Migros Ostschweiz realisieren zehn neue Ladestationen. Accessed on December, 2020. [Online]. Available: <https://www.sak.ch/ueber-sak/medien/medienmitteilungen-vorjahre>
- [101] Swisstopo - Swiss Federal Office of Topography. Landscape model: SwissTLM3D. Accessed on June, 2015. [Online]. Available: www.swisstopo.admin.ch/en/knowledge-facts/topographic-landscape-model.html
- [102] Swiss Society of Engineers and Architects, “Norm 380/1: Thermische Energie im Hochbau,” Zurich - Switzerland, 2016.
- [103] —, “Norm 2024: Raumnutzungsdaten für die Energie- und Gebäudetechnik,” Zurich - Switzerland, 2015.
- [104] —, “Norm 2044: klimatisierte Gebäude - Standard Berechnungsverfahren für den Leistungs- und Energiebedarf,” Zurich - Switzerland, 2010.
- [105] J. Seifert, “Bestimmung des realen Luftwechsels bei Fensterlüftung aus energetischer und bauphysikalischer Sicht,” *Fraunhofer-IRB-Verlag*, vol. 3816760023, 2003.
- [106] W. C. Skamarock, J. B. Klemp, J. Dudhia, D. O. Gill, D. M. Barker, W. Wang, and J. G. Powers, “A description of the advanced research WRF version 3,” *National Center for Atmospheric Research*, pp. 3–27, 2008.
- [107] Federal Office of Meteorology and Climatology MeteoSwiss. (2020) Date portal for teaching and research. Accessed October, 2020. [Online]. Available: www.meteoswiss.admin.ch/home/services-and-publications/beratung-und-service/datenportal-fuer-lehre-und-forschung.html
- [108] K. Collins, “Low indoor temperatures and morbidity in the elderly,” *Age and Ageing*, vol. 15, pp. 212–220, 1986.
- [109] M. Beshir and J. Ramsey, “Comparison between male and female subjective estimates of thermal effects and sensations,” *Applied Ergonomics*, vol. 12, pp. 29–33, 1981.
- [110] e. a. Buchmann, M, “Energie nachhaltig konsumieren - nachhaltige Energie konsumieren,” Report, 2011.

- [111] Fachhochschule Nordwestschweiz – Hochschule für Architektur Bau und Geomatik, “Warmwasser-Wärmepumpen Auslegungs- (Dimensionierungs-) Checkliste,” Olten - Switzerland, 2017.
- [112] Velux Schweiz AG, “Gutes Wohnen in der Schweiz,” Aarbug - Schweiz, 2016.
- [113] T. Frank, “Anforderungen an behordentaugliche dynamische Simulationsprogramme,” Swiss Federal Office of Energy, Bern - Switzerland, 2011.
- [114] P. Maire, “Bottom-up heating demand model for multi-utility company,” Semester Project, 2018, Laboratory for Energy Conversion - ETH Zurich - Switzerland.
- [115] Schweizerische Verein des Gas- und Wasserfaches. Haushaltsverbrauch in der Schweiz. Accessed on September, 2019. [Online]. Available: www.wasserqualitaet.svgw.ch/index.php?id=874
- [116] C. F. Reinhart and C. C. Davila, “Urban building energy modeling—A review of a nascent field,” *Building and Environment*, vol. 97, pp. 196–202, 2016.
- [117] A. Grandjean, G. Binet, J. Bieret, J. Adnot, and B. Duplessis, “A functional analysis of electrical load curve modelling for some households specific electricity end-uses,” in *6th International Conference on Energy Efficiency in Domestic Appliances and Lighting (EEDAL’11)*, 2011, pp. 24–p.
- [118] H. Lin, Q. Wang, Y. Wang, R. Wennerstern, and Q. Sun, “Agent-based modeling of electricity consumption in an office building under a tiered pricing mechanism,” *Energy Procedia*, vol. 104, pp. 329–335, 2016.
- [119] Swiss Federal Office of Energy, “Schweizerische Elektrizitätsstatistik 2019,” Ittigen - Switzerland, 2019.
- [120] P. Bertoldi and B. Atanasiu, “Electricity consumption and efficiency trends in European Union,” *Renewable Energy Status Rep*, vol. -, pp. 3–62, 2009.
- [121] P. Bertoldi, B. Hirl, and N. Labanca, “Energy efficiency status report,” *JRC Scientific and Policy Reports*, vol. -, pp. 8–141, 2012.
- [122] J. Nipkow, “Typischer Haushalt-Stromverbrauch,” Swiss Federal Office of Energy, Ittigen - Switzerland, 2013.
- [123] D. Aiulfi, A. Primas, and M. Jakob, “Energieverbrauch von Bürogebäuden und Grossverteilern,” Swiss Federal Office of Energy, Ittigen - Switzerland, 2010.
- [124] M. Yokoya and H. Shimizu, “Estimation of effective day length at any light intensity using solar radiation data,” *International journal of environmental research and public health*, vol. 8, pp. 4272–4283, 2011.

- [125] VELUX Group, “How to evaluate daylight,” Horsholm - Denmark, 2019.
- [126] Swiss Society of Engineers and Architects, “Norm 387/4: Elektrizität in Gebäuden - Beleuchtung: Berechnung und Anforderungen,” Zurich - Switzerland, 2017.
- [127] —, “Norm 2056: Elektrizität in Gebäuden - Energie- und Leistungsbedarf,” Zurich - Switzerland, 2019.
- [128] D. Haegel, “Agent-based modelling of electricity demand,” Semester Project, 2019, Laboratory for Energy Conversion - ETH Zurich - Switzerland.
- [129] R. Dunbar, “Breaking bread: the functions of social eating,” *Adaptive Human Behavior and Physiology*, vol. 3, pp. 198–211, 2017.
- [130] EnergieSchweiz, “Energie-effizienz im Haushalt,” Zurich - Switzerland, 2016.
- [131] M. Griffin, T. Ramsson, and G. Gibson, “Cooking appliances,” *Energy Technology Systems Analysis Programme*, vol. R06, 2012.
- [132] Statistical Office of Estonia, “Household appliances electricity consumption,” Tallin - Estonia, 2013.
- [133] Coop Fachstelle Ernährung and Schweizerische Gesellschaft für Ernährung, “Ess-Trends im Fokus,” Basel - Switzerland, 2009.
- [134] C. Bourrier, F. Corsini, M. Danthurebandara, K. Fuchs, S. Olloz, S. Poulikidou, S. Rufener, and R. Singh, “ETH Sustainability Summer School: Washing Machine,” Zurich - Switzerland, 2011.
- [135] I. Rüdener, U. Eberle, and R. Griebhammer, “Ökobilanz und Lebenszykluskostenrechnung Wäschewaschen: Vergleich des Waschens bei durchschnittlichen Temperaturen mit Waschen bei niedrigen Temperaturen,” Freiburg/Hamburg - Germany, 2006.
- [136] L. Stawreberg, “Energy efficiency improvements of tumble dryers: Technical development, laundry habits and energy labelling,” Karlstad University - Sweden, 2011.
- [137] A. Menezes, A. Cripps, R. A. Buswell, J. Wright, and D. Bouchlaghem, “Estimating the energy consumption and power demand of small power equipment in office buildings,” *Energy and Buildings*, vol. 75, pp. 199–209, 2014.